REGULATION OF LYSOSOME TRAFFICKING AND NUTRIENT HOMEOSTASIS

by

Shefali Krishna

A Dissertation

Presented to the Faculty of Louis V. Gerstner, Jr

Graduate School of Biomedical Sciences,

Memorial Sloan Kettering Cancer Center,

In Partial Fulfillment of the Requirements for the Degree of

Doctor of Philosophy

New York, NY

May, 2017

Michael Overholtzer, PhD
Dissertation Mentor

Date

To my family and friends for their endless support and love.

ABSTRACT

The scavenging of extracellular macromolecules by the engulfment processes of macropinocytosis, phagocytosis or entosis can sustain cell growth in a nutrient-depleted environment. Engulfed macromolecules are contained within vacuoles that are targeted for lysosome fusion to initiate cargo degradation and nutrient export. While much is known about the upstream stages leading to lysosome fusion, surprisingly little is known about the late stages of lysosome function required for vacuole processing and nutrient trafficking. We have shown that vacuoles containing engulfed material undergo mTORC1-dependent fission that redistributes degraded cargo into lysosomal networks. Here we identify the lipid kinase PIKfyve as a regulator of an alternative pathway that distributes engulfed contents in support of intracellular macromolecular synthesis. We find that PIKfyve regulates vacuole size in part through its downstream effector, the cationic transporter TRPML1. Furthermore, PIKfyve promotes recovery of amino acids from vacuoles, suggesting a potential link between PIKfyve activity and lysosomal nutrient export. During amino acid depletion, PIKfyve activity protects Ras-mutant cells from starvation-induced cell death and supports their proliferation. Interestingly, we find that PIKfyve regulates the exit of cholesterol from lysosomal membranes and PIKfyve-dependent cholesterol egress plays a role in maintaining lysosome size and morphology. We also find that PIKfyve regulates the partitioning of lysosomal membrane proteins into distinct microdomains that resemble cholesterol-rich lipid domains. These data identify PIKfyve as a critical regulator of lysosome trafficking and nutrient homeostasis.

BIOGRAPHICAL SKETCH

Shefali Krishna was born on November 8th, 1988 to Shailesh Krishna and Rashmi Krishna in Lucknow, India. She lived in Lucknow during her childhood with her parents, her brother Shantanu Krishna and her extended family. Shefali attended Seth M. R Jaipuria School for her high school training, and discovered her passion for science, particularly biology, during these years. To pursue her interest in biology after graduating high school in 2006, she went on to study Life Sciences with a focus on Cell and Molecular Biology for a Bachelor in Science degree at National University of Singapore, Singapore. During her junior and senior year she worked on cell survival signaling pathways in tumorigenesis in the laboratory of Dr. Shazib Pervaiz, and became fascinated with understanding the basic cell biology of tumor cells. In order to pursue this interest after graduating with her bachelor's degree in 2010, she decided to pursue doctoral studies at Louis V. Gerstner Sloan Kettering Graduate School of Biomedical Sciences at Memorial Sloan Kettering Cancer Center in New York, New York. She joined the lab of Dr. Michael Overholtzer to conduct her graduate research in understanding lysosome trafficking and nutrient homeostasis in normal and tumor cells.

ACKNOWLEDGEMENTS

I would first and foremost like to thank my PhD advisor, Dr. Michael Overholtzer, for being an exceptional mentor. He is a brilliant scientist and it has been awe-inspiring to learn from someone who is so passionate about science. I am extremely grateful to him for his tremendous support throughout my PhD and constant encouragement to do interesting creative science. His scientific insight, supportive guidance and mentorship have helped me become a better scientist and will always encourage me to pursue my goals.

I would also like to thank my thesis committee members, Dr Alan Hall, Dr. Xuejun Jiang and Dr. Philipp Niethammer, who have been extremely supportive and helpful throughout my graduate studies both in sharing ideas as well as resources. Although Dr. Alan Hall is no longer with us, he was a wonderful mentor and has provided many great ideas during the committee meetings and our weekly joint lab meetings. I am very grateful to Dr. Marilyn Resh for sharing ideas and resources from her lab as well as for chairing my thesis defense. I am also thankful to Dr. Eric Baehrecke for many scientific discussions and for being the external examiner for my thesis defense. I am also very grateful to Dr. Cole Haynes, for numerous scientific discussions and sharing many ideas as well as resources from the lab.

I would also like to thank all the current and former members of the Overholtzer lab for being so helpful and making this experience so exciting: Oliver Florey, Qiang Sun, Matej Krajcovic, Sung Eun Kim, Yongchan Lee, Urmi Bandyopadhyay, Jens Hamann, Chan Lee, Ruoyao Chen and Michelle Riegman.

It has been a pleasure working with such talented colleagues and they have made our lab a wonderful place to work.

Next I would like to express my gratitude to our collaborators for their invaluable expertise and resources. In particular, I would like to thank Dr. Wilhelm Palm and Dr. Craig B. Thompson for conducting albumin supplementation assays, their assistance in writing our manuscript and for many useful discussions regarding the nutrient homeostasis project. I would also like to thank Dr. David Iaea and Dr. Frederick Maxfield for their assistance in conducting some filipin staining experiments as well as providing ideas and reagents for the cholesterol project. I am also grateful to Dr. Will Wood for numerous scientific discussions and for sharing ideas related to my thesis project.

I am very thankful to all my friends that I met during graduate school: Deeja Sultan, Richa Gupta, Chong Luo, Nitya Ramkumar, Vidhya Rangaraju, Radhika Raheja, Priya Issuree and Bobby Bowman for making my time in New York so exciting and enjoyable.

Finally, I am extremely grateful to my family for their endless support throughout my career. I would to thank my parents, Rashmi Krishna and Shailesh Krishna for encouraging me to pursue science, specially my mother for always motivating me to follow my dreams. I would also like to thank my brother Shantanu Krishna, my sister-in-law Deviyani Srivastava, and my extended family in the US – Vimal Srivastava, Andrea Srivastava, Nisha Newman, Newman, Ramesh Srivastava and Sushila Srivastava, for all their love and support during these years.

TABLE OF CONTENTS

CHAPTER 1: Introduction

1.1 NUTRIENT HOMEOSTASIS

Cell proliferation requires bulk production of proteins, lipids and nucleic acids, which places a heavy demand on cellular nutrient and energy supplies. This is particularly true for cancer cells, where normal cell cycle control is often disrupted and proliferation occurs in a dysregulated manner. Nutrient uptake primarily occurs through plasma membrane transporters that import the metabolites provided by the surrounding vasculature. The high rates of cancer cell proliferation often lead to a metabolic crisis in tumors, which can be countered in part by angiogenesis or the upregulation of plasma membrane transporters for key metabolites like glucose (GLUT1), leucine (LAT1) and glutamine (ASCT2) (Jones and Thompson, 2009; Pavlova and Thompson, 2016; Wang and Holst, 2015). However, the rapid expansion of solid tumors often outpaces vascular supply, causing an increased dependence of tumor cells on alternative mechanisms of nutrient acquisition. In addition to cancer cells, non-transformed cells, such as macrophages, neurons, cardiomyocytes, and epithelial and endothelial cells, must also function within ischemic tissues during stroke, heart attack, or injury, or within hypovascular tumor microenvironments, which places a demand on alternative pathways that can allow for the recycling and scavenging of nutrients needed for cell survival. These pathways include

autophagy, macropinocytosis and forms of cell engulfment like phagocytosis and entosis, which are discussed in the following sections.

1.2 NUTRIENT RECYCLING AND SCAVENGING PATHWAYS

1.2.1 Autophagy

Macroautophagy (referred to as autophagy) is a molecular pathway activated upon cellular stresses like starvation, growth factor depletion, hypoxia or infection, whereby cells sequester intracellular components that undergo lysosomal degradation (He and Klionsky, 2009). Nutrient starvation (in particular amino acid starvation) leads to inactivation of the nutrient responsive kinase mTORC1 that relieves the autophagy pre-initiation complex consisting of “ULK1/2-ATG13-FIP200”. This complex acts in concert with the Class III PI3K complex containing “VPS34-VPS15-Beclin1-Atg14L” to initiate the nucleation of double membrane phagophores around the cytosolic cargo (Figure 1.1) (Debnath et al., 2015). Phagophore expansion and autophagosome formation is mediated by the LC3 and Atg12 conjugation systems, which is followed by lysosome fusion to the compartment (Debnath et al., 2015). Degradation of the engulfed contents and nutrient recovery from these autolysosomes then restores the energy balance in the cell (Figure 1.1) (Debnath et al., 2015).

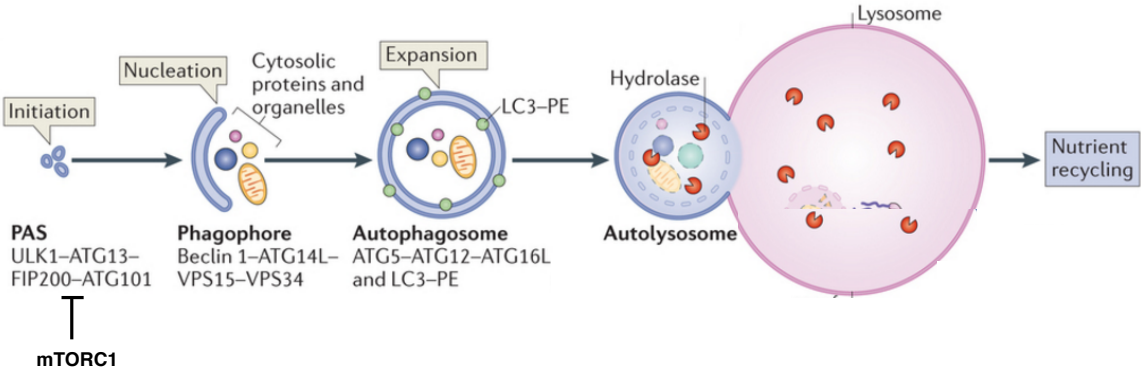

Figure 1.1. Molecular Mechanism of Autophagy. Nutrient deprivation inactivates mTORC1, an inhibitor of autophagy, which relieves the autophagy pre-initiation complex containing "ULK1/2-Atg13-FIP200-Atg101" to initiate formation of pre-autophagosomal structures (PAS). The PAS then undergoes nucleation to form the double membrane phagophore around cytosolic cargo with the help of the "Beclin1-Atg14L-VPS34-VPS15" complex. Further expansion of the phagophores into autophagosomes is directed by "Atg5-Atg12-Atg16L" and the "LC3-PE" conjugation systems. The autophagosomes then fuse with lysosomes to form autolysosomes where the engulfed cargo is degraded and nutrients recycled. Figure adapted from (Debnath et al., 2015).

Autophagy is induced in ischemic tissues where it has been shown to promote cell survival (Guan et al., 2015; Matsui et al., 2007), although prolonged autophagy can also contribute to cell death in some contexts (Descloux et al., 2015). In yeast autophagy is required to support survival during nitrogen starvation by recycling amino acids like leucine, isoleucine and tyrosine (Yang et al., 2006). Similarly, in neonate mice autophagy is upregulated at birth as the placental nutrition is disrupted, and increases plasma concentrations of essential and branched chain amino acids to facilitate survival until milk becomes available (Kuma et al., 2004). Certain cancer types, particularly those with mutations in Ras-family small GTPases (eg. lung and pancreatic tumors), also exhibit an elevated level of autophagy that supports cell survival by recycling glutamine to support mitochondrial metabolism and respiration (Guo et al., 2011; Seo et al.,

2016; Strohecker et al., 2013; Yang et al., 2011). These cancers, demonstrate signs of autophagy “addiction”, where inhibition of autophagy can lead to cell death (Mancias and Kimmelman, 2011). However, while autophagy can recycle intracellular metabolites to support survival, it is unlikely to generated sufficient biomass to support cell proliferation without an exogenous nutrient supply making it critical to understand extracellular nutrient scavenging pathways.

1.2.2 Macropinocytosis

Macropinocytosis is an endocytic pathway involving bulk uptake of solutes by the cell from the extracellular environment. It was first described in rat macrophages in the early 1930s as a morphological process involving plasma membrane ruffles that close back on themselves to form macropinosomes ranging from 0.2-5um in size (Lim and Gleeson, 2011). Macropinocytosis is non-specific with regard to the cargo and requires Rac1/Actin-dependent membrane ruffling (Lim and Gleeson, 2011). Once formed the macropinosomes undergoes extensive tubulation to change shape and size, which is followed by endocytic maturation culminating with lysosome fusion (Racoosin and Swanson, 1993), although sometimes macropinosomes contents can be recycled back to the plasma membrane (Figure 1.2A) (West et al., 1989).

Macropinocytosis has several critical roles in physiology including cell motility, chemotactic responses, antigen presentation as well as pathogen entry (Lim and Gleeson, 2011). Interestingly, recent studies have demonstrated that macropinocytosis can be utilized as a strategy by cells to scavenge nutrients

from the extracellular environment (Commisso et al., 2013; Kamphorst et al., 2013; Yoshida et al., 2015). Similar to autophagy, which recycles intracellular contents and promotes cell survival, Ras-transformed cells upregulate macropinocytosis to engulf nutrients to support proliferation (Commisso et al., 2013; Kamphorst et al., 2013). The macropinocytic uptake of serum albumin by Ras-mutant cells can provide them with numerous amino acids including glutamine, leucine, isoleucine, proline, lysine, valine and alanine (Commisso et al., 2013). These protein-derived amino acids can enter the pyruvate, lactate and TCA cycles to maintain central carbon metabolism and can support the proliferation of Ras-mutant cells during starvation conditions (Commisso et al., 2013; Palm et al., 2015).

Macropinocytic uptake of albumin by Ras-mutant cells or free amino acids by non-transformed cells during leucine depletion can also reactivate mTORC1 signaling in the cell (Palm et al., 2015; Yoshida et al., 2015). Remarkably, mTORC1 inhibition during leucine depletion promotes lysosomal degradation of engulfed albumin and subsequent proliferation of the starving Ras-mutant cells (Palm et al., 2015). The reverse is true during leucine-replete conditions, suggesting a tight regulation of extracellular protein catabolism that is dependent on the nutrient status of the cell (Palm et al., 2015).

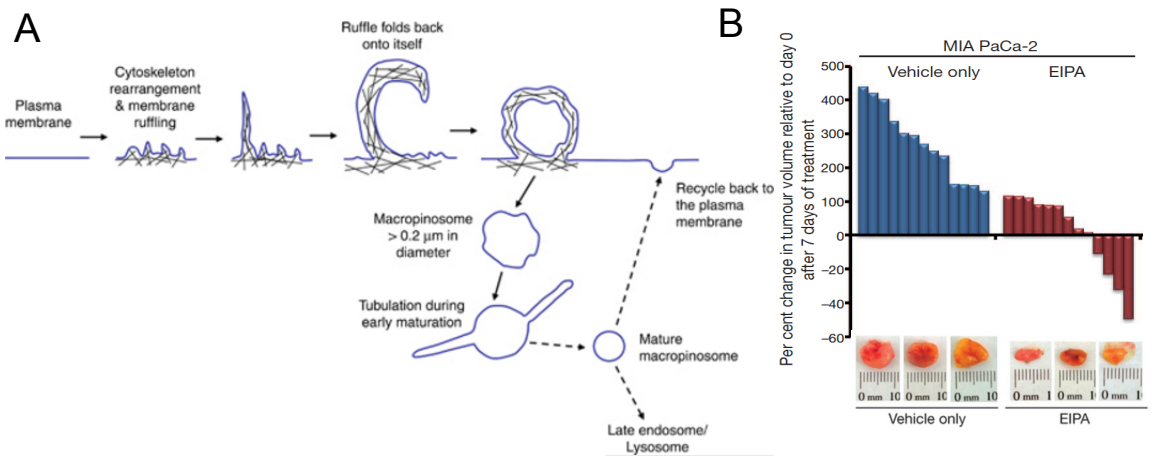

Figure 1.2. The macropinocytosis pathway and its role in tumorigenesis. A) Macropinocytosis involves actin-driven plasma membrane ruffling that leads to non-specific uptake of substrates from the extracellular environment. Macropinosomes formed undergo tubulation during early maturation to change their shape and size, followed by fusion with late endosomes/lysosomes for degradation or recycling of contents back to the plasma membrane. Figure adapted from (Lim and Gleeson, 2011) **B)** Xenografts of Ras-mutant pancreatic cancer cell line MIAPaca-2 in mice treated with macropinocytosis inhibitor EIPA show significantly reduced tumor growth compared to vehicle treated mice. Images at the bottom show the tumor sizes at day 7 of treatment. Figure adapted from (Commisso et al., 2013).

Interestingly, Ras-mutant and hypoxic cells can also scavenge serum lipids and fatty acids through direct import or macropinocytosis to support their growth and metabolism (Kamphorst et al., 2013). Inhibition of macropinocytosis by amiloride derivative EIPA is able to inhibit tumor growth *in vivo* in xenograft models of mutant Ras pancreatic cancer (Figure 1.2B), indicating its importance in tumorigenesis (Commisso et al., 2013). Intriguingly, macropinocytosis can also be utilized by certain amoebae like *Dictyostelium* in a Ras-dependent manner for feeding, suggesting a key evolutionary purpose of this pathway in nutrient scavenging (Chubb et al., 2000; Hoeller et al., 2013).

1.2.3 Phagocytosis

Phagocytosis is defined as the engulfment of large solid particles (>0.5um) like pathogens or dead cell corpses by professional phagocytes (macrophages, neutrophils, dendritic cells and other immune cells), non-professional phagocytes (epithelial cells, endothelial cells and fibroblasts) or unicellular protozoans like amoebae (Stefater et al., 2011). Phagocytic uptake involves recognition of signals on the cargo by cell-surface receptors in phagocytes (eg, phosphatidylserine during apoptotic corpse phagocytosis), that lead to Rac1/Actin-dependent engulfment of the cargo followed by lysosomal degradation (Figure 1.3) (Ravichandran and Lorenz, 2007).

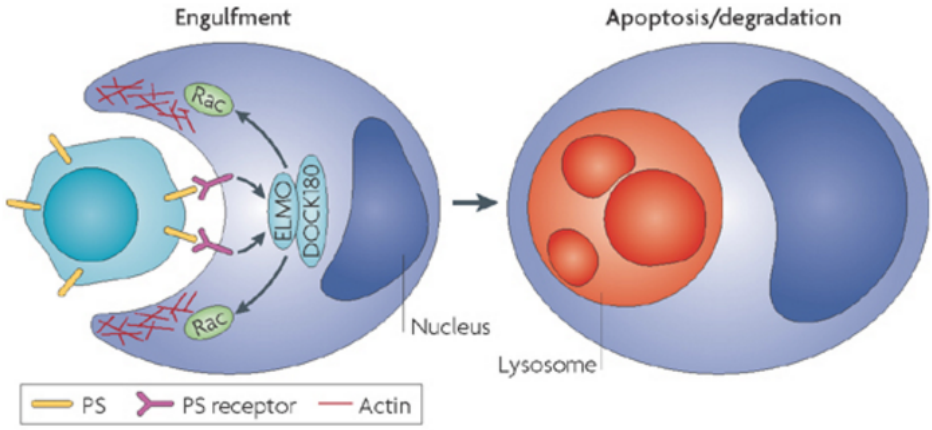

Figure 1.3. Phagocytosis of apoptotic corpses. Engulfment of apoptotic corpses involves recognition of phosphatidylserine expressed by the corpses by PS receptors on phagocytes, which signals to ELMO/DOCK180 complex to activate Rac1/actin signaling. Upon uptake, the corpse-containing phagosome undergoes endocytic maturation culminating with lysosomal degradation. Figure adapted from (Overholtzer and Brugge, 2008).

While phagocytosis in mammalian organisms is primarily required for immune functions including pathogen defense, antigen presentation, tissue homeostasis and inflammation, its evolutionary origin lies in its role for feeding and nutrient uptake in protozoans (Figure 1.4) (Stefater et al., 2011). Indeed,

phagocytosis of bacteria is the primary mechanism of obtaining nutrition in most species of amoebae like *Dictyostelium discoideum, Amoeba proteus* and *Naegleria fowleri* (Stefater et al., 2011).

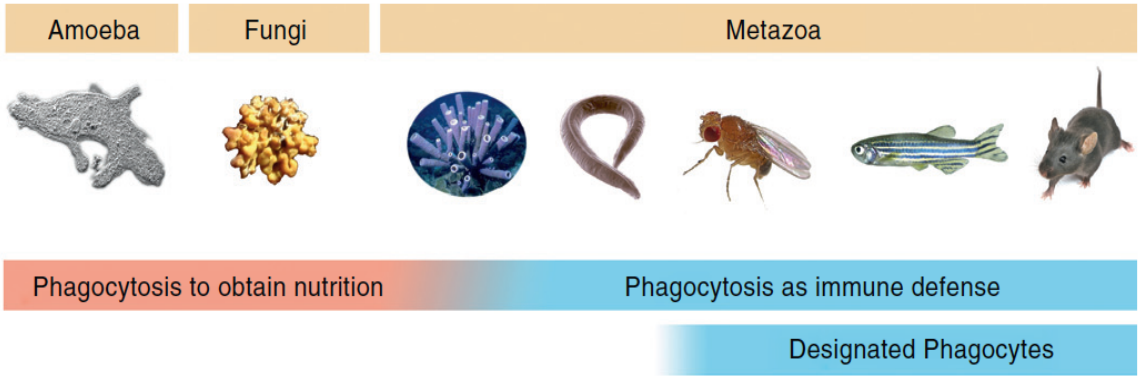

Figure 1.4. Evolutionary role of Phagocytosis. Phagocytosis is used by lower eukaryotes like amoeba primarily as a feeding mechanism to obtain nutrition from the environment. However, in metazoans the role of phagocytosis has evolved into an immune defense with specialized cells called phagocytes performing this function. Figure adapted from (Stefater et al., 2011).

Interestingly, recent studies have shown that phagocytosis of dead cells by mammalian macrophages can serve a similar purpose. Engulfment of apoptotic corpses can provide the engulfing macrophages with amino acids that can reactivate mTORC1 during starvation, suppress starvation-induced cell death and promote proliferation (Krajcovic et al., 2013). Thus, mammalian phagocytes retain this ancient function of phagocytosis and utilize it as an alternative source of nutrition during conditions of metabolic stress.

1.2.4 Cell Cannibalism and Entosis

While phagocytosis primarily involves uptake of pathogens or dead/dying cells, there is growing evidence that “live” cells can also be targeted for

engulfment in a process called cell cannibalism (Overholtzer and Brugge, 2008). Similar to phagocytosis, cell cannibalism is also observed in ancient protozoans as a nutrient scavenging strategy. A species of slime mold called *Dictyostelium caveatum*, when deprived of bacteria, cannibalizes other species of *Dictyostelium* to support its metabolism and survival (Waddell and Vogel, 1985). Indeed, during starvation conditions one *D. caveatum* cell can outcompete 1000 cells of other species by engulfing them piecemeal or in the form of whole cells (Waddell and Vogel, 1985). *Dictyostelium* also utilize cannibalism during their sexual life cycle, whereby the zygote formed after mating engulfs neighboring amoebae for either nutrient uptake or cell wall formation (Erdos et al., 1973). Thus ancient protozoans can utilize cell cannibalism as an important strategy for nutrient recycling to support growth during vegetative and sexual life cycles.

Cannibalism has also been reported in mammalian systems in the form of "cell-in-cell" structures, where a live cell is contained in a vacuole in the outer cell (Overholtzer and Brugge, 2008). These "cell-in-cell" structures have can either be heterotypic (between different cell types) or homotypic (between the same cell type). Most forms of heterotypic cannibalism occurs in the form of leukocytes engulfed into non-leukocyte hosts like hepatocytes, epithelial cells or tumor cells (Overholtzer and Brugge, 2008). Indeed it was recently shown that autoreactive T-cells are cannibalized by host hepatocytes *in vivo* and this process is required for preventing autoimmunity in mice (Benseler et al., 2011). Homotypic cannibalism on the other hand has been observed mostly in fluid exudates containing tumor cells or in primary tumors of breast cancer, colorectal cancer

and melanomas (Overholtzer and Brugge, 2008). Cell cannibalism can occur through phagocytic or non-phagocytic processes, and a mechanism for the latter has been demonstrated in a form of homotypic cell cannibalism called “entosis” (Overholtzer et al., 2007).

Live cell engulfment during entosis involves formation of E-cadherin dependent junctions between neighboring cells (Overholtzer et al., 2007). Intriguingly, there is a requirement of increased Rho-kinase activity in the cell being internalized suggesting an active role of the cell in its own engulfment (Overholtzer et al., 2007). After engulfment, the inner cell can undergo a variety of cell fates like release, division or death, with cell death being the most common (Figure 1.5).

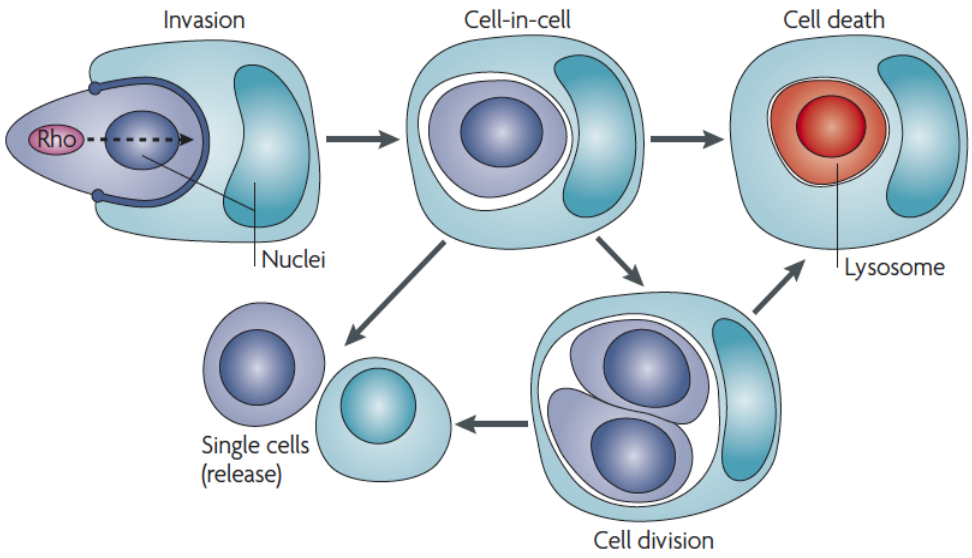

Figure 1.5. Cell fates of cells cannibalized by Entosis. Cells with high Rho-kinase activity are engulfed neighboring cells to form cell-in-cell structures. The engulfed inner cell can have a wide variety of cell fates – they can either be released back into the environment, undergo cell division, or undergo cell death. Most internalized cells undergo cell death in a non-apoptotic manner where the lysosomes of the outer cell fuse to the entotic vacuole thereby killing and degrading the inner cell. Figure adapted from (Overholtzer et al., 2007).

Entotic cell death occurs in a similar fashion to phagosome maturation, where lysosomes from the outer cell fuse to the vacuole to deliver the cathepsin proteases and other degradative enzymes that kill and degrade the inner cell (Florey et al., 2011). Entotic cell corpses can also provide the engulfing cells with nutrients that can reactivate mTORC1 signaling and support their proliferation in starvation conditions. Interestingly, the presence of an entotic vacuole prevents the formation of a cleavage furrow during mitosis of the engulfing cell, leading to increased aneuploidy in populations that undergo entosis (Krajcovic et al., 2011). The generation of aneuploidy and the ability of cells to scavenge nutrients during metabolic stress suggest a pro-survival and potentially pro-tumorigenic role of entosis in cell populations.

1.2 LYSOSOME AS A NUTRIENT SENSING AND SIGNALING HUB

During the above-mentioned engulfment pathways, the cargo containing vacuole undergoes a series of sequential maturation events involving phosphorylation of phosphatidylinositol to form phosphatidylinositol-3-phosphate, recruitment of early endosome marker Rab5, lipidation of autophagy protein LC3, and recruitment of late endosomal/lysosome markers Rab-7 and LAMP1, all of which ultimately lead to lysosome fusion (Florey et al., 2011). The large lysosomal compartments formed degrade the exogenous cargo into nutrients like amino acids, glucose, lipids and nucleic acids. While lysosomes have long been considered to be the terminal degradative stages of maturation, in the recent

years they have also emerged as a major nutrient sensing and signaling hub in the cell (Efeyan et al., 2012). The nutrient responsive kinase mTORC1 localizes to lysosomal membranes to be activated in response to amino acids (Sancak et al., 2008). Amino acids in the lysosome and the cytosol signal to Rag GTPases present on the lysosomal membrane, which recruit mTORC1 by binding to its component Raptor (Figure 1.6A) (Sancak et al., 2008). This recruitment is critical for mTORC1 interaction with its activator Rheb, which is also localized at late endosomes/lysosomes. During amino-acid starvation, mTORC1 falls off from the lysosomes and can no longer interact with Rheb, leading to its inactivation (Sancak et al., 2008). However, as mentioned previously the engulfment and digestion of extracellular cargo is able to provide amino acids activate mTORC1 during starvation, since mTOR can now be recruited to these nutrient rich compartments (Figure 1.6B) (Krajcovic et al., 2013).

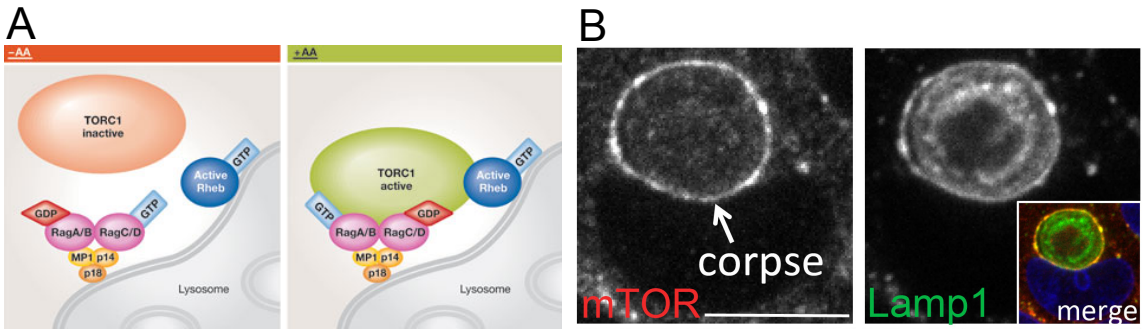

Figure 1.6. mTORC1 signaling at lysosomes. A) In amino acid free conditions, the mTORC1 complex resides in the cytosol in an inactive state. The machinery required for activating mTORC1 is present at the lysosomal membranes. In the presence of amino acids, the p18/MP1/p14 Ragulator, RagA/B and RagC/D complex recruits mTORC1 to the lysosome where it can interact with its Rheb for its activation. Figure adapted from (Duran and Hall, 2012) **B)** mTOR (left panel) can be recruited to lysosomal compartments (LAMP1 lysosome marker, right panel) containing entotic corpses in amino acid free conditions due to corpse degradation and amino acid recovery. Figure adapted from (Krajcovic et al., 2013).

These studies have established that lysosomes act as a critical nutrient signaling hub, whose function is required not only for amino acid sensing and cell signaling but also for nutrient recycling and cell survival during scavenging of extracellular macromolecules. Given its key functions in nutrient trafficking, it is imperative to understand lysosome biology and function during uptake of exogenous cargo. While much work has been done to understand the upstream events during engulfment, the late stages that regulate vacuole maturation post-lysosome fusion and their impact on nutrient trafficking and cell survival are largely unclear with only a few contemporary studies exploring this new field.

1.3 LARGE LYSOSOMAL VACUOLES UNDERGO MTORC1-DEPENDENT MEMBRANE FISSION

A recent study has demonstrated that the large lysosomal compartments formed during entosis and phagocytosis undergo a process of membrane fission that shrinks their size as the engulfed cargo is degraded. This process of vacuole fission is regulated by mTORC1 that is localized on the vacuole membranes, and results in redistribution of the degraded cargo throughout the lysosome network of the engulfing cell (Figure 1.7) (Krajcovic et al., 2013).

Interestingly, a similar process is known to occur during autophagy termed “autophagic lysosome reformation” (ALR), where during long term starvation larger-than-normal autolysosomes undergo tubulation and membrane budding that resets the original lysosome size and number in the cell (Yu et al., 2010). ALR is also regulated by mTORC1 kinase that is reactivated during long-term starvation due to nutrient recovery from autolysosomes (Yu et al., 2010).

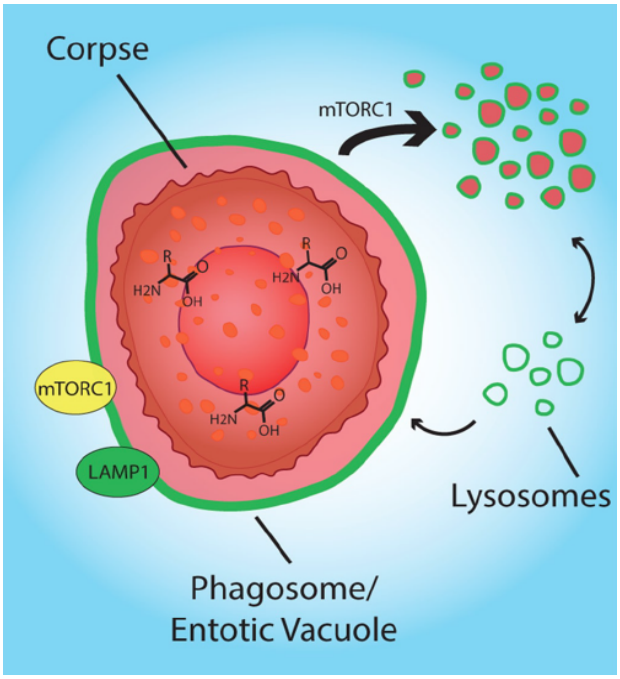

Figure 1.7. mTORC1 regulates entotic vacuole and phagosome fission. The large lysosomal compartments formed during entosis and phagocytosis undergoes a process of membrane fission that shrinks the vacuole size while the cargo is degraded. mTORC1 localizes to these lysosomal compartments and regulates this process of vacuole fission. Fusion of lysosomes to the main vacuole or the vesicles formed through fission helps in redistribution of the cargo into the lysosome network of the engulfing cell. Figure adapted from (Krajcovic et al., 2013).

It has also been shown that TORC1 mediates fission of the yeast vacuole (lysosomal compartment), which could be responsible for nutrient status-dependent changes in yeast vacuole size (Michaillat et al., 2012). These reports demonstrate an evolutionary role for mTORC1 in vacuole fission and lysosome trafficking in response to nutrient stress.

Given that mTORC1 can be activated by amino acids derived from the degrading cargo, it is perhaps uniquely suited to act as a regulator of maturation and fission of the cargo-containing vacuoles. However, there are no other known regulators of vacuole fission during macroendocytic pathways. Also, the consequences of vacuole fission on lysosomal nutrient export and other cellular processes are relatively unexplored.

1.4 THESIS AIMS

While mTORC1 has been demonstrated to play a key role in membrane fission, to date there are no other known regulators of this novel stage of vacuole maturation. Moreover, the functional connection between vacuole fission and nutrient recovery from these compartments, particularly during starvation conditions, remain poorly understood. Further downstream consequences of these processes on different cellular pathways and cell fate decisions are also unexplored.

My thesis aims to identify novel regulators of vacuole fission and nutrient recovery during engulfment. In Chapter 2, we identify the kinase PIKfyve as a critical regulator of vacuole fission during macropinocytosis, phagocytosis and entosis. We demonstrate that PIKfyve regulates fission in an mTORC1-independent manner, functioning in part through the lysosomal cation channel TRPML1. We also demonstrate that PIKfyve plays a key role in regulating nutrient export from the cargo-containing vacuoles, which is critical for supporting the survival and proliferation of the engulfing phagocytes as well as mutant Ras tumor cells.

In Chapter 3, we identify a critical role for PIKfyve in regulating the cholesterol exit from lysosomal membranes, which is required for maintaining intracellular cholesterol levels. We demonstrate that PIKfyve-dependent cholesterol egress from lysosomes plays a key role in maintaining lysosome size and morphology. We also find that PIKfyve regulates the partitioning of lysosomal

membrane proteins into distinct microdomains that resemble cholesterol-rich lipid domains.

In Chapter 4, we explore the unanswered questions raised by the studies described in this dissertation, which include the potential mechanism of PIKfyve-dependent fission and nutrient recovery. In addition, potential roles of these PIKfyve-dependent processes in lipid-raft partitioning, cell signaling and its consequences on immune functions like antigen presentation or disease states like tumorigenesis are also discussed.

CHAPTER 2: PIKfyve regulates vacuole fission and nutrient recovery during engulfment

2.1 INTRODUCTION

We have shown that maturation of macroendocytic vacuoles after lysosome fusion involves membrane fission that shrinks their size as the engulfed material is degraded. At least one mechanism of vacuole shrinkage is regulated by mTORC1 that localizes to vacuole membranes, and results in redistribution of engulfed material throughout endosome/lysosome networks (Krajcovic et al., 2013). In order to explore further how the contents of macroendocytic vacuoles are processed and utilized, we sought to identify other regulators of vacuole dynamics. For example, mTORC1 activity and localization has been shown to be regulated by PIKfyve, a lipid kinase that catalyzes the conversion of PI and PI(3)P into PI5P and PI(3,5)P2 respectively (Bridges et al., 2012; Sbrissa et al., 1999). PIKfyve loss-of function is known to lead to enlargement of late endosomal/lysosomal vesicles, and occurs primarily due to PI(3,5)P2 depletion in the cell (Ikonomov et al., 2001; Nicot et al., 2006; Shisheva, 2001).

PI(3,5)P2 synthesis and turnover is tightly regulated by a multiprotein "PAS" complex containing PIKfyve, its scaffolding agent ArPIKfyve/Vac14, and the antagonistic phosphatase Sac3/Fig4, and their loss-of-function leads to disruption of PI(3,5)P2-dependent cellular functions (Sbrissa et al., 2008; Sbrissa et al., 2007). This pathway plays a key role during development, as

deletions of the PAS complex cause early embryonic lethality in all model organism systems (Shisheva, 2012). The PAS complex, in particular PIKfyve, is also implicated in various disease states including diabetes, neurodegenerative diseases, cancer and microbial pathogenesis (Shisheva, 2012).

A recent study reported that PIKfyve regulates the activation of mTORC1 in adipocytes in response to amino acid or insulin stimulation due to PI(3,5)P2 binding to the WD40 domain of Raptor from the mTORC1 complex and altering its cellular localization (Bridges et al., 2012). While PIKfyve is known to function in the endocytic pathway, how it might regulate the membrane dynamics of macroendocytic vacuoles containing engulfed cargo is unknown. Given that it controls mTORC1 activity and that mTORC1 controls vacuole fission, we investigate the possibility that PIKfyve may also regulate vacuole dynamics, the redistribution of engulfed cargo and cytosolic uptake of nutrients that accumulate in lysosomes following degradation of engulfed cells and macromolecules.

2.2 RESULTS

2.2.1 PIKfyve regulates entotic vacuole, phagosome and macropinosome shrinkage *in vitro* and *in vivo*.

As PIKfyve is reported to maintain lysosome morphology and support mTORC1 activity, we hypothesized that it might regulate the redistribution of the contents of large lysosomal vacuoles that are formed during cell engulfment. To investigate if PIKfyve contributes to resolving the large lysosomal vacuoles that form as a result of the live cell engulfment mechanism entosis, we treated cells with two inhibitors of PIKfyve kinase activity, YM201636 (YM201) (Jefferies et al., 2008) and Apilimod (Cai et al., 2013), and monitored the size of entotic vacuoles through time using H2B-mCherry fluorescence derived from engulfed cells, as we reported previously (Krajcovic et al., 2013). Whereas entotic vacuoles in vehicle-treated MCF10A or HEK-293 cells reduced in size over time as cell corpses were degraded, vacuoles within PIKfyve-inhibited cells failed to shrink over 20 hours, despite the degradation of corpses observed by DIC imaging (Figure 2.1A,B,C). Likewise, the knockdown of PIKfyve expression with two independent shRNAs also slowed vacuole shrinkage (Figure 2.1D). Together, these data indicate a role for PIKfyve in this late stage of vacuole maturation. We also quantified the presence of mCherry-positive vesicles in the cytoplasm of corpse-containing cells, which we have measured previously as a readout of membrane fission (Krajcovic et al., 2013). PIKfyve inhibition significantly reduced the percentage of cells accumulating mCherry vesicles, suggesting that PIKfyve is required in part

to initiate the redistribution of accumulated lysosomal contents back into the endosome network (Figure 2.1E,F).

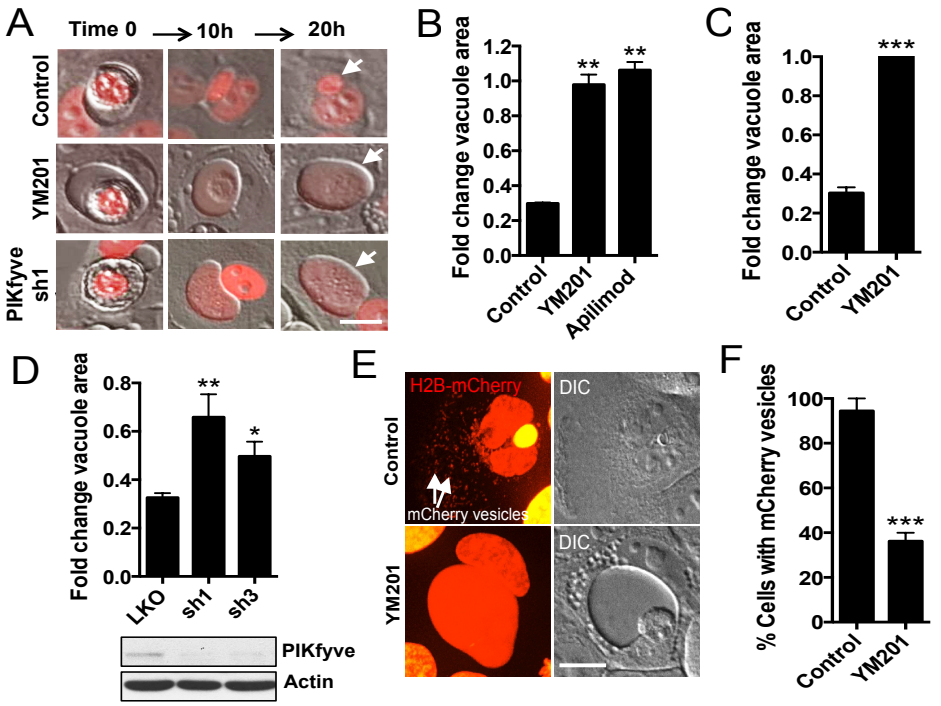

Figure 2.1: PIKfyve regulates vacuole shrinkage and fission during entosis.
A) Entotic vacuoles in MCF10A cells undergo PIKfyve-dependent shrinkage. Images show representative entotic vacuoles containing engulfed cell corpses in control and PIKfyve-inhibited cells (YM201 treatment, middle panels; shRNA knockdown, bottom panels). Note that vacuoles in PIKfyve-inhibited cells fail to shrink over 20 hours despite the degradation of cell corpses (arrows). **B)** Treatment with PIKfyve inhibitors (YM201 and Apilimod) delays entotic vacuole shrinkage. Graph shows fold change in area of entotic vacuoles after 10 hours for control and PIKfyve-inhibited cells as determined by time-lapse microscopy. Total cell number analysed for control n=168, YM201 n=119, Apilimod n=86. **C)** PIKfyve inhibition delays entotic vacuole shrinkage in HEK-293 cells. Graph shows fold change in entotic vacuole area after 10 hours for control and PIKfyve-inhibited cells, determined by time-lapse microscopy. Total cell number analysed for Control n=63, YM201 n=59. **D)** shRNA-mediated PIKfyve knockdowns delay entotic vacuole shrinkage in MCF10A cells. Graph shows quantification of vacuole shrinkage after 10 hours, western blot shows PIKfyve expression in control and knockdown cells. Total cell number analysed for LKO n=131, sh1 n=56, sh3 n=84. **E)** mCherry fluorescence from entotic corpses (H2B-mCherry-expressing MCF10A cells) appears in vesicles in the cytoplasm of control cells (H2B-mCherry, left top panel, arrows; DIC right top panel) as a result of fission, which is blocked in PIKfyve-inhibited cells (bottom panel). **F)** PIKfyve inhibition reduces the appearance of vacuole-derived mCherry vesicles in the cytoplasm of engulfing cells. Graph shows quantification of percentage of entotic corpses in MCF10A cells containing mCherry vesicles after 10 hours in control and PIKfyve-inhibited conditions. Total cell number analysed for Control n=18, YM201 n=17. Error bars show mean±SEM for n=3 independent experiments unless otherwise specified. Scale bars equal 10μm

We next sought to determine if PIKfyve might play a similar role to regulate the resolution of large lysosomal compartments resulting from apoptotic cell phagocytosis. We examined phagosomes in J774.1 macrophages incubated with H2B-mCherry labeled apoptotic corpses. Like entotic vacuoles, apoptotic corpse-containing phagosomes in PIKfyve-inhibited cells exhibited decreased rates of vacuole shrinkage compared to controls, despite the degradation of ingested apoptotic corpses (Figure 2.2A,B).

To further extend these findings to an *in vivo* system, we examined the requirement of the PIKfyve ortholog *ppk-3* for apoptotic phagosome shrinkage during *C. elegans* embryogenesis, where phagocytosis is well known to clear cells that undergo developmentally programmed apoptosis. Using *C. elegans* embryos co-expressing H2B::mCherry and PIP2::GFP in strain *OD95* (Green et al., 2011; McNally et al., 2006), we quantified the shrinkage of phagosomes (indicated by mCherry fluorescence), after the completion of engulfment (indicated by loss of PIP2::GFP from phagosome membranes) (Figure 2.2C,D). Consistent with our *in vitro* studies, *ppk-3* mutant embryos (Nicot et al., 2006) showed significantly decreased rates of phagosome shrinkage compared to wild-type embryos (Figure 2.2C,D).

Finally, to investigate if PIKfyve regulates macropinosome maturation, we monitored macropinosomes in macrophages incubated with fluorescent dextran by time lapse-imaging. Nascent macropinosomes were observed to undergo fusion with lysosomes as measured by co-staining with lysotracker (data not shown), and then rapidly shrink in size over time (Figure 2.3A).

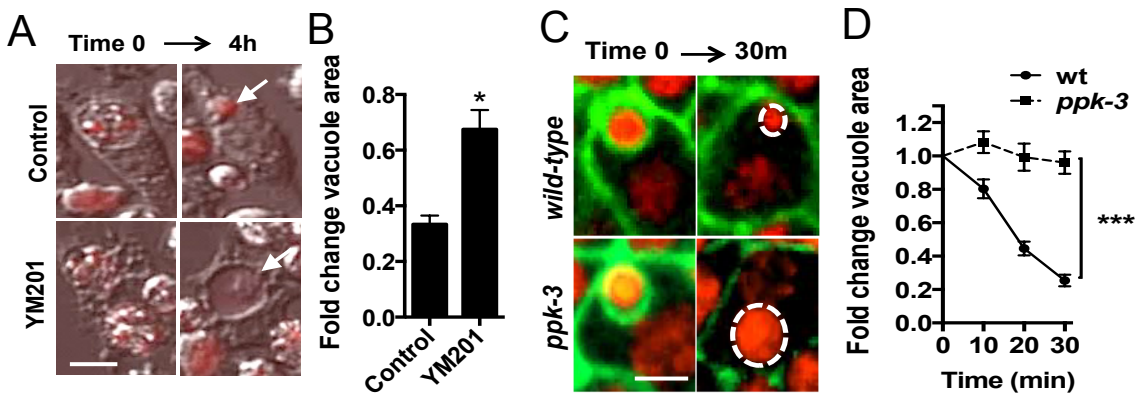

Figure 2.2. PIKfyve regulates phagosome shrinkage *in vitro* and *in vivo*.
A) Apoptotic cell phagosomes undergo PIKfyve-dependent shrinkage in macrophages. Images show representative apoptotic cell phagosomes in control and PIKfyve-inhibited J774.1 mouse macrophages. Note that the PIKfyve-inhibited phagosome (bottom panel, arrow) fails to shrink over 4 hours despite degradation of the engulfed apoptotic corpse. **B)** Treatment of J774.1 macrophages with the PIKfyve inhibitor YM201 delays apoptotic phagosome shrinkage. Graph shows fold change in area of phagosomes after 4 hours. Total cell number analysed for Control n=103, YM201 n=92. **C)** *ppk3* (PIKfyve ortholog) controls phagosome shrinkage during *C. elegans* development. Images show H2B-mCherry and PIP2-GFP fluorescence during apoptotic cell phagocytosis. Note that the *wild-type* phagosome (top panel, circle) undergoes rapid shrinkage while the phagosome in a *ppk3* mutant embryo (bottom panel, circle) shows delayed shrinkage. **D)** Quantification of fold change in area of apoptotic phagosomes, 30 minutes after engulfment in *wild-type* and *ppk3* mutant *C. elegans* embryos, as determined by time-lapse microscopy. Error bars show mean±SEM for n=7 embryos.

The inhibition of PIKfyve blocked the ability of macropinosomes to shrink after lysosome fusion, consistent with the function of PIKfyve in vacuole shrinkage during entosis and phagocytosis (Figure 2.3A,B). We further observed transient recruitment of PIKfyve-eGFP onto macropinosomes as they underwent shrinkage in HEK293 cells (Figure 2.3C,D). PIKfyve inhibition by treatment with YM201 prolonged the association of PIKfyve with macropinosomes, whose sizes remained unchanged over time (Figure 2.3C,D). Taken together, these data demonstrate that PIKfyve controls the maturation of entotic vacuoles, phagosomes and macropinosomes, by functioning at a post-lysosome fusion stage.

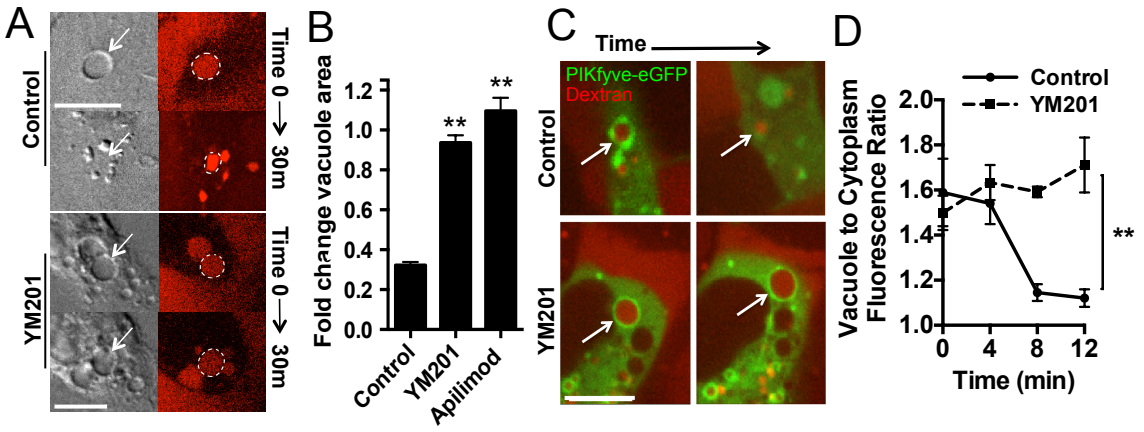

Figure 2.3. PIKfyve regulates macropinosome shrinkage.
A) Images show TMR-Dextran fluorescence from engulfed macropinosomes in J774.1 macrophages. Note that macropinosomes in control, untreated cells (top panels, left DIC white arrows, right Dextran white circles) undergo rapid shrinkage by 30 minutes, whereas in PIKfyve inhibited cells (YM201-treated, bottom panels, left DIC white arrows, right Dextran white circles) macropinosomes fail to shrink. **B)** PIKfyve inhibitors YM201 and Apilimod delay macropinosome shrinkage. Graph shows quantification of fold change in macropinosome area after 30 minutes in control, YM201 and Apilimod treated J774.1 macrophages, measured by confocal time-lapse microscopy. Total cell number analysed for Control n=10, YM201 n=10, Apilimod n=10. **C)** PIKfyve localizes to macropinosomes. Images show PIKfyve-eGFP recruitment to dextran-containing macropinosomes in HEK293 cells. Recruitment occurs in a transient manner in control cells (top panel, arrow), and in a prolonged manner in PIKfyve-inhibited cells (bottom panel, arrow). **D)** PIKfyve localizes to macropinosomes transiently in control vacuoles and in a prolonged manner in YM201 treated cells. Graph shows ratio of fluorescence intensity of PIKfyve-eGFP on the macropinosome vacuole vs cytoplasm in control and YM201 treated cells. Control n=3 and YM201 n=3 cells. For all graphs, error bars show mean±SEM for n=3 independent experiments unless otherwise mentioned. *p<0.05, **p<0.02 (Student's t-test). Scale bars equal 10μm.

2.2.2 PIKfyve controls vacuole shrinkage independent of upstream endocytic functions

As PIKfyve has been suggested to play various roles in lysosome physiology (de Lartigue et al., 2009; Ikonomov et al., 2001, 2006; Jefferies et al., 2008; Kerr et al., 2010; Kim et al., 2014; Nicot et al., 2006; Rusten et al., 2006; Sbrissa et al., 2007), we next examined if PIKfyve might also regulate earlier steps in delivery of extracellular cargo to lysosomes. During entotic cell death, the endosomes containing engulfed cells undergo sequential steps of maturation

involving phosphorylation of phosphatidylinositol to form phosphatidylinositol-3-phosphate, lipidation of autophagy protein LC3, and recruitment of late endosomal marker Rab-7, all of which appeared unperturbed by PIKfyve inhibition (Figure 2.4A,B). During entosis, these upstream maturation events are important for the fusion of lysosomes to entotic vacuoles, which triggers the death of internalized cells (Florey et al., 2011). We found that recruitment of the lysosomal marker Lamp1 (Figure 2.4B), and the rate of entotic cell death (Figure 2.4C) were not significantly altered by PIKfyve inhibition, consistent with normal upstream vesicle-to-lysosome maturation. We also noted by DIC imaging that PIKfyve-inhibited cells appeared to degrade entotic cell corpses with kinetics similar to control cells, even though the large vacuoles failed to undergo fission (Figure 2.1A).

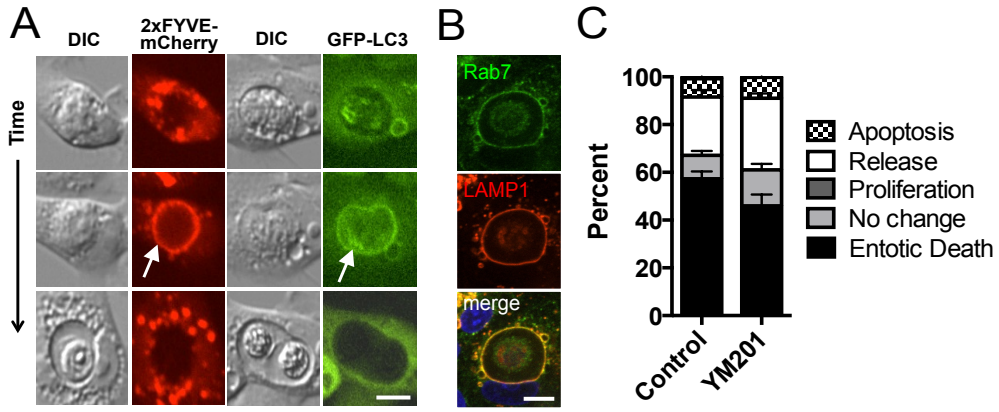

Figure 2.4. PIKfyve does not affect upstream entotic vacuole maturation.A) PIKfyve inhibition has no effect on upstream PI3P formation and LC3 recruitment to the entotic vacuoles. PI3P reporter 2xFYVE-mCherry (DIC first panel, 2xFYVE-mCherry in red second panel, arrow) and GFP-LC3 (DIC third panel, GFP-LC3 in green fourth panel, arrow) localize to entotic vacuoles in PIKfyve-inhibited MCF10A cells. **B)** PIKfyve inhibition has no effect on recruitment of Rab7 (green, top panel) and Lamp1 (red, middle panel) in PIKfyve-inhibited MCF10A cells. **C)** PIKfyve inhibition has no effect on internalized cell fate during entosis. Graph shows quantification of cell fate as entotic death, no change, proliferation, release and apoptosis in control and PIKfyve-inhibited MCF10A cells. Error bars show mean±SEM for n=6 independent experiments. Total cell number analysed for Control n=387, YM201 n=426. No significant differences in cell fate between control and PIKfyve-inhibited cultures were observed. Scale bars equal 10μm.

To examine the effects of PIKfyve inhibition during apoptotic corpse engulfment in macrophages, we investigated acidification and cathepsin protease activity through lysotracker and DQ-BSA staining. Apoptotic phagosomes showed lysotracker and DQ-BSA-positive staining in both control and PIKfyve-inhibited macrophages, consistent with normal acidification and degradative capacity (Figure 2.5A). In contrast, treating cells with the acidification inhibitor Concanamycin A (ConA) effectively prevented lysotracker and DQ-BSA staining (Figure 2.5A). To further monitor the phagocytic engulfment and degradation of apoptotic cells by macrophages, we examined the accumulation of corpse-derived mCherry protein, which is generated by the degradation of ingested H2B-mCherry-expressing apoptotic cells (Krajcovic et al., 2013). mCherry accumulation occurred with similar kinetics in control and PIKfyve-inhibited cells, but was blocked by ConA (Figure 2.5B), consistent with normal phagocytosis and lysosomal degradation of apoptotic cells in PIKfyve-inhibited macrophages.

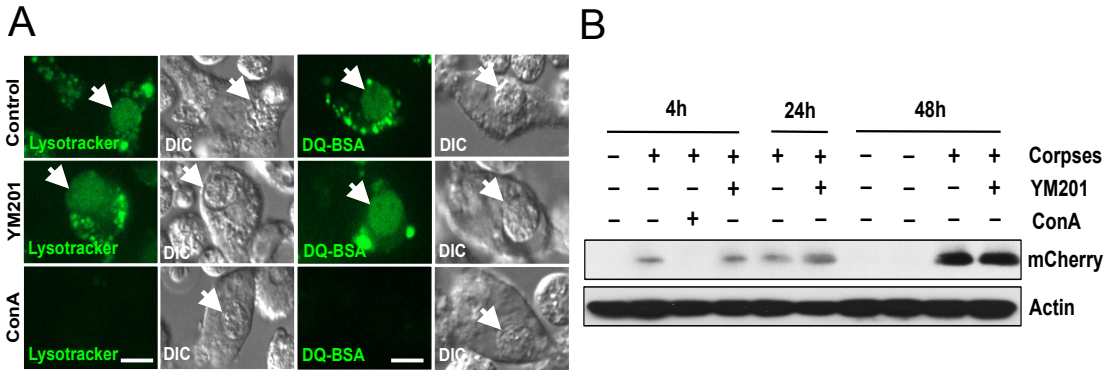

Figure 2.5. PIKfyve does not affect phagosome maturation and degradation.
A) PIKfyve inhibition has no effect on lysotracker positivity (Left panel, Green, DIC, arrow) and DQ-BSA fluorescence (Right panel, Green, DIC, arrow) in J774.1 macrophage phagosomes. Note that lysotracker and DQ-BSA fluorescence are blocked by treatment with Concanamycin A (ConA) (bottom panel). Scale bars equal 10μm. **B)** PIKfyve inhibition has no effect on apoptotic corpse degradation in J774.1 macrophages. Western blot shows kinetics of mCherry derived from digestion of H2B-mCherry of apoptotic corpses at 4 hours, 24 hours and 48 hours, in the presence or absence of YM201 and ConA.

To further address the role of PIKfyve in an experimental system where corpse degradation can be bypassed (Krajcovic et al., 2013), we blocked entotic vacuole shrinkage by treating nutrient-replete cells with the mTOR kinase inhibitor Torin1, until engulfed cell corpses were visibly digested as determined by DIC microscopy (after 16 hours), but vacuoles were still large and intact. We then washed out Torin1 and observed the vacuolar dynamics in the presence or absence of PIKfyve inhibition. While control vacuoles underwent rapid shrinkage after Torin1 washout, PIKfyve inhibition significantly delayed shrinkage (Figure 2.6A,B). Altogether these data support a model where PIKfyve regulates the ability of cells to clear large lysosomal vacuoles independently of the ability of lysosomal proteases to degrade engulfed material.

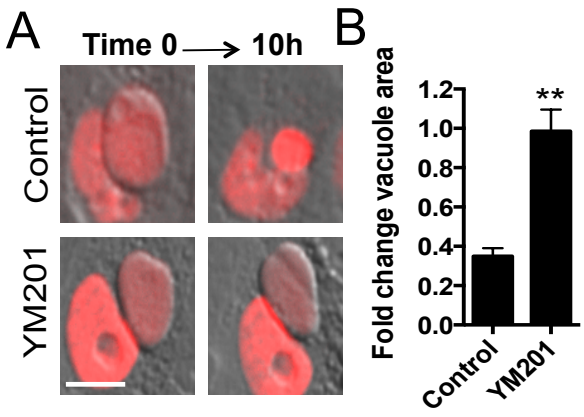

Figure 2.6. PIKfyve regulates vacuole fission downstream of corpse degradation. **A)** Entotic vacuoles in H2B-mcherry expressing MCF10A cells with digested corpses generated by 16h pre-treatment with Torin1 undergo rapid shrinkage in control cells (upper panel), which is blocked in PIKfyve-inhibited cells (bottom panel). Scale bars equal 10μm. **B)** PIKfyve inhibition blocks the shrinkage of vacuoles resulting from prior mTOR inhibition. Graph shows fold change in area of vacuoles pre-treated with Torin1, and then subjected to Torin1 washout and treatment with vehicle control or YM201 for 10 hours. Error bars show mean±SEM for n=3 independent experiments. Total cell number analysed for Control n=74, YM201 n=80.

2.2.3 PIKfyve regulates vacuole fission in an mTORC1-independent manner

We next examined how PIKfyve regulates vacuole shrinkage by interrogating potential downstream effectors. Given the reported role of PIKfyve in supporting mTORC1 activity, and the role of mTORC1 in lysosome fission, we determined the effects of PIKfyve inhibition on mTORC1 activity and localization (Bridges et al., 2012). Both MCF10A cells and J774.1 macrophages cultured in amino acid-free media or treated with Torin1 showed a loss of mTORC1 activity, as monitored by threonine 389 phosphorylation of its downstream target, S6-ribosomal protein kinase (pS6K) (Figure 2.7A,C). In contrast, when PIKfyve was inhibited, both cell types exhibited normal pS6K levels in nutrient-replete media (Figure 2.7A,C). PIKfyve inhibition also had no effect on the reactivation of mTORC1 by amino acids in starved cells (Figure 2.7B,D). We have shown previously that mTOR localizes to corpse-containing lysosomal compartments (Krajcovic et al., 2013), and mTOR co-localization to entotic vacuoles and phagosomes was also unaffected by PIKfyve inhibition (Figure 2.7E,F). These data suggest that PIKfyve does not function upstream of mTORC1 to regulate vacuole shrinkage.

2.2.4 PIKfyve regulates vacuole shrinkage in part through the PI(3,5)P2 effector TRPML1

Since PIKfyve does not function through mTORC1, we investigated the role of effectors of the lipid product generate by PIKfyve kinase activity PI(3,5)P2. PI(3,5)P2 is reported to have three primary effectors in mammalian systems:

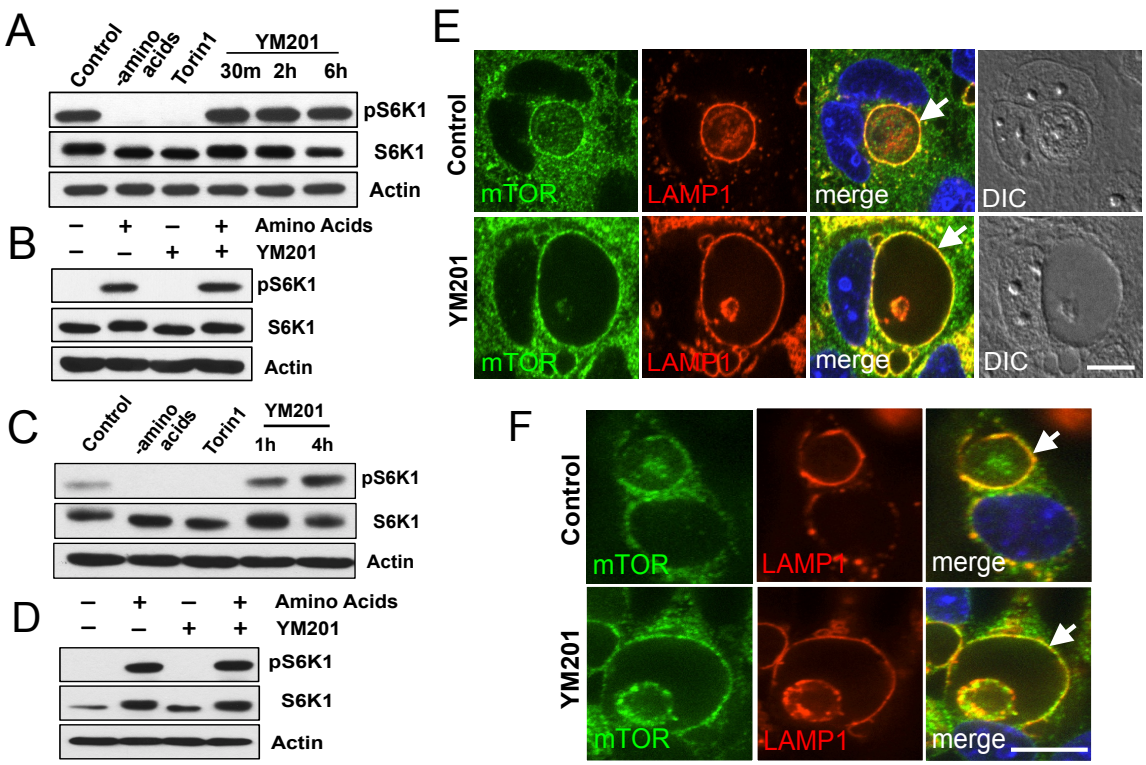

Figure 2.7. PIKfyve regulates vacuole shrinkage through TRPML1 in an mTORC1-independent manner. A) mTORC1 activity in cells cultured in full media is not affected by PIKfyve inhibition. Western blot of MCF10A cell lysates shows phosphorylation of the mTORC1 target S6-kinase threonine 389 (pS6K) in full media (Control), amino-acid starved, Torin1-treated, and YM201-treated conditions, as indicated. PIKfyve inhibition by YM201 treatment for 30 minutes, 2 hours or 6 hours does not affect pS6K levels. **B)** mTORC1 stimulation by amino acids is not affected by PIKfyve inhibition. Western blot shows pS6K levels in amino acid-starved and restimulated MCF10A cells in the presence and absence of YM201. **C)** mTORC1 activity in full media is not affected by PIKfyve inhibition in macrophages. Western blot from J774.1 cell lysates shows phosphorylation of mTORC1 target S6-kinase threonine 389 (pS6K) in full media, amino acid-starved, mTOR-inhibited (Torin1), and PIKfyve-inhibited (YM201) conditions, as indicated. Note that PIKfyve inhibition for 1 hour or 4 hours does not reduce pS6K levels. **D)** mTORC1 reactivation by amino acids is not affected by PIKfyve inhibition. Western blot of J774.1 lysates shows restimulation of pS6K in amino acid-starved cells, by refeeding with full media for 4 hours, in the presence or absence of YM201. Note that PIKfyve inhibition does not block pS6K restimulation. **E)** mTOR localization onto entotic vacuoles in MCF10A cells is not affected by PIKfyve inhibition. Top, mTOR (green) is recruited to a corpse-containing entotic vacuole (arrow), where it colocalizes with Lamp1 (red). Bottom, treatment with the PIKfyve inhibitor YM201 for 18 hours does not inhibit mTOR colocalization with Lamp1 on entotic vacuole (arrow). **F)** mTOR localization on apoptotic phagosomes is not affected by PIKfyve inhibition. Top panels, mTOR (green) is recruited to apoptotic phagosome where it colocalizes with Lamp1 (red) in J774.1 macrophages. Bottom panels, PIKfyve inhibition for 4 hours has no effect on mTOR localization to Lamp1-positive phagosome (arrow). Scale bars equal 10μm.

lysosomal cation channel TRPML1/MCOLN1, autophagy proteins WIPI1/2 (the mammalian homolog of yeast effector Atg18), and actin (Dong et al., 2010; Dove et al., 2004; Hong et al., 2015). We performed shRNA-mediated knockdowns of WIPI1 and WIPI2 and did not observe any effect on vacuolar shrinkage (Figure 2.8A,B,C). And while PIKfyve inhibition led to an accumulation of actin on entotic vacuoles, inhibition of actin by treatment with Latrunculin B had no effect to rescue fission in PIKfyve-inhibited cells, suggesting that actin regulation downstream of PIKfyve is also not related to vacuole shrinkage (Figure 2.8D,E).

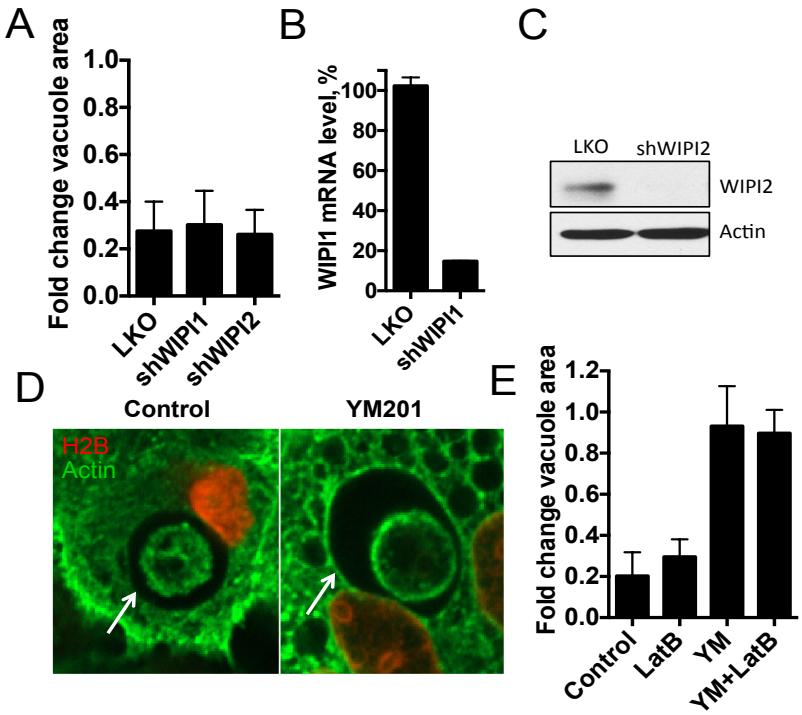

Figure 2.8 PI(3,5)P2 effectors WIPI1,WIPI2, and actin do not regulate vacuole shrinkage. A) shRNA mediated knockdowns of WIPI1 and WIPI2 do not inhibit entotic vacuole shrinkage in MCF10A cells. Graph shows fold change in entotic vacuole area after 10 hours in control and knockdown cells. **B)** Fold knockdowns of WIPI1 expression by the shRNA from A, determined by quantitative RT-PCR. **C)** Western blot shows WIPI2 expression in control and knockdown cells from A. **D)** Treatment of MCF10A cells with PIKfyve inhibitor YM201 leads to accumulation of actin at entotic vacuoles (arrow, right image). Green = immunostaining for Actin. **E)** Treatment of cells with latrunculin B does not rescue vacuole shrinkage in PIKfyve-inhibited cells. Graph shows fold change in entotic vacuole area after 10 hours in control and knockdown cells. Error bars show mean±SD,. Graphs are representative of independent experiments.

TRPML1 has been shown to bind PI(3,5)P2, the lipid product of PIKfyve, to regulate lysosome function, and its mutation underlies the lysosome storage disorder Mucolipidosis IV (Dong et al., 2010; Sun et al., 2000). To examine the role of TRPML1 in vacuole shrinkage, we utilized a previously reported pharmacological inhibitor ML-SI3 (Samie et al., 2013) to acutely inhibit TRPML-1 function. As shown in Figure 2.9A, treatment of cells with ML-SI3 significantly delayed the shrinkage of macropinosomes, demonstrating that TRPML-1 is required for macropinosome maturation in a similar manner to PIKfyve. We also generated shRNA-mediated knockdowns of TRPML1, which led to a slight but reproducible delay in vacuole shrinkage during entosis (Figure 2.9B,C). However, TRPML1 shRNA also affected corpse degradation (data not shown), suggesting that TRPML1 could be required for general lysosome function. In order to further examine a role for TRPML1 downstream of PIKfyve in regulating vacuole shrinkage, we hypothesized that overexpressing the channel might rescue the effects of PIKfyve inhibition, similar to what has been shown for other endosomal compartments (Dong et al., 2010). Indeed, upon treatment with PIKfyve inhibitors, vacuole shrinkage was rescued in cells overexpressing TRPML1-eGFP, but not in adjacent, non-expressing control cells (Figure 2.9D,E). Interestingly, TRPML1 overexpression had no effect on Torin1-induced increase in vacuole size, (Figure 2.9E), supporting a model that TRPML1 and mTORC1 function in an independent pathway of resolving large lysosomal vacuoles that have accumulated extracellular macromolecules.

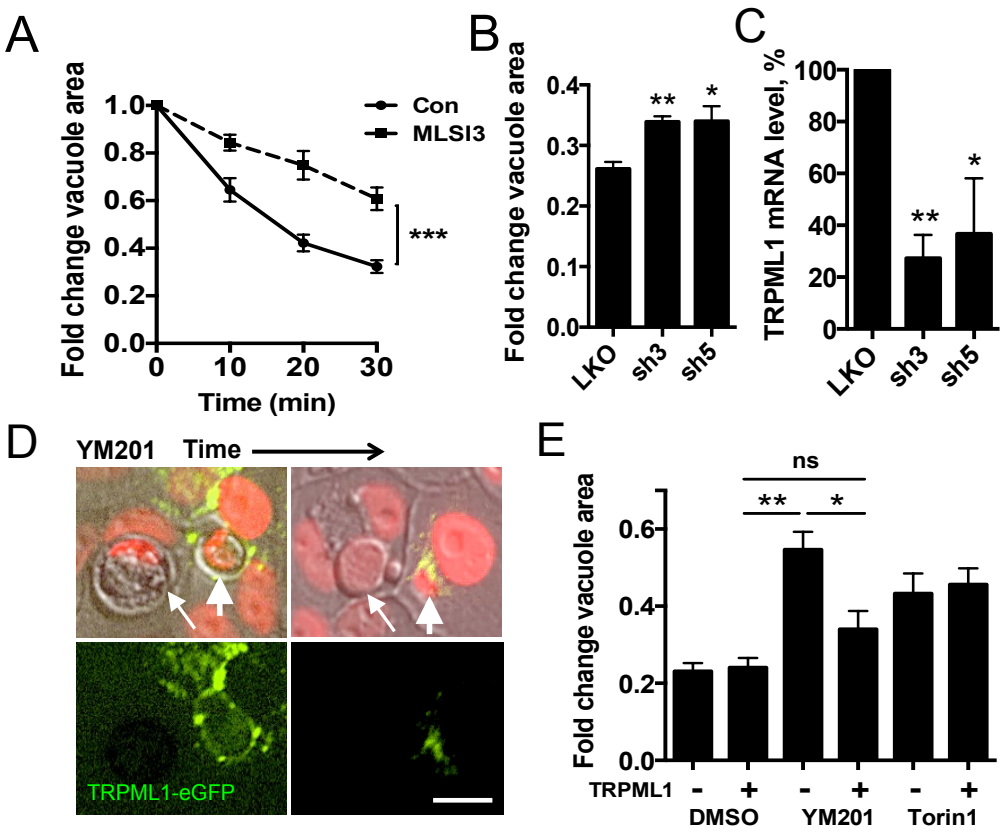

Figure 2.9. TRPML1 regulates vacuole shrinkage downstream of PIKfyve.
A) TRPML1 inhibitor ML-SI3 delays macropinosome shrinkage in J774.1 macrophage cells. Graph shows fold change in area of macropinosomes after 30min.Total cell number analysed for Control n=12, ML-SI3 n=15. **B)** shRNA-mediated TRPML1 knockdowns delay entotic vacuole shrinkage in MCF10A cells. Graph shows fold change in entotic vacuole area after 10 hours in control and knockdown cells. Total cell number analysed for LKO n=60, sh3 n=85, sh5=74. **C)** Fold knockdowns of TRPML1 expression by the shRNAs from B, determined by quantitative RT-PCR. **D)** TRPML1 overexpression rescues entotic vacuole shrinkage in PIKfyve-inhibited MCF10A cells (YM201 0.2μM). Note that entotic vacuole in TRPML1-eGFP-expressing cell (green, right arrow) shrinks rapidly while control vacuole in adjacent, non-expressing cell (left arrow) fails to shrink as corpse is degraded. **E)** TRPML1-eGFP overexpression rescues entotic vacuole shrinkage in PIKfyve-inhibited (YM201 0.2μM), but not mTOR-inhibted (Torin1 1μM), MCF10A cells. Graph shows fold change in vacuole area after 20 hours for control, PIKfyve and mTOR-inhibited MCF10A cells, with or without TRPML1-eGFP expression as measured by time-lapse microscopy. Total cell number DMSO TRPML1 Neg n=78, DMSO TRPML1 Pos n=72, YM201 TRPML1 Neg n=60, YM201 TRPML1 Pos n=42, Torin TRPML1 Neg n=50, Torin TRPML1 Pos n=39. Error bars show mean±SEM for n=3 independent experiments. For all graphs, *p<0.05, **p<0.02 (Student's t-test).

2.2.5 Lysosomal cation fluxes regulate vacuole fission downstream of PIKfyve

The regulation of vacuole maturation by PIKfyve and its effector ion channel TRPML-1 led us to consider that lysosomal ion fluxes may be linked to vacuole fission regulated by PIKfyve. As TRPML-1 is a known cation channel that can efflux calcium, we treated cells with an inhibitor of calcium signaling at lysosomes, *trans*-Ned 19, which is an NAADP antagonist. NAADP signaling mobilizes calcium release from lysosomal cation channels including TRPML1, and *trans*-Ned 19 has been shown to block calcium release from lysosomes (Lee et al., 2015). Consistent with TRPML1 loss-of-function, *trans*-Ned 19 induced a significant delay in entotic vacuole shrinkage (Figure 2.10A), but also delayed corpse degradation (data not shown). To examine if *trans*-Ned 19 could affect vacuole shrinkage independent of upstream degradation events, we performed a washout experiment where we blocked vacuole shrinkage by inhibiting PIKfyve with YM201, until engulfed cell corpses were visibly digested as determined DIC microscopy (after 16 hours), but the vacuoles were still large and intact. We then washed out YM201 and observed the vacuolar dynamics in the presence or absence of *trans*-Ned 19. While control vacuoles underwent rapid shrinkage after YM201 washout, *trans*-Ned 19 treated vacuoles showed significantly delayed shrinkage (Figure 2.10B). These data suggest a role for NAADP-dependent calcium signaling at lysosomes in redistribution of lysosomally accumulated material downstream of PIKfyve activity.

The effect of lysosomal calcium efflux could suggest a role for increased cytosolic calcium concentrations in vacuole shrinkage. To test this, we increased cellular calcium levels by treatment with calcium ionophore Ionomycin, but this did not rescue the effects of PIKfyve inhibition on vacuole shrinkage (Figure 2.10C), suggesting that the block in fission resulting from inhibition of PIKfyve may not be due to an inhibition of cytosolic calcium signaling. Alternatively, we reasoned that calcium efflux could function to reduce the high ionic burden generated by engulfed extracellular material in vacuoles. We therefore considered that PIKfyve inhibition may inhibit vacuole shrinkage at least in part by limiting cation efflux, resulting in hyperosmotic stress in the vacuoles. Hence, in order to determine if manipulation of ionic balances could affect vacuole size, we first pre-treated cells with YM201 to generate large entotic vacuoles. We then examined the effects of hypertonic or hypotonic medium, which would induce vacuolar efflux or influx of water (Florey et al., 2015), on vacuole shrinkage. Indeed, while vacuoles in YM201-treated cells did not shrink (Figure 2.10D upper panel, 2.10E), vacuoles in YM201 treated cells cultured in hypertonic medium underwent rapid shrinkage associated with the appearance of mCherry vesicles in the cytoplasm (Figure 2.10D lower panel, 2.10E). Conversely, while vacuoles shrank normally after the washout of YM201, treatment with hypotonic medium was sufficient to completely prevent vacuole shrinkage (Figure 2.10E). These data suggest a role for the efflux of lysosomal cations downstream of PIKfyve and TRPML1 in controlling vacuole shrinkage.

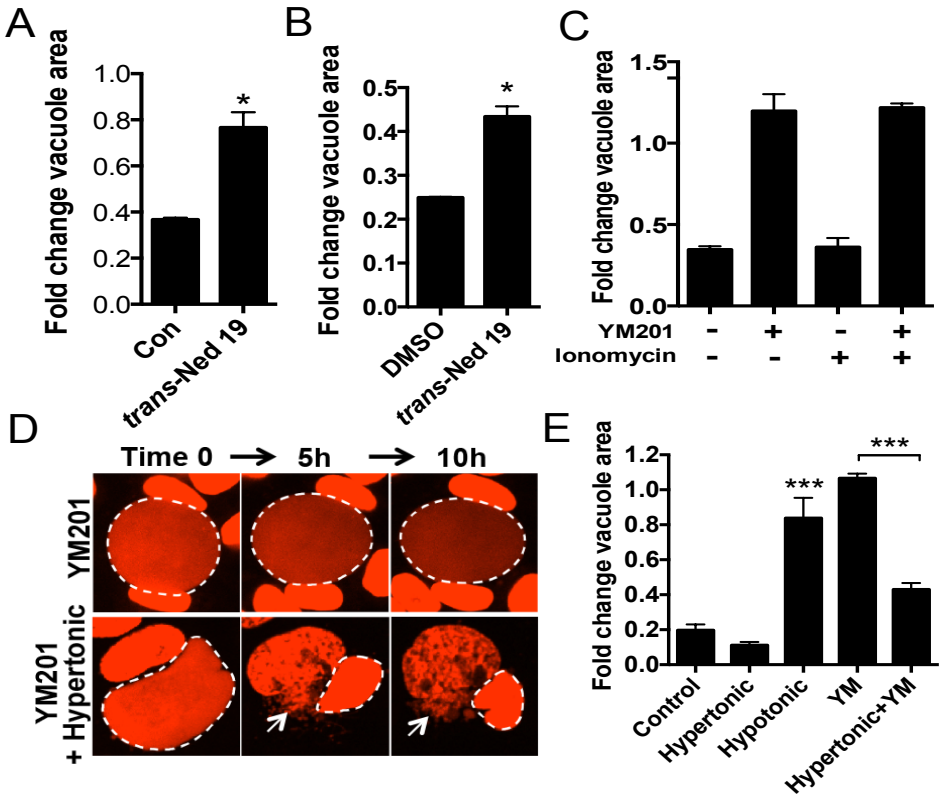

Figure 2.10: Lysosomal cation fluxes regulate vacuole fission downstream of PIKfyve. A) Treatment of MCF10A cells with *trans*-Ned 19 delays entotic vacuole shrinkage. Graph shows fold change in area of entotic vacuoles after 10 hours. Total cell number control n=81 *trans*-Ned 19 n=85. **B)** Treatment of MCF10A cells with *trans*-Ned 19 delays shrinkage of vacuoles resulting from pre-treatment with PIKfyve inhibitor YM201. Graph shows fold change in area of vacuoles pre-treated with YM201, and then subjected to YM201 washout and treatment with vehicle control or *trans*-Ned 19 for 10 hours. Total cell number Control n=96, *trans*-Ned 19 n=90. **C)** Treatment with Ionomycin does not rescue effects of PIKfyve inhibition on vacuole fission. Graphs show fold change in area of vacuoles treated with YM201 with or without Ionomycin. Total cell number Control n=32 ,YM n=38, Ionomycin n=30, Ionomycin+YM n=30. **D)** Treatment with hypertonic medium rescues the effects of PIKfyve inhibition. Vacuoles generated from YM201 pre-treatment in MCF10A cells do not undergo shrinkage in YM201 full media conditions (top panel, circle), but undergo rapid shrinkage and fission in YM201 with hypertonic media (bottom panel, circle) with mCherry vesicles accumulating in the cytosol (arrow). **E)** Graph shows fold change in area of vacuoles pre-treated with YM201, and then subjected to hypertonic or hypotonic medium for 10 hours. Total cell number Control n=41, Hypertonic n=39, Hypotonic n=35, YM n=35, Hypertonic +YM n=39. For all graphs, error bars show mean±SEM for n=3 independent experiments, *p<0.05, **p<0.02 (Student's t-test).

2.2.6 PIKfyve regulates nutrient recovery from phagosomes

We have reported previously that nutrients recovered from engulfed corpses can support cell survival and proliferation during starvation (Krajcovic et al., 2013). To determine if amino acid export from phagosomes required PIKfyve activity, we quantified the incorporation of radiolabeled amino acids from phagocytosed apoptotic corpses into GFP synthesized by macrophages, an assay we published previously to quantify nutrient recovery (Krajcovic et al., 2013). As shown in Figure 2.11A, PIKfyve inhibition reduced the amount of radiolabeled amino acid incorporation, but had no effect on engulfment or degradation, as evidenced by similar levels of mCherry protein derived from ingested and degraded apoptotic cells, consistent with the regulation of nutrient recovery by PIKfyve. To further examine if PIKfyve activity was required for the utilization of engulfed nutrients, we investigated amino acid signaling and cell proliferation in control and PIKfyve-inhibited cultures. We have shown that nutrient recovery from phagosomes reactivates mTORC1 under starvation conditions, as monitored by restoration of pS6K levels when macrophages cultured in amino acid-free media are fed with apoptotic corpses (Krajcovic et al., 2013). While PIKfyve had no effect on mTORC1 activity when stimulated by free amino acids (Figure 2.7B,D), PIKfyve inhibition was able to block mTORC1 reactivation when amino acids were supplied in the form of engulfed apoptotic corpses (Figure 2.11B), consistent with defective lysosomal amino acid export.

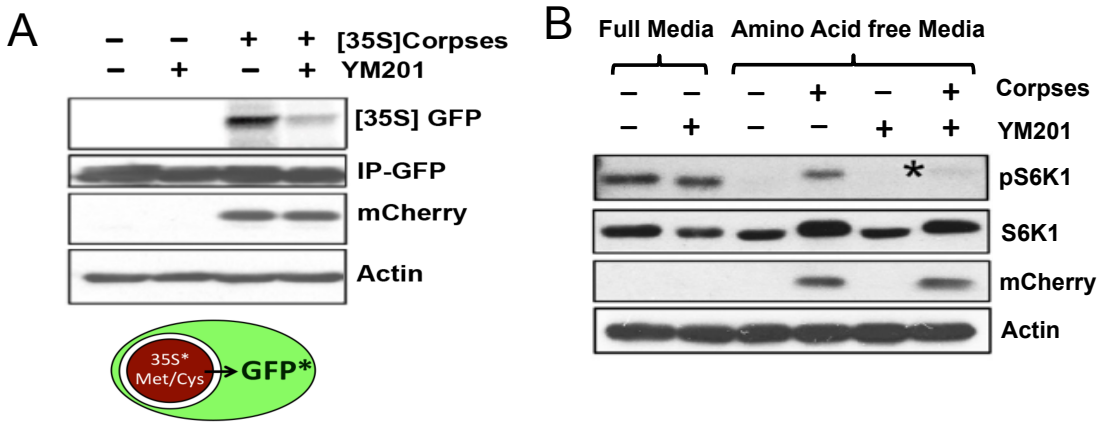

Figure 2.11. PIKfyve regulates amino acid export and signaling from phagosomes. **A)** PIKfyve inhibition blocks amino acids efflux from phagosomes. Blot shows 35S-cysteine and methionine incorporation into macrophage-expressed GFP (top lane), following phagocytosis of H2B-mCherry expressing apoptotic corpses. Note that PIKfyve inhibition reduces levels of radiolabeled GFP, but does not affect the engulfment and degradation marked by the presence of free mCherry. Cartoon shows a schematic of the radiolabeled amino acid incorporation into GFP. **B)** mTORC1 reactivation by apoptotic corpse engulfment is blocked by PIKfyve inhibition. Western blot shows pS6K phosphorylation in J774.1 macrophages cultured in full or amino acid-free media, in the presence or absence of apoptotic corpses and the PIKfyve inhibitor YM201. Note that the loss of pS6K in amino acid-starved cells is rescued by apoptotic corpses (lane 4), and this rescue is blocked by PIKfyve inhibition (lane 6, asterisk).

Finally, as J774.1 macrophages are a proliferative cell line, we further examined the ability of apoptotic corpses to support J774.1 macrophage proliferation by quantifying fold changes in cell number over time in starved and corpse-fed cultures. As shown in Figure 2.12A,B, feeding macrophages with apoptotic cell corpses under amino acid-free conditions supported proliferation in PIKfyve-dependent manner. Taken together, these data support a model that PIKfyve is required for the recovery of nutrients from phagosomes in macrophages.

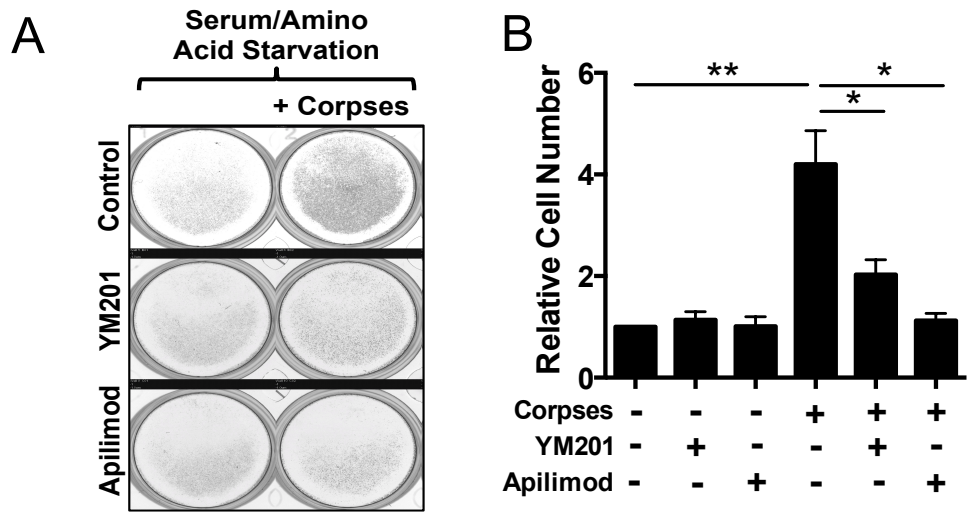

Figure 2.12 PIKfyve regulates apoptotic corpse-dependent cell proliferation in starving macrophages. A) Rescue of macrophage proliferation during starvation by apoptotic cell engulfment is blocked by PIKfyve inhibition. Images show representative crystal violet-stained J774.1 macrophage cultures in serum/amino acid-free media, in the presence or absence of apoptotic corpses and 2μM YM201 or 0.1μM Apilimod. **B**) Fold change in cell number of J774.1 macrophages cultured in serum/amino acid starvation media, with or without the indicated PIKfyve inhibitors, and in the presence or absence of apoptotic corpses. For all graphs, error bars show mean±SEM for n=3 independent experiments, *p<0.05, **p<0.02 (Student's t-test).

2.2.7 PIKfyve is required for albumin-dependent growth of Ras-transformed cells

It has been reported recently that Ras-transformed cells utilize macropinocytosis of albumin to support their growth under nutrient-deprived conditions (Commisso et al., 2013). We hypothesized that PIKfyve might regulate nutrient recovery during this process, similar to its function during apoptotic cell phagocytosis. To examine the effect of PIKfyve inhibition on cell proliferation that is dependent on macropinocytosis, we took advantage of a recently published system that allows cells to grow utilizing extracellular proteins. K-Ras G12D knock-in mouse embryo fibroblasts (MEFs) are unable to proliferate during leucine depletion, but cell

proliferation is restored by supplementing medium with 3% BSA (Palm et al., 2015). By using this system, we found that treatment with the PIKfyve inhibitors Apilimod and YM201 abolished the BSA-dependent rescue of proliferation of cells cultured in leucine-free media (Figure 2.13A,B), while having no effect on growth in leucine-replete conditions (Figure 2.13C). It has been shown that mTOR inhibition by treatment with Torin1 actually increases the growth of K-Ras G12D MEFs during starvation due to increased lysosomal degradation of BSA (Palm et al., 2015). We also found that the inhibition of PIKfyve abolished the Torin1-dependent increase in proliferation (Figure 2.13A). Similar to the inhibition of PIKfyve with pharmacological agents, the siRNA-mediated knockdown of PIKfyve expression also inhibited albumin-dependent growth of K-Ras G12D MEFs, while having no effect in nutrient-replete conditions (Figure 2.13D,E,F).

Importantly, PIKfyve inhibition had no effect on the uptake and degradation of BSA, as evidenced by DQ-BSA fluorescence that was similar between control and Apilimod-treated cells, but strongly decreased when cells were treated with lysosomal cathepsin protease inhibitors (Figure 2.14A,B,C).

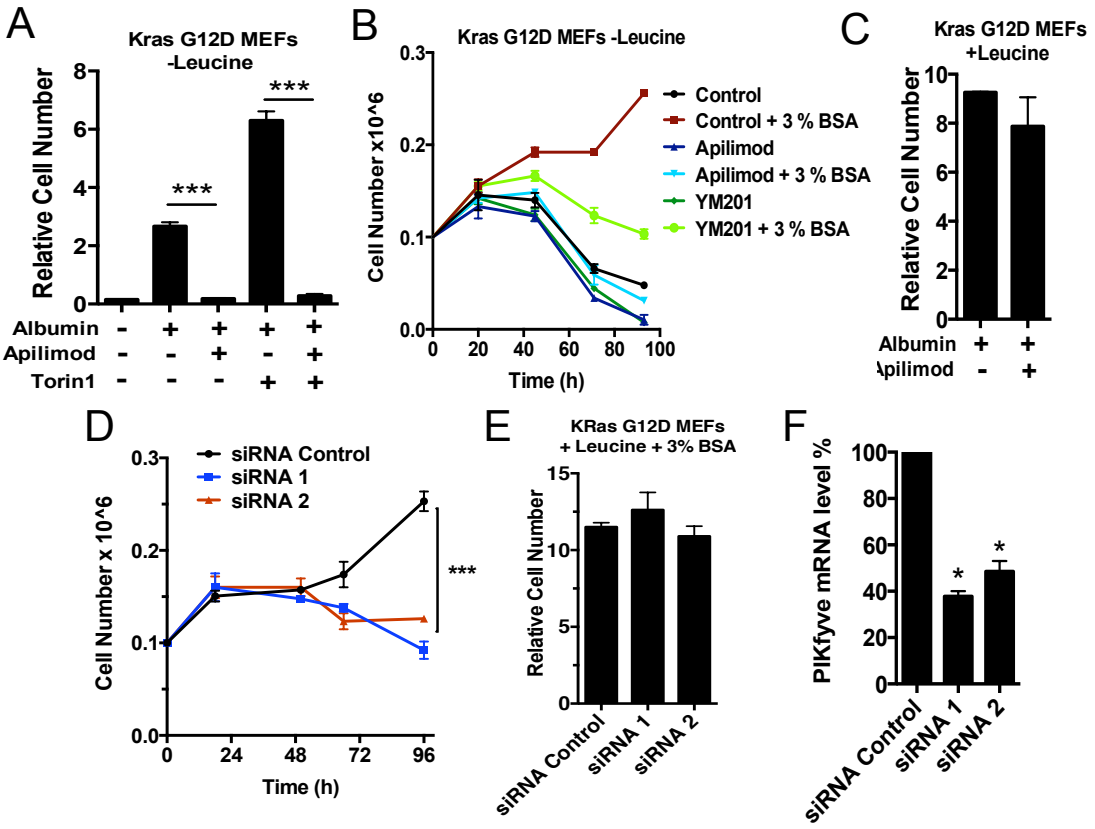

Figure 2.13: PIKfyve regulates albumin-dependent growth of Kras G12D MEFs. A) Rescue of leucine-starved Kras G12D MEF cell growth by engulfment of albumin requires PIKfyve activity. Graph shows relative change in cell number in leucine-free conditions from day 0 to day 4 in the presence or absence of 3% BSA supplementation, and treatment with Apilimod or Torin1. Note that treatment with the PIKfyve inhibitors Apilimod and YM201 abolished the BSA-dependent rescue of cell proliferation and the Torin1-dependent increase in cell proliferation during leucine deprivation. **B)** Rescue of leucine-starved Kras G12D MEF cell growth by engulfment of albumin requires PIKfyve activity. Graph shows kinetics of change in absolute cell number in leucine-free conditions in the presence or absence of 3% albumin supplementation, and treatment with Apilimod (0.1μM) or YM201 (4μM). **C)** PIKfyve inhibition does not significantly affect the growth of Kras G12D MEFs in full media conditions. Graphs show relative change in cell number in leucine-replete media from day 0 to day 2 with albumin supplementation, in the presence or absence of the PIKfyve inhibitor Apilimod (0.1μM). **D)** siRNA-mediated PIKfyve knockdowns inhibit albumin-dependent growth of leucine-starved Kras G12D MEFs. Graph shows relative change in cell number in leucine-free conditions from day 0 to day 4 with albumin supplementation. **E)** siRNA-mediated PIKfyve knockdowns do not affect the growth of Kras G12D MEF cells in full media conditions. Graphs show relative change in cell number in leucine-replete media from day 0 to day 2 with albumin supplementation. **F)** Fold knockdowns of PIKfyve expression by the shRNAs from D,E, as determined by quantitative RT-PCR. All Graphs show representative data from one of three independent experiments, error bars show mean±SD, ***p<0.01.

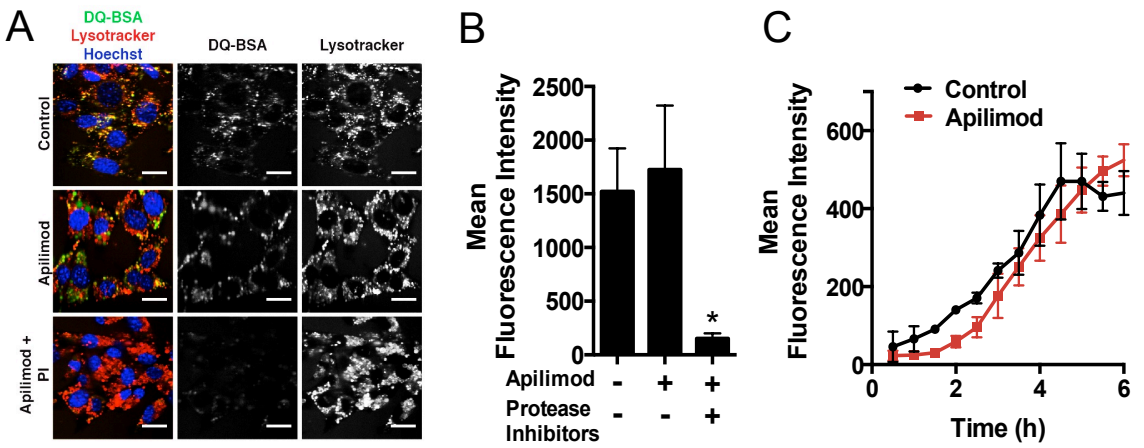

Figure 2.14. PIKfyve does not affect uptake or degradation of albumin. A) PIKfyve inhibition does not affect lysotracker staining or BSA degradation in Kras G12D MEFs. Images show merge of lysotracker and DQ-BSA fluorescence (top left), and individual DQ-BSA (top center) and lysotracker (top right) fluorescence channels in control, Apilimod-treated, and Apilimod plus protease inhibitor (PI)-treated Kras G12D MEFs. **B)** Quantification of mean fluorescence intensity of DQ-BSA for Kras G12D MEFs treated as in Figure 5B. **C)** Quantification of the kinetics of mean fluorescence intensity of DQ-BSA over 6 hours between control and Apilimod-treated Kras G12D MEFs. All graphs show representatives of three independent experiments, error bars show mean±SD. *p<0.05, **p<0.02 (Student's t-test).

We further examined the BSA-mediated growth of tumor cells derived from a Kras-mutant mouse model of pancreatic cancer KRPC (Lito et al., 2014), and human cancer cells MiaPaca-2 (pancreatic cancer, Kras mutant) and T24 (bladder cancer, H-Ras mutant). PIKfyve inhibition consistently blocked cell proliferation when starvation media were supplemented with 3% BSA (Figure 2.15A,B,C), while having no effect in full media conditions (Figure 2.15 D,E,F), demonstrating that PIKfyve is required for albumin-dependent growth of Ras-mutant cancer cells.

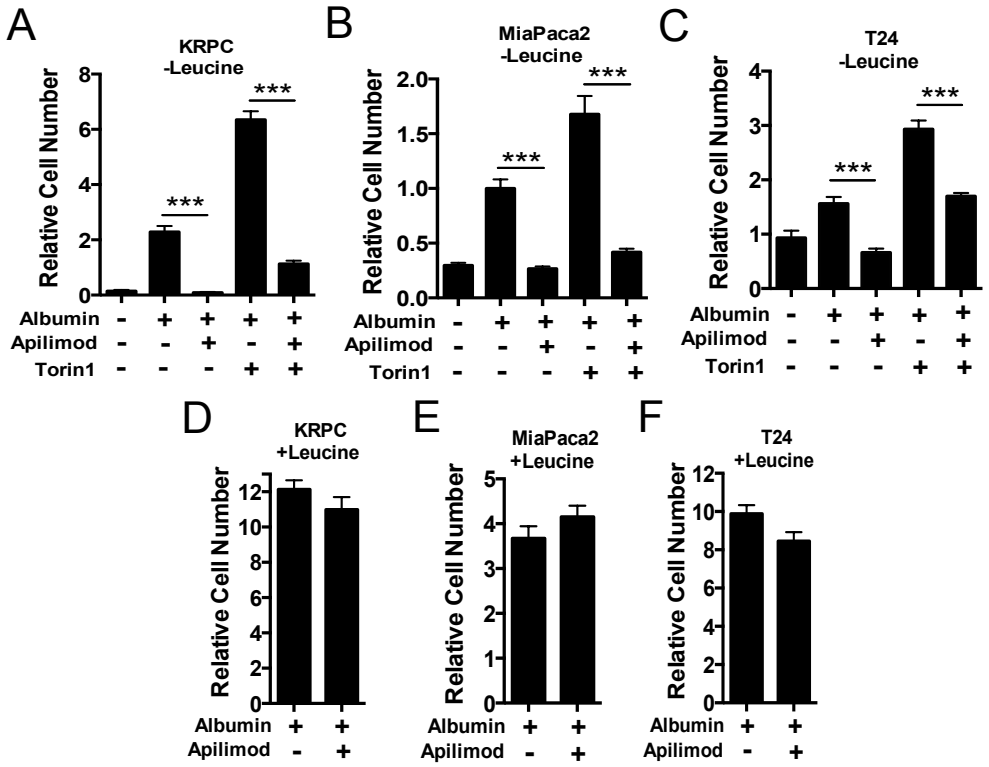

Figure 2.15. PIKfyve activity regulates albumin-dependent growth of leucine-starved mutant Ras tumor cells while having no affect in full media conditions. Graph shows relative change in cell number in leucine-free conditions from day 0 to day 4 for the indicated cell lines: **A)** KRPCs **B)** MiaPaca2 and **C)** T24. Apilimod was used at 0.6μM for KRPC, MiaPaca2 and T24 cells. Graphs show relative change in cell number of Kras G12D MEFs, **D)** KRPCs **E)** MiaPaca2 and **F)** T24 in leucine-replete media from day 0 to day 2 with albumin supplementation, in the presence or absence of the PIKfyve inhibitor Apilimod (0.6μM for KRPC, MiaPaca2 and T24 cells). All graphs show representatives of three independent experiments, error bars show mean±SD. *$p<0.05$, **$p<0.02$ (Student's t-test).

2.3 DISCUSSION

The data presented here establish that PIKfyve controls a late stage of macroendocytic vacuole maturation, involving redistribution of engulfed cargo to lysosome networks. While a role for PIKfyve in regulating lysosome morphology has been established previously (Ikonomov et al., 2001; Nicot et al., 2006; Rudge et al., 2004), mechanistic studies have suggested conflicting functions of PIKfyve in maintaining lysosomal pH, supporting proteolytic degradation, or promoting lysosome fusion (de Lartigue et al., 2009; Ho et al., 2015; Ikonomov et al., 2001, 2006; Jefferies et al., 2008; Kerr et al., 2010; Kim et al., 2014; Nicot et al., 2006; Rusten et al., 2006; Sbrissa et al., 2007). Recent studies have also concluded that PIKfyve is required for engulfment by phagocytosis, phagolysosome formation and cargo degradation (Dong et al., 2010; Kim et al., 2014). Although we cannot completely rule out upstream functions, we find here that PIKfyve is not required for the engulfment or degradation of apoptotic corpses during phagocytosis by macrophages, or during *C. elegans* embryogenesis *in vivo.* Further, the ingestion and degradation of serum albumin by macropinocytosis is unaffected by PIKfyve inhibition. Our findings instead implicate PIKfyve in controlling the ability of the cell to clear large lysosomal vacuoles and redistribute their contents. It is conceivable that the different substrates used for engulfment between our study and others (Dong et al., 2010; Kim et al., 2014) could account for some of the observed effects, as we note that latex beads used as phagocytosis substrates cannot be degraded and redistributed by uptake into the cytosol.

Although previous studies have shown that both PIKfyve and TRPML1 can regulate mTORC1 (Bridges et al., 2012; Wong et al., 2012), we found that PIKfyve functions largely independently of mTORC1 to control vacuole shrinkage. PIKfyve activity was required for mTORC1 activation in our systems only under conditions when cells are dependent on nutrients supplied by engulfment, an effect we speculate may be due to reduced nutrient recovery from macroendocytic vacuoles upon PIKfyve inhibition. We find evidence instead that PIKfyve may control vacuole shrinkage at least in part through its effector, the Ca2+ channel TRPML1, as its inhibition slows vacuole shrinkage in a similar manner to PIKfyve inhibition, and shrinkage is rescued in PIKfyve-inhibited cells by TRPML1 overexpression. Interestingly, TRPML1 overexpression does not rescue vacuole shrinkage induced by mTOR inhibition, consistent with PIKfyve and mTORC1 controlling vacuolar shrinkage through separate pathways. While we find that PIKfyve is not required for the degradation of engulfed corpses, TRPML1 loss of function does slow corpse degradation (data not shown), similar to a recent report (Dayam et al., 2015), suggesting that TRPML1 has PIKfyve-independent upstream functions. Perhaps basal ion fluxes controlled by TRPML1 are generally required to maintain lysosome function and further TRPML1 activation by PIKfyve is required to support the shrinkage of macroendocytic vacuoles that harbor complex substrates undergoing degradation.

Cargo degradation would alter the osmotic potential in the vacuole and perhaps require this increased ionic flux at the lysosomal membrane. Consistent with this model, changing the ionic balance of the cells by using hypertonic

medium was sufficient to completely rescue vacuole shrinkage due to PIKfyve inhibition. While we cannot exclude a general effect of hypertonic medium conditions on vacuole shrinkage, our data suggest that PIKfyve might regulate vacuole size by altering the osmotic balance in the vacuole via TRPML1-dependent ion flux. Indeed, several studies have reported that Fab1, the yeast ortholog of PIKfyve, is activated during conditions of hyperosmotic stress and generates PI(3,5)P2 which causes fragmentation of the yeast vacuole (Figure 2.16A,B) (Dove et al., 1997; Gary et al., 1998; Jin et al., 2016). Thus is it possible that there is an evolutionarily conserved link between PIKfyve activity and osmotic regulation in controlling vacuole dynamics.

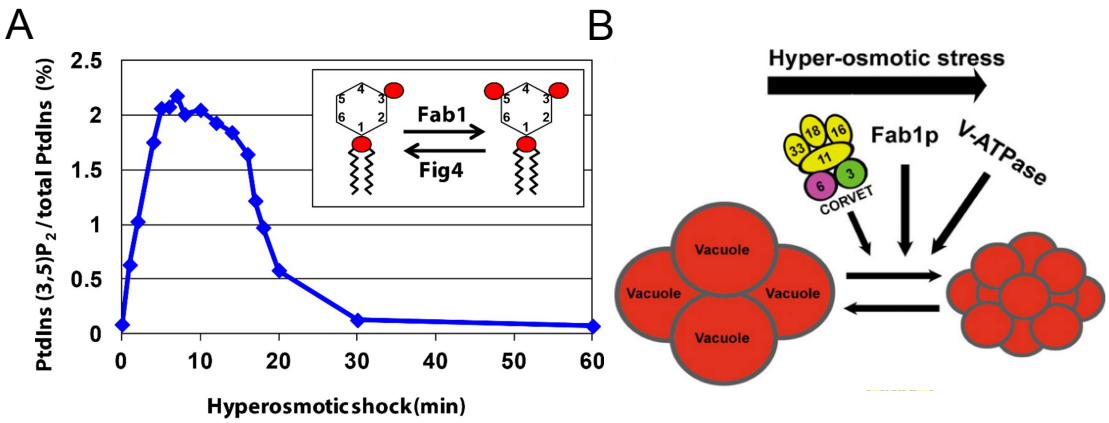

Figure 2.16. PI(3,5)P2 and vacuole size regulation during hyperosmotic shock in yeast. A) Levels of PI(3,5)P2 increase transiently increase over 20-fold during hyperosmotic stress before returning back to normal. Image adapted from (Jin et al., 2016). **B)** Hyperosmotic stress causes fragmentation of yeast vacuole that is dependent on Fab1, CORVET Complex and V-ATPase. Image adapted from (Dove et al., 2009). Fab1 is the yeast ortholog of PIKfyve.

The precise mechanism of how this osmoregulation occurs, the source of the TRPML1-effluxed lysosomal ions, and other potential PIKfyve effectors that could regulate vacuole fission remains to be elucidated. We note that the removal of calcium from culture medium does not appear to affect the shrinkage

of macropinosomes (Figure 2.17), suggesting that lysosomal calcium originating from sources other than engulfed substrates could also contribute. One such potential source is the ER, which has been implicated in maintaining lysosomal calcium that is effluxed by TRPML1 (Garrity et al., 2016). It is also important to point out that while we favor a model that TRPML1 may function as an effector of PIKfyve in this context, our data do not exclude a parallel relationship. Also, while we have not found evidence to support a role for the WIPI1/2 and actin, we cannot exclude the possibility that there are other unknown PI(3,5)P2 effectors that may be regulating vacuole shrinkage.

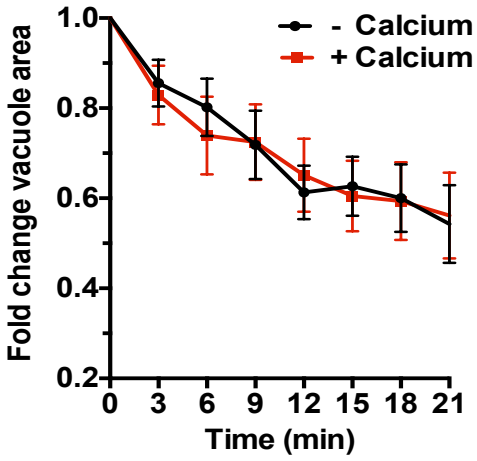

Figure 2.17. Calcium from the media does not affect vacuole shrinkage. Calcium-free media has no effect on macropinosome shrinkage in J774.1 macrophages. Graph shows fold change in vacuole area over time in calcium-free and calcium-replete media. Error bars show mean±SD, graph is representative of independent experiments. Total cell number analysed for –calcium n= 5 and +calcium n=5.

In addition to supporting vacuole shrinkage, we also find that PIKfyve facilitates the utilization of nutrients from engulfed substrates, suggesting a potential link between shrinkage and nutrient export, which could occur by several mechanisms. The role of calcium and hypertonicity in the resolution of

large vacuoles may suggest that ion transport may directly facilitate the cytosolic uptake of amino acids in the lysosome. Alternatively, the redistribution of degraded cargo from large vacuoles into the entire lysosome network alters the surface area-to-volume ratio, which could contribute to enhanced export. Perhaps analogously, starvation is known to increase the absorptive surface area of intestinal epithelial cells by 2-3-fold, in order to maximize nutrient uptake from the intestinal lumen (Gupta and Waheed, 1992). The fission of large macroendocytic vacuoles is predicted to increase surface area-to-volume by at least 10-fold (Figure 2.18), and may therefore increase the efficiency of nutrient export significantly. Finally, it is also possible that PIKfyve controls nutrient export more directly by supporting the activity of amino acid and other nutrient transporters whose identities remain poorly characterized.

Surface Area to Volume Equation
SA is Surface Area, V is volume, r is radius, n is number of vesicles
$SA{:}V_{sphere} = 3 / r_{sphere}$

Assuming corpse radius of 5μm and vesicle radius of 0.5μm:
$SA{:}V_{corpse} = 3 / 5 = 0.6$
$SA{:}V_{vesicle} = 3 / 0.5 = 6$
$SA{:}V_{vesicle} > SA{:}V_{corpse}$ ***by 10 fold***

Since $n \times V_{vesicle} = V_{corpse,}$
$Total\ SA_{vesicles} > Total\ SA_{corpse}$ ***by 10 fold***

Figure 2.18. Surface Area-to-Volume changes during vacuole fission. Surface Area-to-Volume (SA:V) ratio of a vesicle is larger than that of a corpse-containing vacuole, by the fold difference in their radii. Equation shows calculations of SA:V of a sphere with radius of 5μm (approximate size of an entotic vacuole or phagosome) compared to one with radius of 0.5μm (similar to, or larger than, a vesicle budded from a large vacuole), where SA:V ratio is 10-fold larger. Since the total volume of all vesicles is predicted to be similar to the volume of the corpse-containing vacuole, the total surface area of all the vesicles would increase by at least 10-fold. If vesicle size is smaller than 0.5μm radius, then SA:V would increase by more than 10-fold.

We also find that during starvation conditions, PIKfyve-dependent nutrient recovery is required for survival and proliferation of engulfing phagocytes or mutant Ras cells, while having no effect on cell proliferation in nutrient replete conditions. In conclusion, our data are consistent with a model where cells in nutrient deplete conditions are dependent on engulfment of extracellular cargo (Figure 2.19). Upon lysosome fusion, the cargo-containing vacuoles undergo a process of PIKfyve-membrane fission that redistributes their contents into the lysosome network of the cells and enhances nutrient export from these compartments (Figure 2.19). This alternative nutrient scavenging strategy can promote macromolecule synthesis and support the survival and proliferation of engulfing cells in nutrient starvation.

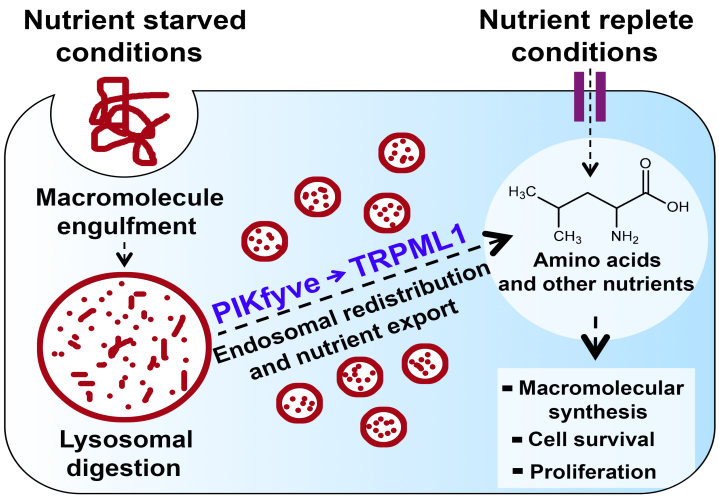

Figure 2.19. Model depicting the role of PIKfyve in regulating vacuole fission and nutrient export during engulfment. In nutrient replete conditions, amino acids can be taken up by plasma membrane transporters and utilized for macromolecule synthesis and survival. In nutrient starved conditions, cells engulf extracellular macromolecules that undergo lysosome fusion and degradation. The cargo-containing vacuoles undergo a PIKfyve-dependent event of membrane fission that redistributes the cargo in lysosomes of the engulfing cell. This role of PIKfyve is mediated in an mTORC1-independent manner in part by its downstream effector lysosomal cation channel TRPML1. PIKfyve also regulates nutrient export from these compartments, which is required for the survival and proliferation of engulfing cells during nutrient starved conditions.

2.4 MATERIALS AND METHODS:

2.4.1 Cell culture and Reagents:

MCF10A cells were obtained from American Type Culture Collection (ATCC, Manassas, VA) and cultured as described (Florey et al., 2011). J774.1 mouse macrophages (ATCC), EL4 cells (kind gift from Dr. Julie Blander, Mt Sinai Hospital, NY), HEK293 (ATCC), Kras G12D Mouse Embryonic Fibroblasts (MEFs) (kind gift from Dr. Scott Lowe, MSKCC, NY), KRPC (Lito et al., 2014), MiaPaca2 (ATCC) and T24 (ATCC) cells were cultured in DMEM plus 10% heat-inactivated fetal bovine serum (FBS) with penicillin/streptomycin (pen/strep). U937 cells (ATCC) were cultured in RPMI-1640 medium plus 10% FBS and pen/strep. Amino acid–free medium was prepared by dialyzing heat-inactivated FBS (for J774.1) or horse serum (for MCF10A) as described (Krajcovic et al., 2013) and adding to amino acid-free base media at 10% final. Hypertonic and hypotonic medium were prepared by addition of 200mM sucrose or 60% water to full growth media respectively. Calcium- free media was prepared by adding dialyzed heat-inactivated FBS to calcium free DMEM (21068028, Thermo Fisher Scientific, USA), and calcium replete media was prepared by addition of 1.8mM calcium to the calcium-free media. MCF10A, HEK293 or U937 cells expressing H2B-mCherry, 2xFYVE-mCherry or GFP-LC3 were prepared by retroviral transduction with pBabe-H2B-mCherry, 2XFYVE-mCherry (FYVE domain from Hrs) and pBabe-GFP-LC3 respectively. Cells were treated with YM201636 (524611, Calbiochem, EMD Millipore, Massachusetts) at 0.4μM for MCF10A cells, 0.8μM for HEK293 cells and 0.8μM-1μM for J774.1 cells, Apilimod

(STA5326, Axon1369, Axon Medchem, Netherlands) at 0.1μM, LatrunculinB (L5288, Sigma) at 5μM, ML-SI3 at 50μM Torin1 (Tocris Bioscience, Bristol, UK) at 0.5μM, *trans*-Ned 19 at 250μM, Ionomycin at 1μM, Concanamycin A (Sigma) at 0.1μM and protease inhibitors at 2 μM E-64, 2 μM Pepstatin A and 10 μM Leupeptin unless otherwise indicated. Cells were treated with lysotracker Green DND-26 (Invitrogen) at 50nM, 10kD-70kD TMR-Dextran (Invitrogen) at 250μg/ml and DQ-BSA Green (Invitrogen) at 10μg/ml.

2.4.2 Constructs and cDNA Transfection

$1x10^6$ MCF10A-H2B-mCherry cells were nucleofected with TRPML1-eGFP with Amaxa Nucleofector Solution V (Lonza, Switzerland) and assayed 72h post-transfection. $1x10^6$ HEK293 cells were plated in 6-well plates, transfected with 4μg PIKfyve-eGFP construct using Lipofectamine 2000 the next day and assayed 48h post-transfection. The pEGFPC1-TRPML1 construct was a kind gift from Dr. Shmuel Muallem, NIH, Bethesda, MD. PIKfyve-eGFP constructs were a kind gift from Dr. Frederic Meunier, University of Queensland, Australia and Dr. Assia Shisheva, Wayne State University, MI.

2.4.3 Measuring vacuole shrinkage by time-lapse microscopy

To quantify vacuole shrinkage, cells were plated on glass-bottom 6-well plates (MatTek, Ashland, MA) and imaged the next day in 37°C and 5% CO_2 live-cell incubation chambers, as described (Krajcovic et al., 2013). Differential Interference Contrast (DIC) and fluorescence images were obtained every 15 minutes for 24-48 hours. Area of entotic vacuoles and phagosomes were determined by mCherry fluorescence and quantified manually using Elements

software. The time point of mCherry protein diffusion from the nucleus of the corpse to the vacuole during entosis or phagocytosis was determined to be the time zero, and vacuole area was quantified at 10h and 4h respectively as described (Krajcovic et al., 2013). Cell fates of internalized cells were quantified as entotic death, release, no change, apoptosis and proliferation.

2.4.4 Measuring macropinosome shrinkage by confocal microscopy

J774.1 macrophages were cultured on 35mm glass-bottomed dishes (MatTek, Ashland, MA) in full medium with 200 U/ml interferon-γ for 48 h, or transfected HEK293 cells were cultured on 35mm glass-bottomed dishes and imaged at 37°C and 5% CO_2 live-cell incubation chambers with 10-70kD Texas-Red Dextran (0.1mg/ml) and lysotracker green (50nM, Invitrogen) added to the media. DIC and fluorescent images were acquired in 0.5μm z-steps, at maximum speed, using the Ultraview Vox spinning-disk confocal system (Perkin Elmer) coupled to a Nikon Ti-E microscope as described(Krajcovic et al., 2013). The time points where dextran macropinosomes became positive for lysotracker staining were considered to be time zero. In J774.1 macrophages, macropinosome areas were quantified at time zero and 30min manually using Volocity software, for the z-planes with maximum area.

2.4.5 Imaging *C. elegans* apoptotic phagocytosis

The H2B::mCherry and PIP2::GFP expressing *ppk3* mutant was generated by crossing the H2B::mCherry and PIP2::GFP expressing OD95 strain with *ppk3 n2668* mutant strain (AC257). Both strains were obtained from the *Caenorhabditis* Genetics Center (University of Minnesota, Minneapolis, MN).

Embryos at the 100-cell stage obtained from dissected gravid hermaphrodites were imaged by confocal microscopy as described (Florey et al., 2011). DIC and fluorescent images of the engulfment of apoptotic corpse (ABplpappap) by neighboring cell (ABplpappaa) at 1μm z-stacks were acquired every 4min. The time point of mCherry protein diffusion from the nucleus of the apoptotic corpse to the vacuole was determined to be the time zero, and vacuole area was quantified at 30min.

2.4.6 Western Blotting

Cell Lysis was performed in ice-cold RIPA buffer, followed by SDS-PAGE and western blotting, using anti-PIKfyve (ab137907; Abcam), anti–S6-Kinase (9202; Cell Signaling), anti–phospho-S6-kinase threonine 389 (9234; Cell Signaling), anti-actin (A1978; Sigma), anti-mCherry (ab125096; Abcam), anti-GFP (11814460001; Roche) and anti-Wipi-2 (8567; Cell Signaling) antibodes.

2.4.7 Immunofluorescence

Immunofluorescence was performed on cells cultured on glass-bottom dishes (MatTek) as described previously (Overholtzer et al., 2007). Cells were fixed in 1:1 chilled Methanol:Acetone at -20°C for 5 minutes. The antibodies used for IF were anti-mTOR (2983; Cell Signaling), anti-Lamp1 (for MCF10A cells; BD555798), anti-Lamp1 (for J774.1 mouse macrophages; BD553792), anti-actin (A1978; Sigma) and anti-Rab7 (9367; Cell Signaling, Danvers, MA). Confocal microscopy was performed using the Ultraview Vox spinning-disk confocal system (Perkin Elmer, Waltham, MA) to acquire Z-stack images using Volocity software (Perkin Elmer).

2.4.8 RNAi

$1x10^5$ MCF10A cells were seeded per well in a six-well plate, followed by lentiviral transduction with control empty LKO.1 vector or the targeted hairpin vectors against PIKfyve, TRPML1, WIPI1 or WIPI2. After 48 hours of transduction, cells expressing the shRNAs were selected using puromycin (2μg/ml) and assayed. siGenome SMART pool siRNAs against mouse *PIKfyve*, and Control 2 non-targeting siRNAs, were obtained from Dharmacon. $2x10^5$ MEF cells were seeded per well in six-well plate, followed by lipofectamine (Invitrogen) transfection with 250nM control or targeted siRNA against PIKfyve for 6 hours. After 24 hours of transfection, cells were subject to BSA supplementation assays.

2.4.9 Quantitative PCR

Total RNA was extracted from shRNA expressing cells using TRIzol® Plus RNA Purification Kit (12183-555, Thermo Fisher Scientific, USA). Quantitative PCR was performed using the Bio-Rad iCycler real-time system (MyiQ), with SYBR green detection (iScript One-Step RT-PCR Kit with SYBR green (Bio-Rad). Samples were analyzed by the standard curve method in triplicate. Primers against *WIPI1* (QT00066458), *TRPML1* (QT00094234), *GAPDH* (QT01192646), *mPIKfyve* (QT00127799) and *mGAPDH* (QT01658692) were obtained from Qiagen.

2.4.10 Phagocytosis & Crystal Violet Assays

We plated $1×10^5$ J774.1 mouse macrophages onto six well tissue culture plastic plates and cultured them in full medium with 200 U/ml interferon-γ for 48 h. After 48hours, cells were washed three times in PBS and fed with $2x10^6$ apoptotic cell

corpses in amino acid free media for western blotting or serum and amino acid free media for crystal violet (CV) assays. Apoptotic corpses were prepared by UV irradiation of U937 cells expressing H2B-mCherry for western blotting, and EL4 cells for CV assays by overnight incubation and harvesting by centrifugation. 48h after addition of corpses, macrophages were washed three times in PBS and lysed for western blotting or fixed with 4% paraformaldehyde for CV. Fixed cells were stained with 0.1% Crystal Violet Solution and dried overnight before taking images of the plates using the Optronix Gelcount colony counter (Oxford Optronix Ltd., Oxford, UK). The crystals were dissolved in 10% acetic acid and the absorbance at 590nm quantified using spectrophotometry. 35S-Cysteine/Methionine radiolabeling assay was conducted as described previously (Krajcovic et al., 2013).

2.4.11 Lysotracker and DQ-BSA Imaging

J774.1 mouse macrophages were plated on glass-bottom dishes and cultured them in full medium with 200 U/ml interferon-γ for 48 h and pretreated with vehicle or inhibitors for one hour. LysoTracker or DQ-BSA staining was performed by adding 50 nM LysoTracker Green (Invitrogen, Carlsbad, CA) or 0.1mg/ml DQ-BSA (Invitrogen, Carlsbad, CA) to culture media for 30 min before imaging live cells using confocal and time-lapse microscopy.

2.4.12 BSA supplementation Assays

Cell Proliferation assays in full medium or in leucine-free media with or without BSA supplementation were performed in Kras G12D MEFs, KRPC, MiaPaca-2 and T24 cell lines as described (Palm et al., 2015). Fold change in cell number

from day 0 to day 4 for leucine-free conditions, and day 0 to day 2 for leucine-replete conditions was quantified.

2.4.13 Statistics and Representative Figures

Error bars show mean±SEM from n=3 independent experiments unless otherwise indicated. P-values were obtained using two-tailed unpaired Student's t-test as all comparisons were between two groups - control and experimental. Western blots and immunofluorescence images are representatives from least 3 independent experiments unless otherwise indicated.

CHAPTER 3: PIKfyve regulates cholesterol trafficking and metabolism

3.1 INTRODUCTION

PIKfyve regulates vacuole fission and nutrient export from engulfed substrates, which promotes the survival and proliferation of engulfing cells. While in the previous study amino acid export was measured, it is possible that export of other nutrients such as glucose, lipids and nucleic acids could also be regulated, particularly if the control of fission by PIKfyve is linked to nutrient export. Like extracellular protein, lipids have also shown to be scavenged from the serum by Ras-mutant cells to support growth and metabolism (Kamphorst et al., 2013). In particular, increased cholesterol uptake and biosynthesis have been observed in many cancer types (Beloribi-Djefaflia et al., 2016; Guillaumond et al., 2015).

Cholesterol levels in the cell are maintained by either extracellular uptake or intracellular biosynthetic pathways. Cholesterol biosynthesis occurs from acetyl-CoA through a 20-step reaction in the cytosol and the ER (Moore et al., 2010). In addition, cells can also take up cholesterol from circulating lipoprotein particles like LDL through receptor-mediated endocytosis (Moore et al., 2010). Upon binding to the LDL receptor (LDLR), LDL is internalized into endosomes that fuse with lysosomes to degrade it into cholesterol while the receptor is recycled back to the plasma membrane (Figure 3.1) (Moore et al., 2010). In the lysosomal lumen, free cholesterol binds to Niemann-Pick C2 (NPC2), which tranfers the molecule to transmembrane protein Niemann-Pick C1 (NPC1) (Kwon et al., 2009). NPC1 then directs the bound cholesterol for insertion into the lysosomal membrane, which is then exported to the ER, plasma membrane and

peroxisomes through poorly understood mechanisms (Chu et al., 2015; Moore et al., 2010). Loss-of-function of NPC1 and NPC2 prevents cholesterol from being incorporated in the lysosome membrane, leading to its accumulation in the lysosome lumen. This impairment of cholesterol efflux can decrease intracellular cholesterol concentrations, which triggers the SCAP-SREBP complex to move from the ER to the Golgi where it is cleaved. Cleaved SREBP then translocates to the nucleus to upregulate the transcription of cholesterol biosynthetic and uptake genes like LDLR and HMG-CoA Reductase (Figure 3.1) (Moore et al., 2010). Conversely, high cholesterol levels leads to reduced transcription of LDLR and HMG-CoA, while increasing the expression of cholesterol efflux transporters ABCA1 and ABCG1 through transcription factors liver X receptors (LXR) and retinoid X receptors (RXR) (Moore et al., 2010).

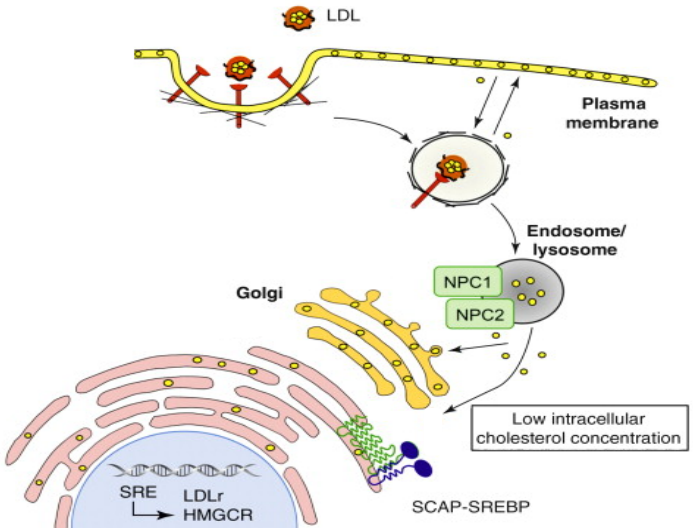

Figure 3.1. LDL and cholesterol trafficking in the cell. LDL binds to the LDL receptor (LDLR) at the plasma membrane and undergoes receptor-mediated endocytosis. The receptor is recycled back to the plasma membrane whereas LDL undergoes lysosomal degradation to generate cholesterol. Cholesterol is bound to NPC2 in the lysosome lumen and transferred to NPC1, which directs its exit into the ER, Golgi or plasma membrane. If this pathway is impaired, it leads to low intracellular cholesterol concentrations, which activates the SCAP-SREBP pathway at the ER and Golgi. SREBP is cleaved and translocates to the nucleus to upregulate cholesterol biosynthetic and uptake genes like HMGCR and LDLR. Figure adapted from (Moore et al., 2010).

Cholesterol is a key metabolite in the cell, with many functions including steroid hormone production, vitamin D synthesis, cell signaling and nerve conduction. It is also a critical part of the cell membranes and is essential to maintaining membrane rigidity and fluidity. Additionally, cholesterol is required for the formation and maintenance of higher order membrane microdomains that can partition proteins and lipids (Simons and Ehehalt, 2002). These microdomains can compartmentalize different cellular processes and are shown to be essential for IgE signaling, TCR antigen receptor signaling, viral entry and membrane fission events (Simons and Ehehalt, 2002).

Dysregulation of cholesterol function and homeostasis is observed in many disorders including atherosclerosis, stroke, pathogen infection, lysosome storage diseases as well as carcinogenesis. In cancers, intracellular cholesterol levels have been shown to be upregulated by increased HMG-CoA activity and LDLR expression. Increased cholesterol accumulation in plasma membrane microdomains can also upregulate Akt, EGFR and HER2 growth signaling pathways, which could contribute to tumor growth and development (Adam et al., 2007; Chen and Resh, 2002; Zhuang et al., 2005). While interactions between lysosomal cholesterol trafficking pathways and cancer cell growth have been reported, it is unclear if specific perturbations in this pathway play an important role in tumorigenesis.

Given the critical role of cholesterol uptake pathways in normal and transformed cells, and the regulation of lysosomal nutrient export by PIKfyve, we investigated the possibility that PIKfyve is required for the cholesterol export and trafficking from lysosomes, thereby altering cholesterol homeostasis in the cell. Also, the endogenous localization of cholesterol can be observed through a direct stain (filipin), making this a useful strategy to image lysosomal nutrient export in the cell.

3.2 RESULTS

3.2.1 PIKfyve regulates cholesterol trafficking from lysosomal membranes

Given that PIKfyve regulates nutrient export from large lysosomal compartments during engulfment, we hypothesized that it would regulate cholesterol export from lysosomes as well. In this model, PIKfyve inhibition would cause accumulation of cholesterol in the lumen of lysosomes, in a manner similar to NPC1 (as shown in Figure 3.1). To investigate the role of PIKfyve in cholesterol export from lysosomal compartments, MEFs treated with PIKfyve or NPC1 inhibitors overnight were immunostained with the cholesterol staining reagent filipin. Vehicle-treated cells stained positively for filipin primarily at the plasma membrane and some cytosolic vesicles (Figure 3.2A left panel), while cells treated with U18666A, a drug that inhibits NPC1, showed increased luminal filipin staining within lysosomes (Figure 3.2A right panel). Interestingly, in contrast to U18666A-treated cells, PIKfyve-inhibited cells demonstrated increased intracellular filipin staining at the membranes of enlarged lysosomal vacuoles, with absence of staining in the lumen (Figure 3.2A middle panels). To validate the effect of PIKfyve inhibition on intracellular cholesterol content in another cell line, a dose response with YM201 was performed in U2OS osteosarcoma cell line, and a similar effect was observed (Figure 3.2B). These results suggest that PIKfyve inhibition leads to accumulation of cholesterol in the limiting membrane of lysosomes.

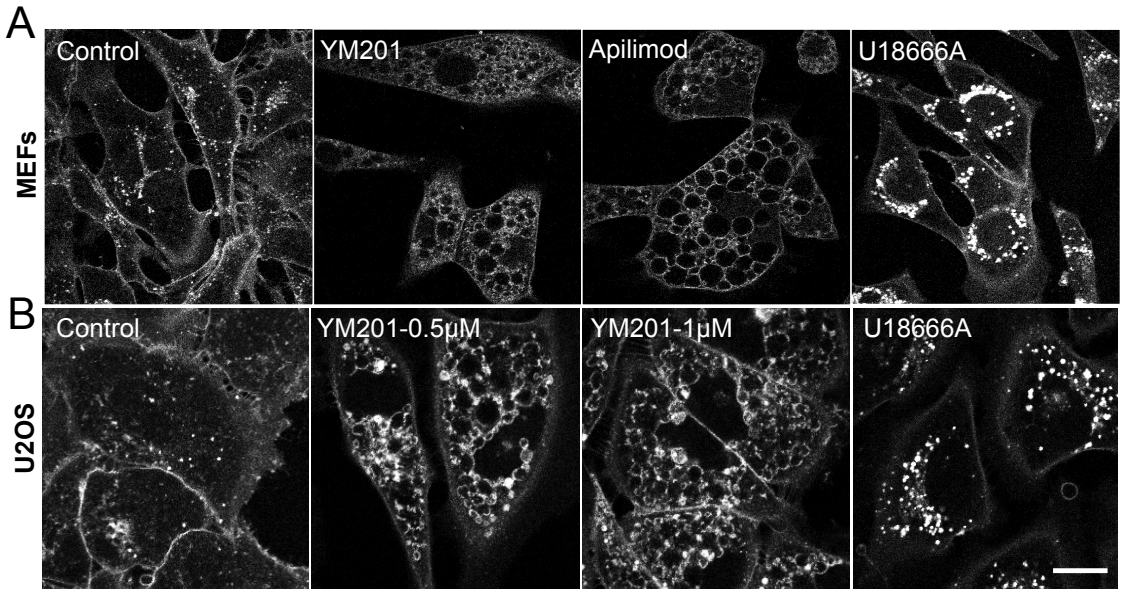

Figure 3.2. PIKfyve regulates cholesterol trafficking in the cell. A) PIKfyve regulates cholesterol exit from lysosomal membranes in MEFs. Image shows filipin staining at the plasma membrane and intracellular vesicles in control cells (Control, left panel), whereas overnight treatment with PIKfyve inhibitors (YM201, Apilimod, middle panels) increased filipin staining at the membranes of enlarged lysosomal vacuoles with absence of staining in the lumen. Overnight treatment with NPC1 inhibitor (U18666A, right panel) increased luminal staining within lysosomes. **B)** PIKfyve regulates cholesterol exit from lysosomal membranes in U2OS cells. . Image shows filipin staining at the plasma membrane and intracellular vesicles in control cells (Control, left panel), whereas overnight treatment with YM201 (0.5μM,1μM, middle panels) increased filipin staining at the membranes of enlarged lysosomal vacuoles with absence of staining in the lumen. Overnight treatment with NPC1 inhibitor (U18666A, right panel) increased luminal staining within lysosomes. Images show confocal slices of a single xy-plane. Scale bars equal 10μm.

To examine if analogous to overnight treatment, short-term PIKfyve inhibition would show a similar effect, MEFs were subject to 4h treatment with PIKfyve inhibitors and stained for filipin. While control cells showed weak staining at the plasma membrane and some intracellular vesicles (Figure 3.3A), PIKfyve-inhibited cells showed dramatically increased intracellular vesicular staining (Figure 3.3A), with the enlarged vacuoles showing membrane staining and empty lumens (Figure 3.3A, inset). Quantification of the whole cell mean fluorescent

intensity showed an approximately 1.7-fold increase in total filipin staining in the cells with PIKfyve inhibition (Figure 3.3B).

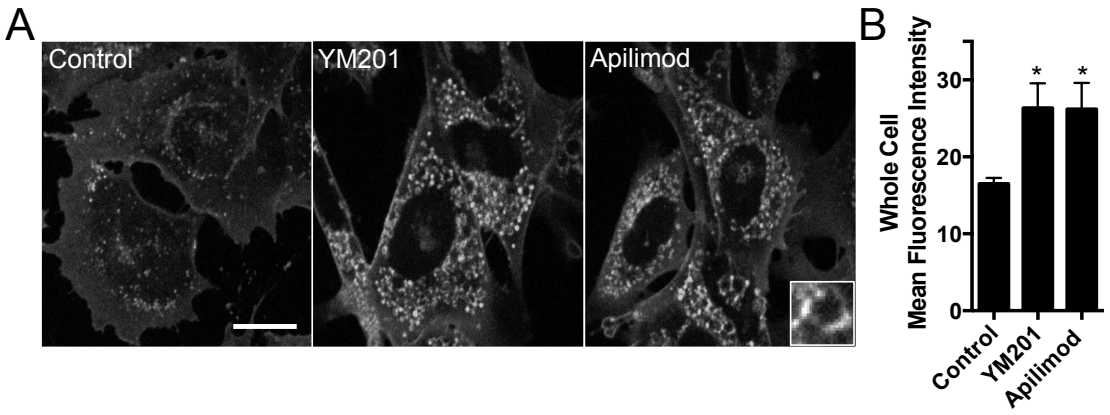

Figure 3.3. Short-term PIKfyve inhibition regulates cholesterol trafficking in the cell. A) Image shows weak filipin staining at the plasma membrane and intracellular vesicles in control MEFs (Control, left panel), whereas 4hours of treatment with PIKfyve inhibitors (YM201, Apilimod, middle and right panels) increased filipin staining at the membranes of enlarged lysosomal vacuoles with absence of staining in the lumen. Inset shows a zoomed in image of an enlarged vacuole with filipin staining at the membrane. Images show confocal slices of a single z-plane. Scale bars equal 10μm. **B)** PIKfyve inhibition increased mean fluorescent intensity of filipin staining in whole cells. Graph shows quantification of whole cell mean fluorescent intensity in cells after 4hours of control, YM201 and Apilimod treatment. Error bars show mean±SD, for Control n=3 and YM201 n=3 cells. *p<0.05 (Student's t-test).

To examine if cholesterol was accumulating on lysosomal membranes, we treated MCF10A cells expressing lysosomal marker LAMP1-GFP with PIKfyve inhibitors and U18666A, followed by filipin staining. While some lysosomes in control cells show weak colocalization with filipin (Figure 3.4A top panel), almost all the lysosomes in PIKfyve-inhibited and U18666A-treated cells show increased colocalization with filipin (Figure 3.4A, lower panels). Importantly, quantification of the total lysosomal filipin fluorescence indicated that PIKfyve-inhibited and U18666A-treated cells have at least 3- to 4-fold higher filipin staining (Figure 3.4B). While lysosomes in both U18666A and YM201-treated cells showed increased filipin fluorescence, U18666A treatment led to cholesterol

accumulation in the lumen of the lysosomes whereas YM201 treatment led to cholesterol accumulation in the lysosomal membrane, in the absence of luminal staining (Figure 3.4C). These data suggest that PIKfyve is required for cholesterol exit from the lysosomal membrane, with its inhibition leading to cholesterol accumulation in the limiting membranes of lysosomes.

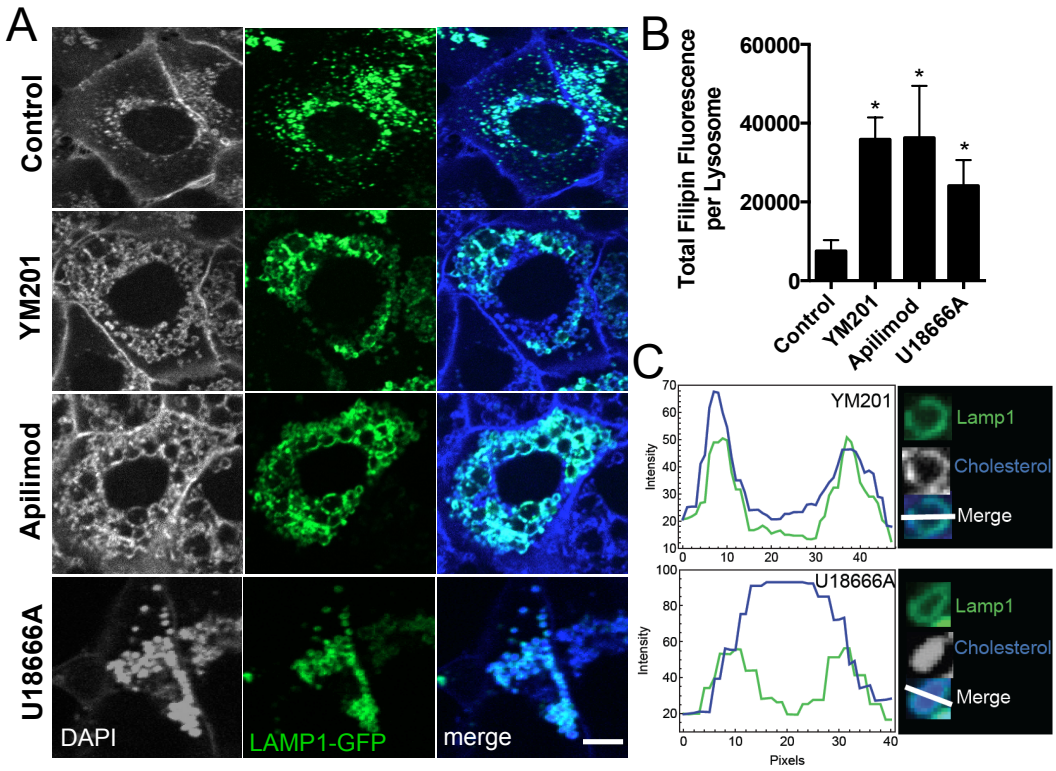

Figure 3.4. PIKfyve regulates cholesterol exit from lysosomal membranes. A) PIKfyve inhibition causes increased filipin staining at lysosomal membranes. Top panel, some lysosomes (green) in control MCF10A cells expressing LAMP1-GFP show weak colocalization with filipin (grayscale). Middle panels, lysosomes in cells treated with YM201 and Apilimod for 3 hours show increased colocalization with filipin at the lysosomal membranes. Bottom panel, lysosomes in cells treated with U18666A for 3 hours show increased colocalization with filipin in the lysosome lumen. **B)** PIKfyve inhibition increases total filipin fluorescence per lysosome. Graph shows total fluorescent intensity of filipin staining per lysosome in the cell. Error bars show mean±SD for Control n=3, YM201 n=3, Apilimod n=3 and U18666A n=3 cells, *p<0.05 (Student's t-test). **C)** PIKfyve inhibition causes increased filipin staining at lysosomal membranes with absent staining in the lumen. Line-scan imaging of lysosomes in YM201-treated cells (top panel) show higher filipin intensity at lysosomal membrane (colocalization with LAMP1-GFP), whereas U18666A-treated cells (bottom panel) show higher filipin intensity within the lysosome lumen. Images show confocal slices of a single xy-plane. Scale bars equal 10μm.

3.2.2 PIKfyve regulates cholesterol biosynthetic and uptake pathways

Cholesterol exit from the lysosomes is required for its utilization by the cell and inhibition of this efflux induces a cellular sterol depletion response, which leads SREBP cleavage and increased transcription of *HMG-CoA* and *LDLR* (Brown and Goldstein, 1997). Since PIKfyve regulates cholesterol exit from the lysosomal membranes, we hypothesized that PIKfyve inhibition would upregulate the cholesterol biosynthetic pathways. Indeed, treatment of cells with PIKfyve inhibitors led to increased cleavage of SREBP-1 and SREBP-2 proteins (Figure 3.5A,B). PIKfyve inhibition also increased the level of LDLR protein in cells compared to vehicle treatment (Figure 3.5C). As expected U18666A treatment also increased SREBP cleavage and LDLR protein levels in the cells, although the effect was not to the same extent as with PIKfyve inhibition (Figure 3.5).

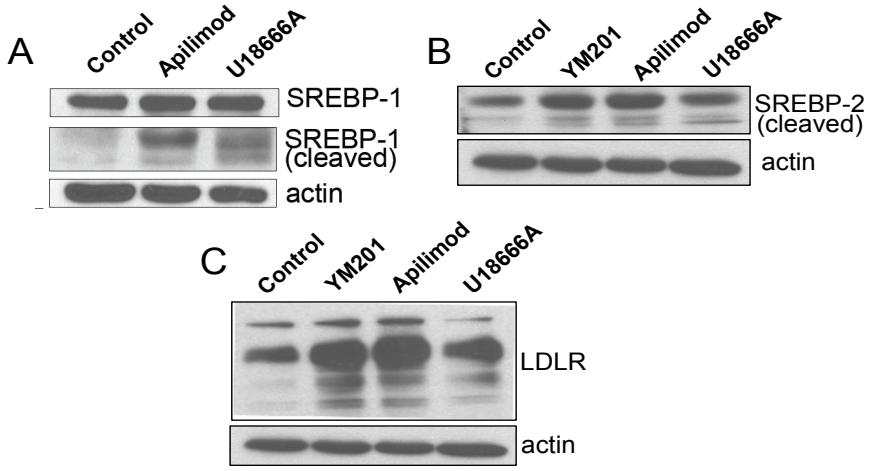

Figure 3.5. PIKfyve regulates SREBP cleavage and LDLR expression. A) PIKfyve inhibition causes SREBP-1 cleavage. Western blot in MEFs shows cleavage of SREBP-1 in PIKfyve-inhibited (Apilimod) and NPC1-inhibited (U18666A) conditions compared to controls. **B)** PIKfyve inhibition causes SREBP-2 cleavage. Western blot in MEFs shows cleavage of SREBP-2 in PIKfyve-inhibited (YM201, Apilimod) and NPC1-inhibited (U18666A) conditions compared to controls. **C)** PIKfyve inhibition upregulates expression of LDLR at the protein level. Western blot in MEFs shows increased LDLR protein levels in PIKfyve-inhibited (YM201, Apilimod) and NPC1-inhibited (U18666A) conditions compared to controls.

Similarly PIKfyve inhibition also increased the expression of LDLR and HMG-CoA reductase at the mRNA levels over time (Figure 3.6). These data suggest that PIKfyve inhibition upregulates cholesterol biosynthetic pathways in the cell, potentially as a response to cholesterol depletion induced by its accumulation in the lysosomal membranes.

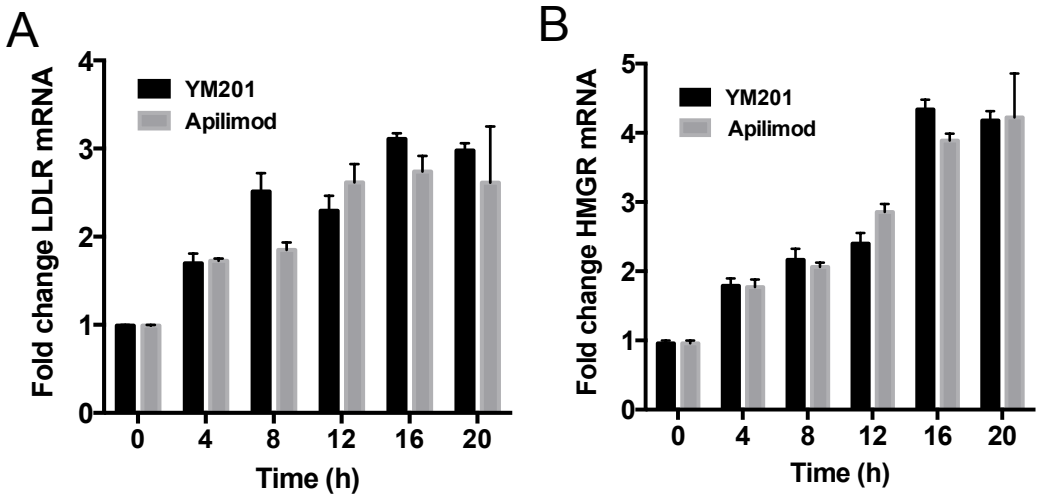

Figure 3.6. PIKfyve regulates the mRNA expression of genes involved in cholesterol uptake and biosynthetic pathways. A) PIKfyve inhibition in MEFs increased LDLR mRNA levels overtime. Graph shows fold change in LDLR mRNA levels with 4-20 hours of treatment with PIKfyve inhibitors YM201 and Apilimod. **B)** PIKfyve inhibition in MEFs increased HMGCR mRNA levels overtime. Graph shows fold change in HMGCR mRNA levels with 4-20 hours of treatment with PIKfyve inhibitors YM201 and Apilimod. Error bars show mean±SD.

3.2.3 PIKfyve regulates cholesterol exit from lysosomal membranes downstream of NPC1

Given that NPC1 is required for cholesterol transfer from the lysosomal lumen to the limiting membrane, and PIKfyve regulates the exit of cholesterol from the lysosome membrane, we hypothesized that NPC1 functions upstream of PIKfyve in the same pathway. To investigate this, cells were simultaneously inhibited for NPC1 (U18666A) and PIKfyve (YM201/Apilimod) and stained for cholesterol with filipin. Indeed, cells with dual inhibition of NPC1 and PIKfyve showed increased filipin staining in the lysosomal lumen similar to NPC1-inhibited cells (U18666A) (Figure 3.7). These results are consistent with a model that PIKfyve is required for cholesterol exit from lysosomal membranes downstream of NPC1.

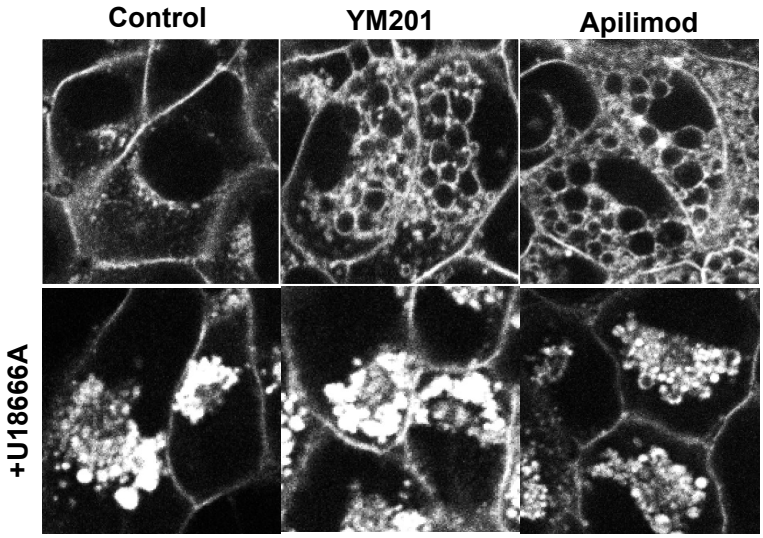

Figure 3.7. PIKfyve regulates cholesterol exit from lysosomes downstream of NPC1. Dual inhibition of PIKfyve and NPC1 in MCF10A cells causes accumulation of cholesterol within lysosome lumens. PIKfyve inhibition by YM201 and Apilimod increased filipin staining at lysosomal membranes (top panel), whereas simultaneous NPC1 inhibition by U18666A increased filipin staining in the lysosome lumen in control (bottom left) and PIKfyve-inhibited cells (bottom middle and right image). Images show confocal slices of a single xy-plane. Scale bars equal 10μm.

3.2.4 PIKfyve-dependent cholesterol trafficking regulates lysosome morphology

The cholesterol content of cellular membranes is known to impact membrane morphology, fluidity, fission events as well as lipid packing (Simons and Ehehalt, 2002). PIKfyve plays a key role in maintaining lysosome size, with its inhibition leading to cytosolic vacuolation due to enlarged lysosomes. We hypothesized that cholesterol accumulation in the lysosome membranes in response to PIKfyve inhibition could contribute to lysosomal enlargement. In this model, preventing cholesterol export from the lumen to the limiting membrane by NPC1 inhibition would be predicted to reduce lysosomal enlargement in PIKfyve-inhibited cells.

Indeed, while PIKfyve-inhibited cells contain enlarged lysosomes, simultaneous inhibition of NPC1 was able to rescue this effect. While the average lysosome size in PIKfyve-inhibited cells was much higher compared to control and NPC1 cells as expected (Figure 3.8A,B), it was significantly lower in the dual-inhibited cells. These data suggest a potential role for cholesterol in PIKfyve-dependent regulation of lysosome size. It is possible that the enlarged lysosomes and reduced lysosome fission observed during PIKfyve inhibition is due to excessive cholesterol accumulation in the limiting membrane of lysosomes, which could severely limit membrane bending and vesicle budding.

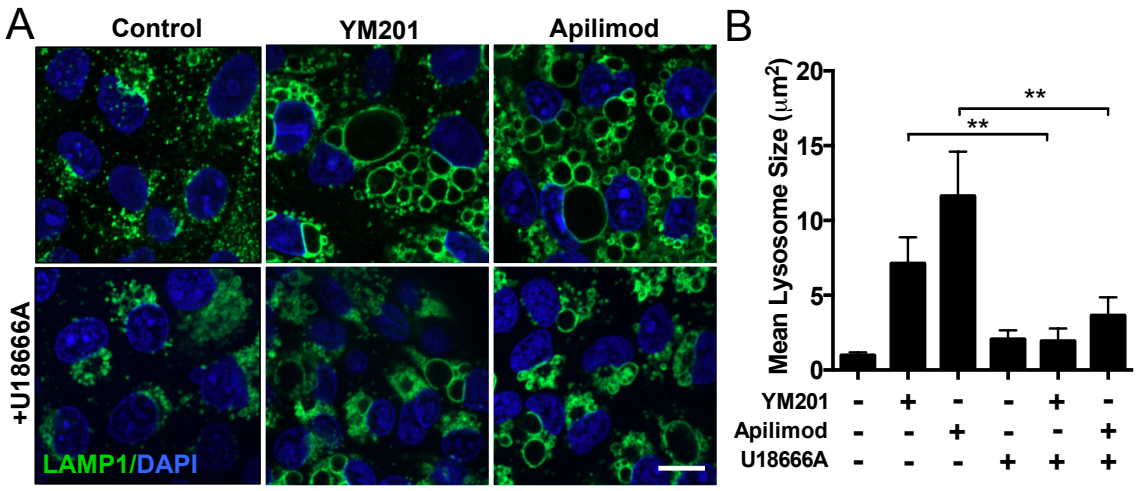

Figure 3.8. PIKfyve-dependent cholesterol trafficking regulates lysosome size. A) Dual inhibition of PIKfyve and NPC1 rescues lysosomal enlargement in PIKfyve-inhibited MCF10A cells. Top, PIKfyve inhibition with YM201 and Apilimod increased lysosome size as seen by LAMP1 immunofluorescent staining (top panel), which was rescued by simultaneous treatment with NPC1 inhibitor U18666A (bottom panel). Images show confocal slices of a single z-plane. Scale bars equal 10μm. **B)** Graph shows mean lysosome size in MCF10A cells treated with YM201 and Apilimod, with or without U18666A treatment. Error bars show mean±SD for Control n=3, YM201 n=3, Apilimod n=3 and U18666A n=3 cells, *p<0.05 (Student's t-test).

3.2.5 PIKfyve regulates formation of microdomains on lysosomal membranes

Cholesterol is known to regulate formation of higher order microdomains within membranes that can partition proteins and lipids. Interestingly, it was recently reported that micrometer-scale cholesterol enriched domains can form on the yeast vacuole under different cellular stresses that partitions vacuole membrane proteins, in a manner dependent on the yeast PIKfyve ortholog Fab1 (Toulmay and Prinz, 2013). Given the observed role of PIKfyve in regulating cholesterol content of lysosomal membranes, we examined if lysosomal proteins

in mammalian cells would also undergo partitioning in a PIKfyve-dependent manner.

In order to image these small micrometer-sized domains, we monitored the large lysosomal compartments formed during entosis in breast tumor MCF7 cells expressing LAMP1-GFP. Interestingly, we observe partitioning of LAMP1 into micrometer scale domains on the entotic vacuole membrane in a subset of cells (Figure 3.9A). We performed detailed analysis of lysosomal transmembrane as well as recruited cytosolic proteins to further determine the components of these domains. Intriguingly, the PIKfyve effector TRPML1 partitioned together with LAMP1 in the microdomains (data not shown), while Rab7 effectors FYCO and RILP and mTORC1 activator RagB partitioned away from the LAMP1 domains on the vacuole (Figure 3.9B, data not shown). These preliminary data suggest a potential pattern of transmembrane proteins localizing in domains separate from cytosolic proteins. This pattern of partitioning indeed resembles the lipid domains seen on the yeast vacuole that are enriched in cholesterol in the partitions containing cytosolic proteins (Toulmay and Prinz, 2013).

Interestingly, we observe that these domains can persist for long periods of time, although sometimes they spontaneously resolve resulting in a smooth pattern of LAMP1 on the entotic vacuole (Figure 3.9C). Given that PIKfyve can regulate cholesterol content of lysosomal membranes, we hypothesized that PIKfyve inhibition might alter the observed domain architecture. Indeed, PIKfyve inhibition by treatment of YM201 led to rapid resolution of these domains (Figure 3.9D). These data suggest that PIKfyve activity is required for the maintenance of

the domain architecture, potentially due to its role in regulating lysosomal membrane cholesterol content.

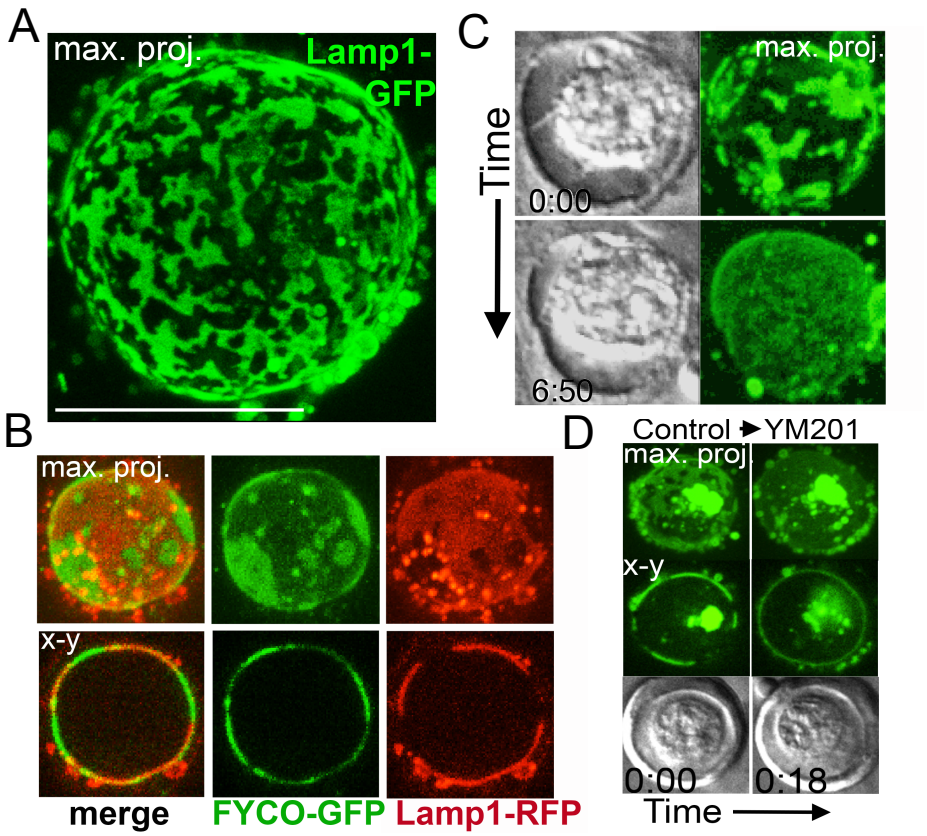

Figure 3.9. PIKfyve regulates formation of microdomains on lysosomal membranes and partitioning of lysosomal proteins. A) LAMP1 is partitioned into microdomains in entotic vacuoles. Image shows maximum projection of a corpse-containing entotic vacuole containing MCF7 cells expressing LAMP1-GFP. **B)** Lysosomally recruited cytosolic protein FYCO (green) is partitioned in microdomains away from LAMP1 (red). Maximum projection (top) and single z-plane (bottom) of an entotic corpse in MCF7 cells expressing FYCO-GFP and LAMP1-RFP. **C)** Membrane microdomains can resolve spontaneously. Image shows maximum projection an entotic corpse (DIC, top left panel) with LAMP1-GFP microdomains (green, top right panel) resolves spontaneously to form a smooth continuous pattern (bottom panel). **D)** PIKfyve regulates the resolution of membrane microdomains. Image shows maximum projection (top panel), single z plane (middle panel) and DIC (bottom panel) of LAMP1-GFP microdomains on an entotic corpse treated with YM201. Scale bars equal 10μm.

3.3 DISCUSSION

The data presented here establish a novel role for PIKfyve in regulating cholesterol exit from lysosomes. Since the role of PIKfyve in amino acid export is potentially due to changes in the surface area to volume ratio of macroendocytic vacuoles, it would likely regulate the export of nutrients generally. Therefore we hypothesized that it would regulate cholesterol efflux from the lysosome lumen to the cytosol and its inhibition would cause accumulation of cholesterol in the lumen. Instead, our data show that while PIKfyve does regulate cholesterol egress from the lysosome, its inhibition causes increased accumulation of cholesterol in the limiting membrane of lysosomes rather than the lumen. These data suggest that PIKfyve plays a very specific role in regulating cholesterol export in the endocytic pathway (Figure 3.10). Future studies with genetic loss-of-function of PIKfyve and NPC1 will be needed to further interrogate this model.

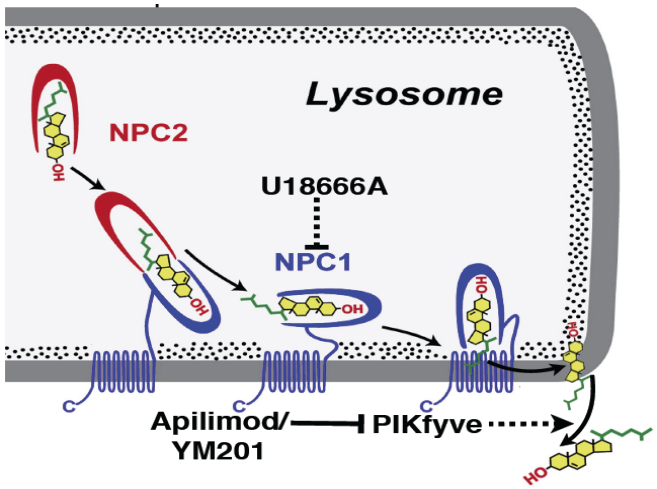

Figure 3.10. Model depicting the role of PIKfyve in regulating cholesterol exit from lysosomes. In the lysosomal lumen, NPC2 binds to free cholesterol and transfers it to transmembrane NPC1. NPC1 then delivers the cholesterol to the lysosomal membrane, following which PIKfyve regulates its exit from the membrane to the ER or plasma membrane. Inhibition of NPC1 by U18666A causes accumulation of cholesterol in the lysosome lumen, whereas inhibition of PIKfyve by YM201 and Apilimod causes accumulation of cholesterol in the limiting membrane of lysosomes. Figure adapted from (Kwon et al., 2009).

However the exact mechanism of how PIKfyve mediates this cholesterol efflux from the lysosomal membrane is unclear and remains to be uncovered. In the lysosomal lumen free cholesterol binds to NPC2 that delivers it to transmembrane NPC1, which then directs it to the lysosomal membrane (Kwon et al., 2009). The mechanisms regulating the egress of cholesterol from the lysosomal membrane have not been well studied. While some studies suggest a role for NPC1 in cholesterol exit from the lysosomal membrane, others speculate the requirement of additional cytosolic cholesterol binding proteins or even vesicular fission mechanisms (Kwon et al., 2009). One study has identified a role for ORP5, an ER resident OSBP-related protein, in regulating cholesterol efflux from the lysosomal membrane to the ER downstream of NPC1 (Du et al., 2011). ORP5 loss-of-function, similar to PIKfyve inhibition, leads to accumulation of cholesterol in the lysosomal membrane and is speculated to interact with NPC1 at ER-lysosome contact sites (Du et al., 2011). Interestingly, it was also recently reported that peroxisome-lysosome contacts mediated by peroxisomal PI(4,5)P2 could regulate cholesterol transport from the lysosomal membrane to peroxisomes (Chu et al., 2015). It is likely that PIKfyve, its lipid products PI(3,5)P2/PI5P and their effectors might interact with ORP5 downstream of NPC1 or help mediate organelle contacts that could potentially regulate cholesterol efflux from the lysosomal membrane. Additionally, given the role of PIKfyve in regulating vacuole fission, it is also possible that cholesterol is transported from the lysosomal through PIKfyve-dependent vesicle fission.

We also find that PIKfyve-dependent cholesterol efflux from the lysosome has critical consequences for the cell. The impairment of cholesterol transport to the ER/cytosol triggers the SREBP-dependent sterol starvation response in the cell that leads to an upregulation of cholesterol biosynthetic and uptake pathways. While the current study was conducted in non-transformed cells, it is likely that in the context of cholesterol uptake by tumor cells PIKfyve inhibition would prevent cholesterol efflux and thereby reduce its utilization by the cell. However since subsequent upregulation of biosynthesis could compensate for this reduction, a combined inhibition of PIKfyve and cholesterol biosynthesis (using HMG-CoA Reductase Inhibitors/Statins) could be a useful strategy to prevent cholesterol utilization by tumor cells.

Additionally, we find that cholesterol in the lysosomal membrane may have significant consequences for membrane dynamics and morphology. Due to its unique structure, cholesterol can increase ordering and packing of lipids in the membrane, which consequently decrease its fluidity and permeability to polar molecules (Simons and Vaz, 2004). However excess membrane cholesterol could increase membrane rigidity enough to significantly impair diffusion of ions and solutes across the membrane and also prevent membrane bending (Ikonen, 2008). We find that the accumulation of cholesterol due to PIKfyve inhibition may contribute to lysosome enlargement. Removal of excess cholesterol from the lysosomal membrane by NPC1 inhibition can rescue the lysosome enlargement defect seen by PIKfyve inhibition. These data are consistent with a model that cholesterol in the lysosome membrane could prevent its fission, perhaps by

increasing its rigidity and preventing sufficient membrane bending to allow vesicle budding. While PIKfyve has been shown to maintain lysosome size through calcium-dependent membrane fission, our data suggest that a contributing mechanism by which PIKfyve maintains lysosome size is by removing cholesterol from the lysosomal membrane. Although further studies are needed to corroborate this, it is also possible that PIKfyve-dependent cholesterol efflux is required for nutrient export through surface area changes by vacuole fission or direct alteration of membrane transporter activity.

We also find that PIKfyve regulates formation of microdomains on the lysosomal membrane. Cholesterol regulates the ordering of specific lipids into “raft-like” membrane microdomains that have been shown to partition different proteins on the yeast vacuole in a Fab1-dependent manner (Toulmay and Prinz, 2013). We observe similar partitions formed on the lysosomal compartments containing entotic corpses that are regulated in a similar fashion by PIKfyve. While we were unable to perform immunofluorescence staining on these structures as fixation of the cells destabilized the domain architecture, future studies with fluorescent lipid dyes might help ascertain their cholesterol and lipid content. The observation that PIKfyve inhibition resolves these partitions and causes cholesterol accumulation in the lysosome membrane suggests that they are likely “raft-like” cholesterol enriched domains. Finally, these microdomains could have important consequences for the proteins they partition, potentially affecting their activity or binding partners. In particular, the PIKfyve-dependent partitioning of its effector TRPML1 into microdomains with different lipid content

could be critical for its function in regulating calcium flux and hence vacuole fission. Indeed, rafts-like domains have been shown to specifically recruit machinery for mediating fission events (Ciarlo et al., 2010). The precise function of these domains in regulating the activity of the proteins partitioned and their effects on membrane dynamics needs to be explored further.

3.4 MATERIALS AND METHODS

3.4.1 Cell culture, Constructs and Reagents

MCF10A cells were obtained from American Type Culture Collection (ATCC, Manassas, VA) and cultured as described (Florey et al., 2011). MEFs (ATCC) and MCF7 cells (ATCC) were cultured in DMEM plus 10% heat-inactivated fetal bovine serum (FBS) with penicillin/streptomycin (pen/strep). U2OS cells (kind gift from Frederick Maxfield) were cultured in McCoy's 5A Media 10% heat-inactivated fetal bovine serum (FBS) with penicillin/streptomycin (pen/strep). MCF10A and MCF7 cells expressing LAMP1-GFP were prepared by retroviral transduction with pRetro-LAMP1-GFP construct as described previously (Florey et al., 2011). $1x10^6$ MCF7 cells were nucleofected with LAMP1-RFP and FYCO-GFP with Amaxa Nucleofector Solution V (Lonza, Switzerland) and imaged 24h post-transfection. Cells were treated with YM201636 (524611, Calbiochem, EMD Millipore, Massachusetts) at 0.4μM for MCF10A cells and 1μM for MEFs and MCF7 cells, Apilimod (STA5326, Axon1369, Axon Medchem, Netherlands) at 0.1μM for MCF10A cells and 10-25nM for MEFs, U18666A (16-381-0, Tocris Biosciences, Bristol, UK) at 20μg/ml for MCF10A and 10μg/ml for MEFs unless otherwise indicated.

3.4.2 Western Blotting

Cell Lysis was performed in ice-cold RIPA buffer, followed by SDS-PAGE and western blotting, using anti–SREBP1 (557036; BD Biosciences), anti–SREBP2 (557037; BD Biosciences), anti-LDLR (ab30532; Abcam) and anti-actin (A1978; Sigma) antibodies.

3.4.3 Immunofluorescence Staining and Analysis

Filipin fluorescence staining was performed on cells cultured on glass-bottom dishes. Briefly, MEFs or MCF10A cells were plated at density of 50-100K per dish. After treatment with inhibitors the cells were fixed with 3% paraformaldehyde for 30 minutes at room temperature, following which they were quenched with 1.5mg/ml glycine solution for 15 minutes. The cells were then stained with 0.05mg/ml Filipin III (Sigma) solution for 2 hours and imaged using a UV filter set (340-380nm excitation) using the Ultraview Vox spinning-disk confocal system (Perkin Elmer, Waltham, MA) to acquire Z-stack images using Volocity software (Perkin Elmer). Mean whole cell filipin fluorescent intensity was quantified manually using ImageJ software and total filipin fluorescence per lysosome (Total filipin fluorescence of lysosomes in the cell/Total lysosome number in the cell) was quantified manually using Volocity software. Immunofluorescence for LAMP1 was performed on cells cultured on glass-bottom dishes (MatTek) as described previously (Overholtzer et al., 2007). Cells were fixed in 1:1 chilled Methanol:Acetone at -20°C for 5 minutes. The antibody used for IF was anti-Lamp1 (BD555798). Confocal microscopy was performed using the Ultraview Vox spinning-disk confocal system (Perkin Elmer, Waltham, MA) to acquire Z-stack images using Volocity software (Perkin Elmer). Lysosomal size (area of lysosomes) was determined by LAMP1 fluorescence and quantified manually using Volocity software.

3.4.4 Microdomain Imaging

MCF7 cells stably transfected with LAMP1-GFP or transiently transfected with FYCO-GFP/LAMP1-RFP were plated on glass-bottom dishes (MatTek) and imaged the next day in 37°C and 5% CO_2 live-cell incubation chambers. Entotic vacuole showing partitioning of LAMP1 into microdomains were imaged by time-lapse confocal microscopy. DIC and fluorescent images were acquired in 0.5µm z-steps, at maximum speed, using the Ultraview Vox spinning-disk confocal system (Perkin Elmer) coupled to a Nikon Ti-E microscope as described (Krajcovic et al., 2013).

3.4.5 Quantitative PCR

Total RNA was extracted from shRNA expressing cells using TRIzol® Plus RNA Purification Kit (12183-555, Thermo Fisher Scientific, USA). Quantitative PCR was performed using the Bio-Rad iCycler real-time system (MyiQ), with SYBR green detection (iScript One-Step RT-PCR Kit with SYBR green (Bio-Rad). Samples were analyzed by the standard curve method in triplicate. Primers against *mLDLR* (QT00109823), *mHMGCR* (QT01037848) and *mGAPDH* (QT01658692) were obtained from Qiagen.

3.4.6 Statistics and Representative Figures

Error bars show mean±SD unless otherwise indicated. P-values were obtained using two-tailed unpaired Student's t-test as all comparisons were between two groups - control and experimental. Western blots and immunofluorescence images are representatives from least 3 independent experiments unless otherwise indicated.

CHAPTER 4: Conclusion and Future Perspectives

4.1 SUMMARY

The regulation of vacuole fission, lysosome trafficking and nutrient export during engulfment is poorly understood. In my thesis we have identified the lipid kinase PIKfyve as a critical regulator of vacuole fission that redistributes engulfed cargo into the lysosome network during the processes of macropinocytosis, phagocytosis and entosis. We find that PIKfyve regulates vacuole fission and shrinkage in an mTORC1-independent manner, in part through its downstream effector TRPML1. Lysosomal cation fluxes and osmotic changes regulate vacuole fission downstream of PIKfyve and TRPML1. We also find that PIKfyve promotes the recovery of nutrients from macroendocytic vacuoles during engulfment, suggesting a potential link between PIKfyve activity and lysosomal nutrient export. During nutrient depletion, PIKfyve-dependent nutrient recovery protects engulfing cells from starvation-induced cell death. In particular, we find that PIKfyve activity is required to support the albumin-dependent growth of Ras-mutant cells during leucine starvation. These data identify PIKfyve as a critical regulator of vacuole fission and nutrient recovery during engulfment.

We have also found that PIKfyve is required for cholesterol exit from the lysosomal membrane downstream of NPC1. This PIKfyve-dependent cholesterol efflux is required for maintaining intracellular cholesterol levels and its inhibition induces SREBP cleavage and activation of sterol biosynthetic pathways. We also find that PIKfyve-mediated cholesterol exit is required to maintain lysosome size

and morphology. PIKfyve activity is also required for the formation of membrane microdomains on the large lysosomal compartments containing entotic corpses. These microdomains partition lysosomal membrane proteins like LAMP1/TRPML1 and cytosolic proteins like FYCO/RILP/RagB into distinct sections of the membrane. These data identify a role for PIKfyve in regulating cholesterol trafficking at the lysosomal membrane with critical consequences on lysosome size, morphology and microdomain formation.

4.2 FUTURE DIRECTIONS

4.2.1 Molecular Mechanism of PIKfyve-dependent fission and nutrient recovery

We have demonstrated that PIKfyve activity is critical for regulating vacuole fission during engulfment. While we have found that PIKfyve regulates fission in an mTORC1-independent pathway through TRPML1 and lysosomal cation fluxes, the molecular machinery required for vesicle budding is still unclear. Vesicle fission can occur through different pathways in the cell involving clathrin, caveolin, dynamin, retromer, sorting nexins, COPI and COPII. It has been shown that clathrin and its adaptor proteins regulate budding from autolysosomes during ALR (Rong et al., 2012). We have also found that inhibition of clathrin as well as dynamin delays entotic vacuole fission (data not shown), suggesting a role for clathrin-dependent vesicle budding during this process. It will be important to investigate through future studies if PIKfyve and TRPML1-dependent ion fluxes affect the recruitment or activity of clathrin and

dynamin during vacuole fission. Similarly, PIKfyve-dependent cholesterol exit from lysosomal membranes could also regulate vacuole fission during engulfment, as cholesterol concentration affects membrane curvature and budding (Simons and Ehehalt, 2002). Identification of the molecular machinery for fission will not only explain the mechanism of vacuole shrinkage, but also help in understanding the link between vacuole fission and nutrient recovery. So far the only two known regulators of vacuole fission, namely mTORC1 and PIKfyve, also regulate nutrient recovery (Figure 2.11, data not shown). However, both kinases can have critical effects on translation, cell growth and proliferation. The effect of inhibition of vesicle budding machinery on nutrient export would help clarify their relationship.

4.2.2 Role of PIKfyve in tumorigenesis

Our findings demonstrate that PIKfyve is required for Ras-mutant cells to scavenge nutrients by macropinocytosis. Ras-mutant cells show an increased dependence on nutrient recovery by macropinocytosis during starvation to satisfy their high metabolic demand (Commisso et al., 2013). This could be of particular importance for pancreatic cancers (>90% have Kras mutations) that are known to be nutrient-deprived due to limited vascularization (Hidalgo, 2010). Since both autophagy and macropinocytosis require lysosome function for nutrient recovery, the use of lysosome inhibitors for pancreatic cancer may hold therapeutic potential. Our data identify PIKfyve as a potential therapeutic target, as its inhibition blocks the ability of Ras-mutant cells to scavenge nutrients by inhibiting

vacuole shrinkage and nutrient export. PIKfyve inhibition has minimal effects on the proliferation of control cells and of Ras-mutant cells in nutrient-replete media, suggesting this strategy could specifically target tumor cells in a nutrient-poor microenvironment. Given that the PIKfyve inhibitor Apilimod is currently in clinical trials for autoimmune disorders and is well tolerated in patients (Burakoff et al., 2006; Krausz et al., 2012), this drug may have potential therapeutic value for patients with Ras-driven cancers.

It is interesting to note that while mTORC1 and PIKfyve both regulate the shrinkage of macroendocytic vacuoles, their inhibition has opposing effects on albumin-mediated rescue of cells harboring oncogenic Kras mutations. mTORC1 inhibition has been shown to increase cell proliferation during starvation by upregulating lysosomal degradation of engulfed albumin (Palm et al., 2015). During Kras-driven pancreatic tumorigenesis *in vivo*, mTORC1 inhibition enhances tumor cell proliferation in the central, nutrient-deprived regions while inhibiting proliferation at the nutrient-replete tumor edges (Palm et al., 2015). Our data demonstrate that PIKfyve inhibition can block the proliferation of starved Ras-mutant cells even when they are mTORC1-inhibited, suggesting that a combined strategy of mTORC1 and PIKfyve inhibition may be an approach to limit proliferation in both nutrient-replete and nutrient-deprived regions of cancers.

4.2.3 Role of PIKfyve and vacuole fission in Antigen Presentation

We have shown that PIKfyve is required for redistribution of the degraded cargo contained in the macroendocytic vacuoles into the lysosome network of the engulfing cell. While we have investigated nutrient trafficking and export, the macroendocytic vacuoles formed can also contain other cargo like antigen. Exogenous antigen can be taken up by phagocytes like dendritic cells via macropinocytosis or phagocytosis. Once engulfed, antigen is processed by the dendritic cell and presented on the cell surface with major histocompatibility complex molecules (MHC) to enable their recognition by T-cells for an adaptive immune response (Villadangos and Schnorrer, 2007). Exogenous antigen is either presented through the traditional MHC Class II pathway involving degradation through the endocytic route or through the MHC Class I cross presentation pathway involving retrograde transport of antigen into the cytosol followed by proteasomal processing (Villadangos and Schnorrer, 2007). We have found that PIKfyve can regulate MHC Class II presentation from antigen-expressing apoptotic corpses as measured by T-cell proliferation and IL-2 production (data not shown), although the exact mechanism underlying this effect is still unclear. This effect could be due to the role of PIKfyve in phagosome fission that would redistribute antigen in the lysosome network of the phagocyte, thereby increasing the surface-area to volume ratio and potentially enhancing the interaction of antigen and MHC Class II molecules. Alternatively, it is also possible that this effect could be due the role of PIKfyve in regulating the cholesterol content and microdomain formation on lysosomal membranes. MHC

Class II complexes are known to cluster on “raft-like” domains on the plasma membrane, and depletion of cholesterol on the plasma membrane impairs antigen presentation (Anderson et al., 2000). Therefore, it is possible that PIKfyve-dependent cholesterol export and microdomain formation regulates MHC Class II clustering or its interaction with degraded antigen itself. Also, whether this effect is specific to apoptotic corpses or any MHC Class II presentation pathway including bacterial pathogen engulfment is also currently unknown. Additionally, if this effect were due to PIKfyve’s role in vacuole fission, it would also be important to investigate if other regulators like mTORC1 and TRPML1 also affect antigen presentation. Investigating the role of PIKfyve and vacuole fission during this process will not only help understanding the mechanism of antigen presentation but also shed light on the effect of this late stage of phagosome maturation on subsequent immune responses by the engulfing phagocytes.

4.2.4 Role of PIKfyve-dependent membrane microdomains in cell signaling

We have found that lysosomal membranes can partition proteins into distinct domains in a PIKfyve-dependent fashion, similar to the “raft-like” lipid domains seen on the yeast vacuole. Lysosomal transmembrane proteins like LAMP1 and TRPML1 cluster in the same domain, and cytosolic proteins that are recruited to the lysosomes such as RILP, FYCO and RagB partition away from LAMP1. While these domains are a unique phenomenon observed in both yeast and now mammalian systems, their functional role remains unclear. It is possible that

similar to lipid domains seen on the plasma membrane, this clustering of proteins could have critical consequences for cell signaling. This could be important for proteins or complexes that are recruited to lysosomal membranes for activation, like mTORC1. The presence of amino acids and glucose can be sensed by lysosomal V-ATPase, which binds to Ragulator and Rag GTPases in order to recruit mTORC1 to the lysosomal membrane for its activation. Interestingly, it was shown that yeast V-ATPase and Gtr2 (RagD GTPase ortholog) segregate into mutually exclusive microdomains on the yeast vacuole upon cellular stresses such as glucose starvation. It is possible that microdomain formation is a means to segregate these proteins as a mechanism to regulate mTORC1 activation; hence upon glucose starvation domain partitioning would be an efficient and rapid way to inactivate mTORC1. Indeed, we have also found in mammalian systems that RagB GTPase partitions away from lysosomal transmembrane proteins, in a fashion similar to yeast RagD GTPase. Future studies would be critical to identify the partitioning of other proteins involved in mTORC1 signaling, and to determine if these partitions indeed regulate mTORC1 activation in response to cellular stresses. Similarly, membrane partitioning could play a similar role in regulating Rab7 signaling, given that its effectors RILP/FYCO in mammalian systems and Ivy1 in yeast segregates away from transmembrane lysosomal proteins. Further work would help clarify the role of these membrane microdomains in different cell signaling pathways and also shed light on their regulation by PIKfyve-dependent cholesterol trafficking.

4.3 CONCLUSION

The findings presented in this thesis identify the lipid kinase PIKfyve as a key regulator of lysosome trafficking and nutrient homeostasis in the cell. PIKfyve regulates vacuole fission during the engulfment and the recovery of nutrients from these vacuoles, which is required for survival and proliferation of engulfing phagocytes and Ras-mutant cells. PIKfyve also plays a unique role in regulating cholesterol trafficking from the lysosomal membrane, which has critical consequences for lysosome size and microdomain formation. These novel functions of PIKfyve can have important physiological consequences in immune diseases, tumorigenesis as well as metabolic disorders. In particular, the function of PIKfyve in the growth of Ras-mutant cells identifies it as a novel therapeutic target for Ras-dependent tumors like pancreatic cancers. Further work with *in vivo* models will help understand the role of PIKfyve-dependent vacuole fission and nutrient homeostasis in different physiological contexts.

REFERENCES

Adam, R.M., Mukhopadhyay, N.K., Kim, J., Di Vizio, D., Cinar, B., Boucher, K., Solomon, K.R., and Freeman, M.R. (2007). Cholesterol sensitivity of endogenous and myristoylated Akt. Cancer research *67*, 6238-6246.

Anderson, H.A., Hiltbold, E.M., and Roche, P.A. (2000). Concentration of MHC class II molecules in lipid rafts facilitates antigen presentation. Nature immunology *1*, 156-162.

Beloribi-Djefaflia, S., Vasseur, S., and Guillaumond, F. (2016). Lipid metabolic reprogramming in cancer cells. Oncogenesis *5*, e189.

Benseler, V., Warren, A., Vo, M., Holz, L.E., Tay, S.S., Le Couteur, D.G., Breen, E., Allison, A.C., van Rooijen, N., McGuffog, C.*, et al.* (2011). Hepatocyte entry leads to degradation of autoreactive CD8 T cells. Proceedings of the National Academy of Sciences of the United States of America *108*, 16735-16740.

Bridges, D., Ma, J.T., Park, S., Inoki, K., Weisman, L.S., and Saltiel, A.R. (2012). Phosphatidylinositol 3,5-bisphosphate plays a role in the activation and subcellular localization of mechanistic target of rapamycin 1. Molecular biology of the cell *23*, 2955-2962.

Brown, M.S., and Goldstein, J.L. (1997). The SREBP pathway: regulation of cholesterol metabolism by proteolysis of a membrane-bound transcription factor. Cell *89*, 331-340.

Burakoff, R., Barish, C.F., Riff, D., Pruitt, R., Chey, W.Y., Farraye, F.A., Shafran, I., Katz, S., Krone, C.L., Vander Vliet, M.*, et al.* (2006). A phase 1/2A trial of STA 5326, an oral interleukin-12/23 inhibitor, in patients with active moderate to severe Crohn's disease. Inflammatory bowel diseases *12*, 558-565.

Cai, X., Xu, Y., Cheung, A.K., Tomlinson, R.C., Alcazar-Roman, A., Murphy, L., Billich, A., Zhang, B., Feng, Y., Klumpp, M.*, et al.* (2013). PIKfyve, a class III PI kinase, is the target of the small molecular IL-12/IL-23 inhibitor apilimod and a player in Toll-like receptor signaling. Chemistry & biology *20*, 912-921.

Chen, X., and Resh, M.D. (2002). Cholesterol depletion from the plasma membrane triggers ligand-independent activation of the epidermal growth factor receptor. The Journal of biological chemistry *277*, 49631-49637.

Chu, B.B., Liao, Y.C., Qi, W., Xie, C., Du, X., Wang, J., Yang, H., Miao, H.H., Li, B.L., and Song, B.L. (2015). Cholesterol transport through lysosome-peroxisome membrane contacts. Cell *161*, 291-306.

Chubb, J.R., Wilkins, A., Thomas, G.M., and Insall, R.H. (2000). The Dictyostelium RasS protein is required for macropinocytosis, phagocytosis and the control of cell movement. Journal of cell science *113 (Pt 4)*, 709-719.

Ciarlo, L., Manganelli, V., Garofalo, T., Matarrese, P., Tinari, A., Misasi, R., Malorni, W., and Sorice, M. (2010). Association of fission proteins with mitochondrial raft-like domains. Cell death and differentiation *17*, 1047-1058.

Commisso, C., Davidson, S.M., Soydaner-Azeloglu, R.G., Parker, S.J., Kamphorst, J.J., Hackett, S., Grabocka, E., Nofal, M., Drebin, J.A., Thompson, C.B.*, et al.* (2013). Macropinocytosis of protein is an amino acid supply route in Ras-transformed cells. Nature *497*, 633-637.

Dayam, R.M., Saric, A., Shilliday, R.E., and Botelho, R.J. (2015). The Phosphoinositide-Gated Lysosomal Ca Channel, TRPML1, Is Required for Phagosome Maturation. Traffic.

de Lartigue, J., Polson, H., Feldman, M., Shokat, K., Tooze, S.A., Urbe, S., and Clague, M.J. (2009). PIKfyve regulation of endosome-linked pathways. Traffic *10*, 883-893.

Debnath, A., Debnath, K., and O'Faolain, L. (2015). Extraction of group index of lossy photonic crystal waveguides. Optics letters *40*, 193-196.

Descloux, C., Ginet, V., Clarke, P.G., Puyal, J., and Truttmann, A.C. (2015). Neuronal death after perinatal cerebral hypoxia-ischemia: Focus on autophagy-mediated cell death. International journal of developmental neuroscience : the official journal of the International Society for Developmental Neuroscience.

Dong, X.P., Shen, D., Wang, X., Dawson, T., Li, X., Zhang, Q., Cheng, X., Zhang, Y., Weisman, L.S., Delling, M.*, et al.* (2010). PI(3,5)P(2) controls membrane trafficking by direct activation of mucolipin Ca(2+) release channels in the endolysosome. Nature communications *1*, 38.

Dove, S.K., Cooke, F.T., Douglas, M.R., Sayers, L.G., Parker, P.J., and Michell, R.H. (1997). Osmotic stress activates phosphatidylinositol-3,5-bisphosphate synthesis. Nature *390*, 187-192.

Dove, S.K., Dong, K., Kobayashi, T., Williams, F.K., and Michell, R.H. (2009). Phosphatidylinositol 3,5-bisphosphate and Fab1p/PIKfyve underPPIn endo-lysosome function. The Biochemical journal *419*, 1-13.

Dove, S.K., Piper, R.C., McEwen, R.K., Yu, J.W., King, M.C., Hughes, D.C., Thuring, J., Holmes, A.B., Cooke, F.T., Michell, R.H.*, et al.* (2004). Svp1p defines a family of phosphatidylinositol 3,5-bisphosphate effectors. The EMBO journal *23*, 1922-1933.

Du, X., Kumar, J., Ferguson, C., Schulz, T.A., Ong, Y.S., Hong, W., Prinz, W.A., Parton, R.G., Brown, A.J., and Yang, H. (2011). A role for oxysterol-binding protein-related protein 5 in endosomal cholesterol trafficking. The Journal of cell biology *192*, 121-135.

Duran, R.V., and Hall, M.N. (2012). Regulation of TOR by small GTPases. EMBO reports *13*, 121-128.

Efeyan, A., Zoncu, R., and Sabatini, D.M. (2012). Amino acids and mTORC1: from lysosomes to disease. Trends in molecular medicine *18*, 524-533.

Erdos, G.W., Raper, K.B., and Vogen, L.K. (1973). Mating Types and Macrocyst Formation in Dictyostelium discoideum. Proceedings of the National Academy of Sciences of the United States of America *70*, 1828-1830.

Florey, O., Gammoh, N., Kim, S.E., Jiang, X., and Overholtzer, M. (2015). V-ATPase and osmotic imbalances activate endolysosomal LC3 lipidation. Autophagy *11*, 88-99.

Florey, O., Kim, S.E., Sandoval, C.P., Haynes, C.M., and Overholtzer, M. (2011). Autophagy machinery mediates macroendocytic processing and entotic cell death by targeting single membranes. Nature cell biology *13*, 1335-1343.

Garrity, A.G., Wang, W., Collier, C.M., Levey, S.A., Gao, Q., and Xu, H. (2016). The endoplasmic reticulum, not the pH gradient, drives calcium refilling of lysosomes. eLife *5*.

Gary, J.D., Wurmser, A.E., Bonangelino, C.J., Weisman, L.S., and Emr, S.D. (1998). Fab1p is essential for PtdIns(3)P 5-kinase activity and the maintenance of vacuolar size and membrane homeostasis. The Journal of cell biology *143*, 65-79.

Green, R.A., Kao, H.L., Audhya, A., Arur, S., Mayers, J.R., Fridolfsson, H.N., Schulman, M., Schloissnig, S., Niessen, S., Laband, K.*, et al.* (2011). A high-resolution C. elegans essential gene network based on phenotypic profiling of a complex tissue. Cell *145*, 470-482.

Guan, X., Qian, Y., Shen, Y., Zhang, L., Du, Y., Dai, H., Qian, J., and Yan, Y. (2015). Autophagy protects renal tubular cells against ischemia / reperfusion injury in a time-dependent manner. Cellular physiology and biochemistry : international journal of experimental cellular physiology, biochemistry, and pharmacology *36*, 285-298.

Guillaumond, F., Bidaut, G., Ouaissi, M., Servais, S., Gouirand, V., Olivares, O., Lac, S., Borge, L., Roques, J., Gayet, O.*, et al.* (2015). Cholesterol uptake disruption, in association with chemotherapy, is a promising combined metabolic

therapy for pancreatic adenocarcinoma. Proceedings of the National Academy of Sciences of the United States of America *112*, 2473-2478.

Guo, J.Y., Chen, H.Y., Mathew, R., Fan, J., Strohecker, A.M., Karsli-Uzunbas, G., Kamphorst, J.J., Chen, G., Lemons, J.M., Karantza, V.*, et al.* (2011). Activated Ras requires autophagy to maintain oxidative metabolism and tumorigenesis. Genes & development *25*, 460-470.

Gupta, P.D., and Waheed, A.A. (1992). Effect of starvation on glucose transport and membrane fluidity in rat intestinal epithelial cells. FEBS letters *300*, 263-267.

He, C., and Klionsky, D.J. (2009). Regulation mechanisms and signaling pathways of autophagy. Annual review of genetics *43*, 67-93.

Hidalgo, M. (2010). Pancreatic cancer. The New England journal of medicine *362*, 1605-1617.

Ho, C.Y., Choy, C.H., Wattson, C.A., Johnson, D.E., and Botelho, R.J. (2015). The Fab1/PIKfyve phosphoinositide phosphate kinase is not necessary to maintain the pH of lysosomes and of the yeast vacuole. The Journal of biological chemistry *290*, 9919-9928.

Hoeller, O., Bolourani, P., Clark, J., Stephens, L.R., Hawkins, P.T., Weiner, O.D., Weeks, G., and Kay, R.R. (2013). Two distinct functions for PI3-kinases in macropinocytosis. Journal of cell science *126*, 4296-4307.

Hong, N.H., Qi, A., and Weaver, A.M. (2015). PI(3,5)P2 controls endosomal branched actin dynamics by regulating cortactin-actin interactions. The Journal of cell biology *210*, 753-769.

Ikonen, E. (2008). Cellular cholesterol trafficking and compartmentalization. Nature reviews Molecular cell biology *9*, 125-138.

Ikonomov, O.C., Sbrissa, D., and Shisheva, A. (2001). Mammalian cell morphology and endocytic membrane homeostasis require enzymatically active phosphoinositide 5-kinase PIKfyve. The Journal of biological chemistry *276*, 26141-26147.

Ikonomov, O.C., Sbrissa, D., and Shisheva, A. (2006). Localized PtdIns 3,5-P2 synthesis to regulate early endosome dynamics and fusion. American journal of physiology Cell physiology *291*, C393-404.

Jefferies, H.B., Cooke, F.T., Jat, P., Boucheron, C., Koizumi, T., Hayakawa, M., Kaizawa, H., Ohishi, T., Workman, P., Waterfield, M.D.*, et al.* (2008). A selective PIKfyve inhibitor blocks PtdIns(3,5)P(2) production and disrupts endomembrane transport and retroviral budding. EMBO reports *9*, 164-170.

Jin, N., Lang, M.J., and Weisman, L.S. (2016). Phosphatidylinositol 3,5-bisphosphate: regulation of cellular events in space and time. Biochemical Society transactions *44*, 177-184.

Jones, R.G., and Thompson, C.B. (2009). Tumor suppressors and cell metabolism: a recipe for cancer growth. Genes & development *23*, 537-548.

Kamphorst, J.J., Cross, J.R., Fan, J., de Stanchina, E., Mathew, R., White, E.P., Thompson, C.B., and Rabinowitz, J.D. (2013). Hypoxic and Ras-transformed cells support growth by scavenging unsaturated fatty acids from lysophospholipids. Proceedings of the National Academy of Sciences of the United States of America *110*, 8882-8887.

Kerr, M.C., Wang, J.T., Castro, N.A., Hamilton, N.A., Town, L., Brown, D.L., Meunier, F.A., Brown, N.F., Stow, J.L., and Teasdale, R.D. (2010). Inhibition of the PtdIns(5) kinase PIKfyve disrupts intracellular replication of Salmonella. The EMBO journal *29*, 1331-1347.

Kim, G.H., Dayam, R.M., Prashar, A., Terebiznik, M., and Botelho, R.J. (2014). PIKfyve inhibition interferes with phagosome and endosome maturation in macrophages. Traffic *15*, 1143-1163.

Krajcovic, M., Johnson, N.B., Sun, Q., Normand, G., Hoover, N., Yao, E., Richardson, A.L., King, R.W., Cibas, E.S., Schnitt, S.J.*, et al.* (2011). A non-genetic route to aneuploidy in human cancers. Nature cell biology *13*, 324-330.

Krajcovic, M., Krishna, S., Akkari, L., Joyce, J.A., and Overholtzer, M. (2013). mTOR regulates phagosome and entotic vacuole fission. Molecular biology of the cell *24*, 3736-3745.

Krausz, S., Boumans, M.J., Gerlag, D.M., Lufkin, J., van Kuijk, A.W., Bakker, A., de Boer, M., Lodde, B.M., Reedquist, K.A., Jacobson, E.W.*, et al.* (2012). Brief report: a phase IIa, randomized, double-blind, placebo-controlled trial of apilimod mesylate, an interleukin-12/interleukin-23 inhibitor, in patients with rheumatoid arthritis. Arthritis and rheumatism *64*, 1750-1755.

Kuma, A., Hatano, M., Matsui, M., Yamamoto, A., Nakaya, H., Yoshimori, T., Ohsumi, Y., Tokuhisa, T., and Mizushima, N. (2004). The role of autophagy during the early neonatal starvation period. Nature *432*, 1032-1036.

Kwon, H.J., Abi-Mosleh, L., Wang, M.L., Deisenhofer, J., Goldstein, J.L., Brown, M.S., and Infante, R.E. (2009). Structure of N-terminal domain of NPC1 reveals distinct subdomains for binding and transfer of cholesterol. Cell *137*, 1213-1224.

Lee, J.H., McBrayer, M.K., Wolfe, D.M., Haslett, L.J., Kumar, A., Sato, Y., Lie, P.P., Mohan, P., Coffey, E.E., Kompella, U.*, et al.* (2015). Presenilin 1 Maintains

Lysosomal Ca(2+) Homeostasis via TRPML1 by Regulating vATPase-Mediated Lysosome Acidification. Cell reports *12*, 1430-1444.

Lim, J.P., and Gleeson, P.A. (2011). Macropinocytosis: an endocytic pathway for internalising large gulps. Immunology and cell biology *89*, 836-843.

Lito, P., Saborowski, A., Yue, J., Solomon, M., Joseph, E., Gadal, S., Saborowski, M., Kastenhuber, E., Fellmann, C., Ohara, K.*, et al.* (2014). Disruption of CRAF-mediated MEK activation is required for effective MEK inhibition in KRAS mutant tumors. Cancer cell *25*, 697-710.

Mancias, J.D., and Kimmelman, A.C. (2011). Targeting autophagy addiction in cancer. Oncotarget *2*, 1302-1306.

Matsui, Y., Takagi, H., Qu, X., Abdellatif, M., Sakoda, H., Asano, T., Levine, B., and Sadoshima, J. (2007). Distinct roles of autophagy in the heart during ischemia and reperfusion: roles of AMP-activated protein kinase and Beclin 1 in mediating autophagy. Circulation research *100*, 914-922.

McNally, K., Audhya, A., Oegema, K., and McNally, F.J. (2006). Katanin controls mitotic and meiotic spindle length. The Journal of cell biology *175*, 881-891.

Michaillat, L., Baars, T.L., and Mayer, A. (2012). Cell-free reconstitution of vacuole membrane fragmentation reveals regulation of vacuole size and number by TORC1. Molecular biology of the cell *23*, 881-895.

Moore, K.J., Rayner, K.J., Suarez, Y., and Fernandez-Hernando, C. (2010). microRNAs and cholesterol metabolism. Trends in endocrinology and metabolism: TEM *21*, 699-706.

Nicot, A.S., Fares, H., Payrastre, B., Chisholm, A.D., Labouesse, M., and Laporte, J. (2006). The phosphoinositide kinase PIKfyve/Fab1p regulates terminal lysosome maturation in Caenorhabditis elegans. Molecular biology of the cell *17*, 3062-3074.

Overholtzer, M., and Brugge, J.S. (2008). The cell biology of cell-in-cell structures. Nature reviews Molecular cell biology *9*, 796-809.

Overholtzer, M., Mailleux, A.A., Mouneimne, G., Normand, G., Schnitt, S.J., King, R.W., Cibas, E.S., and Brugge, J.S. (2007). A nonapoptotic cell death process, entosis, that occurs by cell-in-cell invasion. Cell *131*, 966-979.

Palm, W., Park, Y., Wright, K., Pavlova, N.N., Tuveson, D.A., and Thompson, C.B. (2015). The Utilization of Extracellular Proteins as Nutrients Is Suppressed by mTORC1. Cell *162*, 259-270.

Pavlova, N.N., and Thompson, C.B. (2016). The Emerging Hallmarks of Cancer Metabolism. Cell metabolism *23*, 27-47.

Racoosin, E.L., and Swanson, J.A. (1993). Macropinosome maturation and fusion with tubular lysosomes in macrophages. The Journal of cell biology *121*, 1011-1020.

Ravichandran, K.S., and Lorenz, U. (2007). Engulfment of apoptotic cells: signals for a good meal. Nature reviews Immunology *7*, 964-974.

Rong, Y., Liu, M., Ma, L., Du, W., Zhang, H., Tian, Y., Cao, Z., Li, Y., Ren, H., Zhang, C*., et al.* (2012). Clathrin and phosphatidylinositol-4,5-bisphosphate regulate autophagic lysosome reformation. Nature cell biology *14*, 924-934.

Rudge, S.A., Anderson, D.M., and Emr, S.D. (2004). Vacuole size control: regulation of PtdIns(3,5)P2 levels by the vacuole-associated Vac14-Fig4 complex, a PtdIns(3,5)P2-specific phosphatase. Molecular biology of the cell *15*, 24-36.

Rusten, T.E., Rodahl, L.M., Pattni, K., Englund, C., Samakovlis, C., Dove, S., Brech, A., and Stenmark, H. (2006). Fab1 phosphatidylinositol 3-phosphate 5-kinase controls trafficking but not silencing of endocytosed receptors. Molecular biology of the cell *17*, 3989-4001.

Samie, M., Wang, X., Zhang, X., Goschka, A., Li, X., Cheng, X., Gregg, E., Azar, M., Zhuo, Y., Garrity, A.G*., et al.* (2013). A TRP channel in the lysosome regulates large particle phagocytosis via focal exocytosis. Developmental cell *26*, 511-524.

Sancak, Y., Peterson, T.R., Shaul, Y.D., Lindquist, R.A., Thoreen, C.C., Bar-Peled, L., and Sabatini, D.M. (2008). The Rag GTPases bind raptor and mediate amino acid signaling to mTORC1. Science *320*, 1496-1501.

Sbrissa, D., Ikonomov, O.C., Fenner, H., and Shisheva, A. (2008). ArPIKfyve homomeric and heteromeric interactions scaffold PIKfyve and Sac3 in a complex to promote PIKfyve activity and functionality. Journal of molecular biology *384*, 766-779.

Sbrissa, D., Ikonomov, O.C., Fu, Z., Ijuin, T., Gruenberg, J., Takenawa, T., and Shisheva, A. (2007). Core protein machinery for mammalian phosphatidylinositol 3,5-bisphosphate synthesis and turnover that regulates the progression of endosomal transport. Novel Sac phosphatase joins the ArPIKfyve-PIKfyve complex. The Journal of biological chemistry *282*, 23878-23891.

Sbrissa, D., Ikonomov, O.C., and Shisheva, A. (1999). PIKfyve, a mammalian ortholog of yeast Fab1p lipid kinase, synthesizes 5-phosphoinositides. Effect of insulin. The Journal of biological chemistry *274*, 21589-21597.

Seo, J.W., Choi, J., Lee, S.Y., Sung, S., Yoo, H.J., Kang, M.J., Cheong, H., and Son, J. (2016). Autophagy is required for PDAC glutamine metabolism. Scientific reports *6*, 37594.

Shisheva, A. (2001). PIKfyve: the road to PtdIns 5-P and PtdIns 3,5-P(2). Cell biology international *25*, 1201-1206.

Shisheva, A. (2012). PIKfyve and its Lipid products in health and in sickness. Current topics in microbiology and immunology *362*, 127-162.

Simons, K., and Ehehalt, R. (2002). Cholesterol, lipid rafts, and disease. The Journal of clinical investigation *110*, 597-603.

Simons, K., and Vaz, W.L. (2004). Model systems, lipid rafts, and cell membranes. Annual review of biophysics and biomolecular structure *33*, 269-295.

Stefater, J.A., 3rd, Ren, S., Lang, R.A., and Duffield, J.S. (2011). Metchnikoff's policemen: macrophages in development, homeostasis and regeneration. Trends in molecular medicine *17*, 743-752.

Strohecker, A.M., Guo, J.Y., Karsli-Uzunbas, G., Price, S.M., Chen, G.J., Mathew, R., McMahon, M., and White, E. (2013). Autophagy sustains mitochondrial glutamine metabolism and growth of BrafV600E-driven lung tumors. Cancer discovery *3*, 1272-1285.

Sun, M., Goldin, E., Stahl, S., Falardeau, J.L., Kennedy, J.C., Acierno, J.S., Jr., Bove, C., Kaneski, C.R., Nagle, J., Bromley, M.C.*, et al.* (2000). Mucolipidosis type IV is caused by mutations in a gene encoding a novel transient receptor potential channel. Human molecular genetics *9*, 2471-2478.

Toulmay, A., and Prinz, W.A. (2013). Direct imaging reveals stable, micrometer-scale lipid domains that segregate proteins in live cells. The Journal of cell biology *202*, 35-44.

Villadangos, J.A., and Schnorrer, P. (2007). Intrinsic and cooperative antigen-presenting functions of dendritic-cell subsets in vivo. Nature reviews Immunology *7*, 543-555.

Waddell, D.R., and Vogel, G. (1985). Phagocytic behavior of the predatory slime mold, Dictyostelium caveatum. Cell nibbling. Experimental cell research *159*, 323-334.

Wang, Q., and Holst, J. (2015). L-type amino acid transport and cancer: targeting the mTORC1 pathway to inhibit neoplasia. American journal of cancer research *5*, 1281-1294.

West, M.A., Bretscher, M.S., and Watts, C. (1989). Distinct endocytotic pathways in epidermal growth factor-stimulated human carcinoma A431 cells. The Journal of cell biology *109*, 2731-2739.

Wong, C.O., Li, R., Montell, C., and Venkatachalam, K. (2012). Drosophila TRPML is required for TORC1 activation. Current biology : CB *22*, 1616-1621.

Yang, S., Wang, X., Contino, G., Liesa, M., Sahin, E., Ying, H., Bause, A., Li, Y., Stommel, J.M., Dell'antonio, G.*, et al.* (2011). Pancreatic cancers require autophagy for tumor growth. Genes & development *25*, 717-729.

Yang, Z., Huang, J., Geng, J., Nair, U., and Klionsky, D.J. (2006). Atg22 recycles amino acids to link the degradative and recycling functions of autophagy. Molecular biology of the cell *17*, 5094-5104.

Yoshida, S., Pacitto, R., Yao, Y., Inoki, K., and Swanson, J.A. (2015). Growth factor signaling to mTORC1 by amino acid-laden macropinosomes. The Journal of cell biology *211*, 159-172.

Yu, L., McPhee, C.K., Zheng, L., Mardones, G.A., Rong, Y., Peng, J., Mi, N., Zhao, Y., Liu, Z., Wan, F.*, et al.* (2010). Termination of autophagy and reformation of lysosomes regulated by mTOR. Nature *465*, 942-946.

Zhuang, L., Kim, J., Adam, R.M., Solomon, K.R., and Freeman, M.R. (2005). Cholesterol targeting alters lipid raft composition and cell survival in prostate cancer cells and xenografts. The Journal of clinical investigation *115*, 959-968.